

University of Windsor

Scholarship at UWindor

Electronic Theses and Dissertations

Theses, Dissertations, and Major Papers

9-27-2018

Thermal Management of Vehicle Interior Temperature for Improvement of Fuel Economy

Rehan Mohsin Rashid
University of Windsor

Follow this and additional works at: <https://scholar.uwindsor.ca/etd>

Recommended Citation

Rashid, Rehan Mohsin, "Thermal Management of Vehicle Interior Temperature for Improvement of Fuel Economy" (2018). *Electronic Theses and Dissertations*. 7564.
<https://scholar.uwindsor.ca/etd/7564>

This online database contains the full-text of PhD dissertations and Masters' theses of University of Windsor students from 1954 forward. These documents are made available for personal study and research purposes only, in accordance with the Canadian Copyright Act and the Creative Commons license—CC BY-NC-ND (Attribution, Non-Commercial, No Derivative Works). Under this license, works must always be attributed to the copyright holder (original author), cannot be used for any commercial purposes, and may not be altered. Any other use would require the permission of the copyright holder. Students may inquire about withdrawing their dissertation and/or thesis from this database. For additional inquiries, please contact the repository administrator via email (scholarship@uwindsor.ca) or by telephone at 519-253-3000ext. 3208.

Thermal Management of Vehicle Interior Temperature for Improvement of Fuel Economy

By

Rehan Mohsin Rashid

A Thesis
Submitted to the Faculty of Graduate Studies
through the Department of Mechanical, Automotive and Materials Engineering
in Partial Fulfillment of the Requirements for
the Degree of Master of Applied Science
at the University of Windsor

Windsor, Ontario, Canada

2018

© 2018 Rehan Rashid

Thermal Management of Vehicle Interior Temperature for Improvement of Fuel Economy

by

Rehan Mohsin Rashid

APPROVED BY:

R. Carriveau

Department of Civil and Environmental Engineering

D. Ting

Department of Mechanical, Automotive and Materials Engineering

A. Sobiesiak, Advisor

Department of Mechanical, Automotive and Materials Engineering

September 11th, 2018

DECLARATION OF ORIGINALITY

I hereby certify that I am the sole author of this thesis and that no part of this thesis has been published or submitted for publication.

I certify that, to the best of my knowledge, my thesis does not infringe upon anyone's copyright nor violate any proprietary rights and that any ideas, techniques, quotations, or any other material from the work of other people included in my thesis, published or otherwise, are fully acknowledged in accordance with the standard referencing practices. Furthermore, to the extent that I have included copyrighted material that surpasses the bounds of fair dealing within the meaning of the Canada Copyright Act, I certify that I have obtained a written permission from the copyright owner(s) to include such material(s) in my thesis and have included copies of such copyright clearances to my appendix.

I declare that this is a true copy of my thesis, including any final revisions, as approved by my thesis committee and the Graduate Studies office, and that this thesis has not been submitted for a higher degree to any other University or Institution.

ABSTRACT

The passenger compartment of a vehicle parked directly under the sun in the summer can reach uncomfortably high temperatures. Solar radiation may affect the durability of surfaces such as a dashboards and leather seats. Extended exposure to high temperature reduces the lifespan of some electronics in the instrument panel. VOCs, Volatile organic compounds, also increase due to high temperatures in the vehicle cabin leading to poor air quality. When the driver and passengers enter the vehicle and turn on the AC system, there is a duration of time wherein there is thermal discomfort. The duration depends on how fast the AC system is able to extract the heat from the cabin and transfer it to the outside. In addition, the amount of heat which is entrapped in the passenger compartment affects the amount of work the AC system has to perform to remove the heat from the compartment. In return, this has a significant effect on fuel consumption.

A transient energy balance model is developed to perform thermal analysis for various thermal inputs. This model is able to provide the temperature distribution and energy accumulation for surfaces inside the cabin.

The primary objective of this research is to optimize factors like glass types, roof insulation, materials, thicknesses, underbody heat insulation, and exterior and interior colours using DFSS–Design for Six Sigma. The optimization of these parameters will reduce the load on the AC system while also improving component durability, air quality, and thermal comfort.

DEDICATION

This thesis is dedicated to my beloved parents, who have always supported me.

I would also like to dedicate this thesis to my respected teachers from high school, who inspired me, and garnished my interest in higher education.

ACKNOWLEDGEMENTS

I would like to sincerely thank my University of Windsor advisor, Dr. Sobiesiak, for providing me with guidance throughout the project. His attention to detail in every aspect of this project was vital to the success of this project.

I would also like to thank my industrial advisors from FCA: Dr. Alaa El-sharkawy for providing technical assistance in model development and DFSS, and Ms. Laura Lorefice, and Mr. Andrea Piovano for providing technical assistance in model verification.

TABLE OF CONTENTS

| | |
|---|-----|
| DECLARATION OF ORIGINALITY | iii |
| ABSTRACT..... | iv |
| DEDICATION | v |
| ACKNOWLEDGEMENTS | vi |
| LIST OF TABLES | x |
| LIST OF FIGURES | xi |
| LIST OF ABBREVIATIONS/SYMBOLS..... | xii |
| CHAPTER 1 INTRODUCTION | 1 |
| 1.1 Problem Statement | 3 |
| 1.2 Objective | 6 |
| 1.3 Methodology | 7 |
| CHAPTER 2 LITERATURE REVIEW | 9 |
| 2.1 The Heat is On | 9 |
| 2.2 Volatile Organic Compounds..... | 10 |
| 2.3 Climate Control Load Reduction | 11 |
| 2.4 Solar Control PVB Glass | 12 |
| 2.5 Impact of Vehicle AC on Fuel Economy..... | 14 |
| 2.6 Fuel Used for Air Conditioning | 15 |

| | |
|--|--------|
| CHAPTER 3 THEORETICAL FRAMEWORK..... | 16 |
| 3.1 Conduction | 16 |
| 3.2 Convection..... | 16 |
| 3.3 Radiation | 17 |
| 3.4 Heat Transfer in Cabin..... | 17 |
| 3.5 First Law of Thermodynamics | 21 |
| 3.6 Heat Equation..... | 21 |
| 3.7 Parameters effecting extent of Heat Transfer | 23 |
| 3.7.1 Mass | 23 |
| 3.7.2 Thickness..... | 24 |
| 3.7.3 Surface Area | 24 |
| 3.7.4 Time..... | 24 |
| 3.7.5 Heat Capacity | 25 |
| 3.7.6 Thermal Conductivity | 25 |
| 3.7.7 Thermal Diffusivity | 25 |
| 3.7.8 Convective Heat Transfer Coefficient | 26 |
| 3.7.9 Emissivity and Absorptivity | 27 |
| 3.7.10 Orientation/View Factor | 28 |
| CHAPTER 4 MATLAB MODEL DEVELOPMENT..... | 29 |
| 4.1 Use of MATLAB..... | 29 |
| 4.2 Partial Differential Equation..... | 29 |
| 4.2.1 Solution of Partial Differential Equation | 30 |
| 4.2.2 Surface Layers | 34 |
| 4.2.3 Types of Boundary Conditions | 35 |
| 4.2.4 Flux Boundary Condition..... | 38 |
| 4.2.5 Convection Boundary Condition | 39 |
| 4.2.6 IR Radiation Boundary Condition..... | 39 |
| 4.2.7 Sample Heat Equation with Boundary Conditions..... | 40 |
| 4.3 Ordinary Differential Equation | 45 |
| 4.4 View Factors and The Greenhouse Effect | 47 |
| 4.5 Coupling and Iterations | 49 |
| 4.6 Output of the Model | 49 |

| | |
|--|----|
| CHAPTER 5 MATLAB MODEL VERIFICATION | 56 |
| 5.1 Final Verification..... | 57 |
| 5.1.1 Model Similarities and Differences | 58 |
| 5.1.2 Model Environment | 59 |
| 5.1.3 Thermal Properties | 60 |
| 5.1.4 Results and Comparison..... | 62 |
| CHAPTER 6 DESIGN FOR SIX SIGMA STUDY | 65 |
| 6.1 Need for DFSS..... | 65 |
| 6.2 DFSS Setup for Optimization | 66 |
| 6.2.1 Signal Input..... | 66 |
| 6.2.2 Noise Factors..... | 67 |
| 6.2.3 Control Factors..... | 68 |
| 6.2.4 L-18 Matrix | 69 |
| 6.3 DFSS Results | 70 |
| 6.4 Verification | 74 |
| 6.4.1 High Ranking Control Factor | 74 |
| 6.4.2 Low Ranking Control Factor | 76 |
| 6.5 Potential Improvements | 77 |
| 6.5.1 Fuel Economy..... | 77 |
| 6.5.2 Thermal Comfort..... | 79 |
| CHAPTER 7 CONCLUSIONS | 80 |
| REFERENCES/BIBLIOGRAPHY..... | 82 |
| APPENDICES | 84 |
| VITA AUCTORIS | 96 |

LIST OF TABLES

| | |
|---|----|
| Table 1: Windshield glass properties | 13 |
| Table 2: Surface areas and heat transfer coefficient | 60 |
| Table 3: Surface layers, materials, thicknesses, and conditions | 61 |
| Table 4: Temperatures at the end of 3-hour soak | 62 |
| Table 5: Compounded Noise Strategy | 67 |
| Table 6: L-18 Control Factors and Levels | 68 |
| Table 7: L18 Matrix grouping | 69 |
| Table 8: L18 Matrix results in kW | 70 |
| Table 9: Control factor ranking for signal to noise ratio and slope | 72 |
| Table 10: Percent change for high ranking control factors | 74 |
| Table 11: Percent change for low ranking control factor | 76 |
| Table 12: Recapture of reduction in heat accumulation | 77 |
| Table 13: Improvement in thermal comfort | 79 |
| Table A1: Thermal properties for various materials | 84 |
| Table A2: Glass properties | 85 |
| Table A3: Surface condition properties | 85 |
| Table A4: View Factor between surfaces | 86 |
| Table A5: L18 Matrix results in MJ | 87 |
| Table A6: Final temperatures for thermal comfort | 95 |

LIST OF FIGURES

| | |
|--|----|
| Figure 1: Daily Temperature Data from Phoenix AZ | 3 |
| Figure 2: Hourly Temperature and Solar Data from Arizona | 4 |
| Figure 3: Vehicle breath temperature during a typical day trip schedule | 10 |
| Figure 4: VOC concentration under static conditions for high and moderate heat | 11 |
| Figure 5: Comparison of soak temperatures between baseline and insulated case | 12 |
| Figure 6: Reduction in temperature due to PVB glass as opposed to baseline glass | 13 |
| Figure 7: Fuel economy impacts of auxiliary loads | 14 |
| Figure 8: Energy Losses in a conventional vehicle | 15 |
| Figure 9: Fuel used by AC system for light duty vehicles in USA | 15 |
| Figure 10: Cabin System Boundary | 18 |
| Figure 11: Breakdown of energy as it enters the system | 19 |
| Figure 12: Block illustration of cabin model | 20 |
| Figure 13: Visual representation of CN scheme | 31 |
| Figure 14: CN scheme applied to heat diffusion equation | 32 |
| Figure 15: System of equations for temperature at each node throughout thickness | 33 |
| Figure 16: Breakdown of layers and boundary conditions for roof surface | 35 |
| Figure 17: Introduction of ghost node to apply boundary condition | 37 |
| Figure 18: Spectrum of solar radiation | 47 |
| Figure 19: Temperature profile from 1st iteration of MATLAB simulation | 51 |
| Figure 20: Temperature profile from 15th and final iteration of MATLAB simulation | 52 |
| Figure 21: Temperature of Roof plotted across surface thickness and time | 54 |
| Figure 22: Heat accumulation inside dashboard surface | 55 |
| Figure 23: Exterior view of Fiat 500L modeled in TAITherm | 57 |
| Figure 24: Interior view of Fiat 500L TAITherm model | 58 |
| Figure 25: Temperature comparison between two models at the end of 3-hour soak | 62 |
| Figure 26: Temperature profile comparison for both models | 63 |
| Figure 27: Parameter diagram for a DFSS study setup | 66 |
| Figure 28: Energy trend across DFSS cases | 71 |
| Figure 29: Signal to noise ratio and slope for control factors and its levels | 73 |
| Figure 30: Reduction of energy transfer into cabin due to roof colour | 75 |
| Figure 31: Reduction of energy transfer into cabin due to glass type | 75 |
| Figure 32: Impact of AC load reduction on fuel economy of a conventional vehicle | 78 |
| Figure 33: Impact of AC load reduction on the range of an electric vehicle | 78 |
| Figure A1: Roof-emissivity at N1. Data set A = F1-black, Data Set B = F3-white | 88 |
| Figure A2: Roof-emissivity at N2. Data set A = F1-black, Data Set B = F3-white | 89 |
| Figure A3: Glass-type at N 1. Data set A = B1-conventional, Data set B = B2-reflective ... | 90 |
| Figure A4: Glass-type at N2. Data set A = B1-conventional, Data set B = B2-reflective | 91 |
| Figure A5: Roof-insulation at N2. Data set A = none, Data set B = C2-default | 92 |
| Figure A6: Roof-insulation at N2. Data set A = C2-default, Data set B=C1-doubled | 93 |
| Figure A7: Roof-insulation at N2. Data set A = C2-default, Data set B = C3-trippled | 94 |

LIST OF ABBREVIATIONS/SYMBOLS

Abbreviations:

| | |
|------|--------------------------------|
| VOCs | Volatile Organic Compounds |
| DFSS | Design for Six Sigma |
| AC | Air Conditioner |
| ODE | Ordinary Differential Equation |
| PDE | Partial Differential Equation |
| PVB | Polyvinyl Butyral |
| FTCS | Forward Time Central Space |
| BTCS | Backward Time Central Space |
| CN | Crank Nicolson |
| IR | Infra-red |

Symbols:

| | |
|---------------|--------------------------------------|
| ε | Emissivity |
| α | Absorptivity/Thermal Diffusivity |
| τ | Transmissivity |
| F | Orientation factor |
| m | Mass |
| ρ | Density |
| A | Area |
| c | Specific Heat Capacity |
| σ | Stephan Boltzmann constant |
| k | Conduction heat transfer coefficient |
| h | Convection heat transfer coefficient |
| Q | Heat |
| x | Dimension of thickness |
| T, U, u | (Unknown) Temperature |

Subscripts:

| | |
|----------|-------------------------|
| ∞ | Exterior air |
| cair | Cabin air |
| wd | Windshield |
| dt | Dashboard |
| rf | Roof |
| rw | Rear window |
| rd | Rear deck |
| fe | Floor/Underbody |
| fw | Firewall/Dashwall |
| sfc | Seat front cushion |
| sfb | Seat front back |
| src | Seat rear cushion |
| srb | Seat rear back |
| dtF | Dashboard opposite side |

CHAPTER 1

INTRODUCTION

Awareness of climate change has given engineers a new direction for innovation. Governments around the world have, at times, enforced stringent emission standards to push the limit of innovation. In the past half century, the automotive industry has been designing internal combustion engines which are more fuel efficient and, at the same time, produce less emissions. Examples of some of the recent innovations in powertrain include variable valve timing, turbocharging in gasoline direct injection systems, and cylinder deactivation. Recently, the automotive industry has reached a state wherein merely innovation in engines alone is not enough to meet the emission standards. Automotive engineers have initiated research in other aspects of vehicles such as the reduction of size and weight of the vehicle, research in aerodynamics to reduce drag, and the hybridization of drivetrain with additions of the electric motor, battery and continuous variable transmission.

There are various other aspects of the vehicle which have not yet been methodically explored. One such aspect is the thermal management of a vehicle cabin. The most rudimentary solution to the thermal problem is to install an AC unit that can cool the interior of the cabin to room temperature. Automakers have used this simple yet effective approach for decades. There have been improvements, but they have been limited to component level, e.g. the efficiency of the AC unit has improved, new coatings and tints of glass have been introduced for higher trim vehicles, and availability of a variety of lighter colour selections for the exterior and interior of the vehicle...

On the contrary, an elaborate approach to the thermal problem is to identify how heat transfers into the cabin, how it is stored, and determine the factors which aid or hinder the transfer. The Optimization of thermal management of the cabin may improve three critical aspects. Firstly, the load on the AC unit can be reduced which, in turn, reduces the fuel consumption and improves fuel economy. Secondly, the thermal comfort of the driver and passengers can be improved. Thirdly, component durability can be improved for objects that are affected by solar radiation.

In a modern vehicle, an AC system can yield an auxiliary load of up to 3 kW which equals about 4 horsepower (Farrington, & Rugh, 2000). The/an AC system consumes a fair amount of power produced by the engine; of all the auxiliary power requirements, an AC system has a great impact on fuel consumption. Using the AC can increase the fuel consumption of a conventional vehicle by up to 20%. This number depends on various factors such as cabin size, ambient temperature, the level of performance of the AC, the duration of the trip etc. Considering a conservative case: if a vehicle drives 6000 km annually with the AC on, then the vehicle's AC consumes one litre of fuel for each 100 km. Thus, the driver utilizes 60 L of extra fuel and produces 138 kg of carbon dioxide emissions in one year. Considering an extreme case: if a vehicle drives 14000 km annually with AC on, then the vehicle's AC consumes two liters of fuel for each 100 km. Thus, the driver utilizes 240 L of extra fuel and produces 644 Kg of carbon dioxide emissions in one year. These numbers are in addition to the regular operation of the vehicle (Natural Resources Canada, 2016).

Every year, with new models of vehicles, product consumers expect more comfort to be part of the innovation. When occupants enter a hot vehicle and either roll down their windows or turn on the AC, there is an initial time gap where occupants of the vehicle experience discomfort. No matter how powerful the AC of the vehicle is, the initial heat wave inside a warm car causes thermal discomfort to the occupants for a small period of time until the AC is able to transfer the heat which is soaked inside the cabin to the outside.

Solar radiation contributes to the temperature of the cabin, but it also affects the durability of surfaces and electrical components due to long term recurrent exposure. Some surfaces like leather degrade due to long exposure; other surfaces like headliner and dashboard plastic lose their adhesion and start to bubble and sag. There are many electronic components in the instrument panel which can also be affected due to recurring cycle of high solar radiation.

A thermally optimized vehicle cabin which lowers the heat load inside the cabin is advantageous for reducing emissions, fuel consumption, thermal discomfort, and improving component durability.

1.1 Problem Statement

Heat load is added to the vehicle cabin via different modes and sources. The sources of heat load include the sun, ambient temperature outside the vehicle, and engine and exhaust system. A vehicle parked in a parking lot is exposed to a combination of these sources.

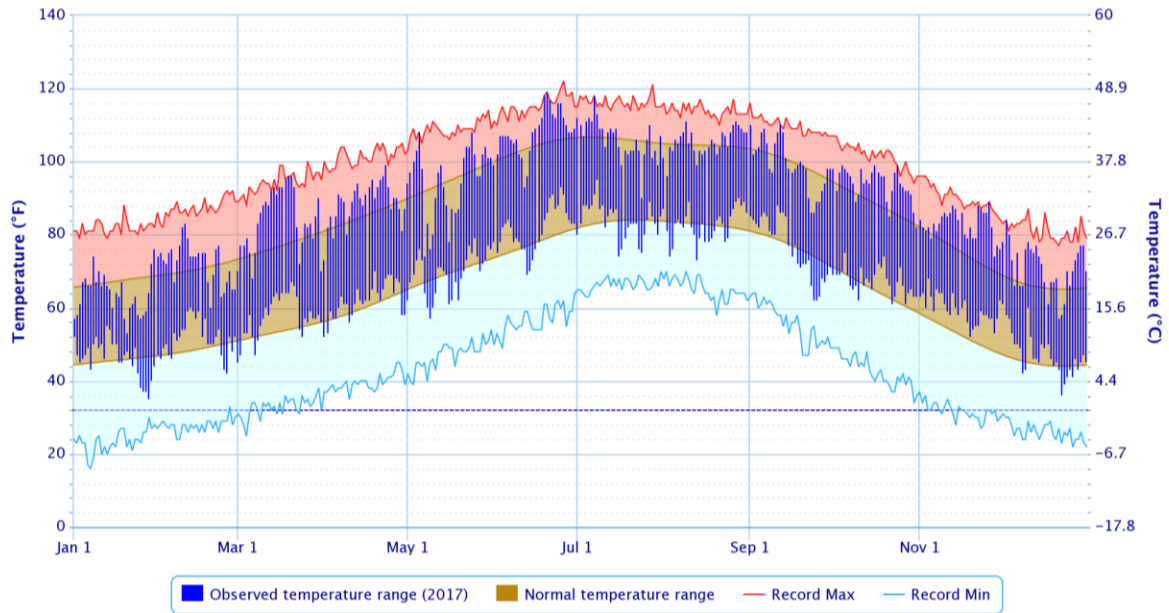


Figure 1: Daily Temperature Data from Phoenix AZ

Figure 1 (US Department of Commerce, & NOAA, 2018) shows the daily temperature range from the city of Phoenix in Arizona, USA for a year. The vertical blue lines display the highest and lowest temperatures of each day. The red markers show the record highest temperatures from previous years. This chart shows the frequency of days with extreme temperature. Taking a look at large North American cities, there are a lot of cities which exceed 99°F or 37.8°C frequently throughout a one-year period. The names of the cities and the number of days within each year when temperature exceeds 99°F or 37.8°C are as follows:

| | |
|-----------------------|-------------------------|
| Phoenix Arizona | 107 days, |
| Las Vegas, Nevada | 70 days, |
| Riverside, California | 24 days, |
| Dallas, Texas | 17 days. (Osborn, n.d.) |

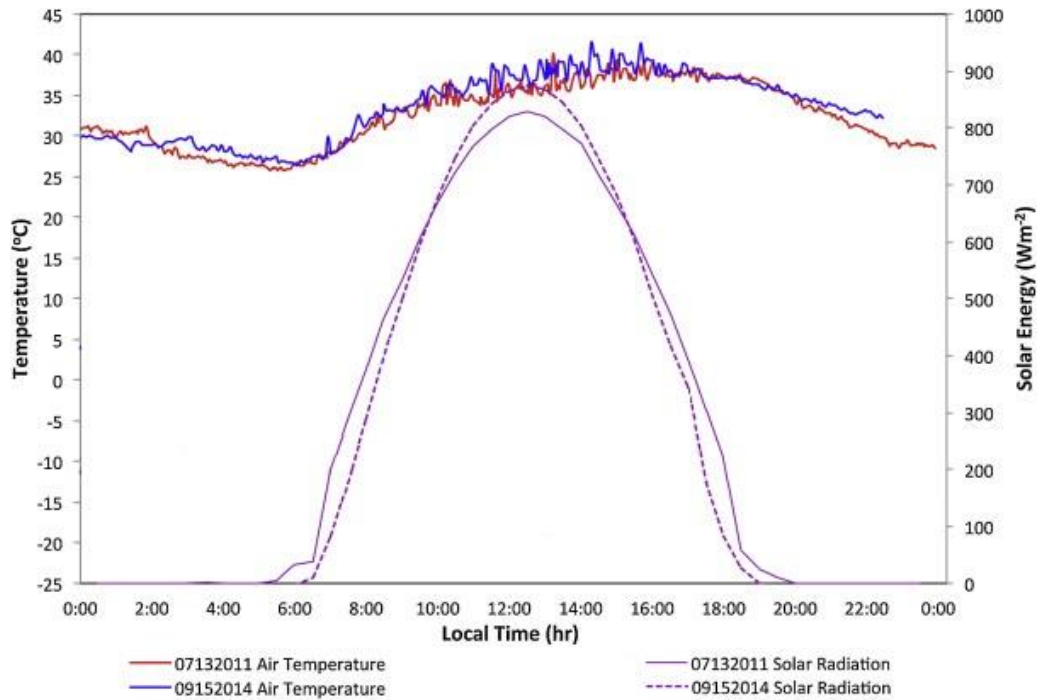


Figure 2: Hourly Temperature and Solar Data from Arizona

Figure 2 (Vanos et al., 2016) shows the hourly air temperature and solar energy distribution from Arizona. The left axis shows the temperature and the right axis shows the solar load. The data is collected from two hot days: one from July and one from September. Solar radiation starts from dawn to dusk, reaching its peak at noon. The air temperature keeps decreasing throughout the night and starts to increase after dawn due to convection with the surfaces located on the ground. These surfaces then become hot by absorbing the solar energy.

In the vehicle cabin, surfaces such as windshields and windows allow the solar radiation to be partially transmitted inside the cabin. Other surfaces such as roofs partially absorb the solar radiation which then gets transferred inside the cabin via conduction and convection. Ambient air outside the vehicle transfers heat to cabin surfaces via convection. Heat passes through the material via conduction and releases inside the cabin via convection. If the vehicle engine is running, then heat load is also added to the cabin via firewall and under the body due to high temperatures of the exhaust system

All these heat sources add heat to the cabin. The cabin absorbs and soaks in this heat load until it reaches a steady state temperature. Steady state temperature is a temperature at which the heat load coming into the cabin is same as the heat load leaving the cabin; thus, there is no net increase in temperature beyond this point.

At a very small scale, a vehicle cabin acts as a greenhouse. The solar radiation gets transmitted through the windshield and windows very easily due to its smaller wavelength. Due to the absorption and soaking of the heat load into the cabin, the interior surfaces inside the cabin increase in temperature and ultimately start radiating their own heat in infrared. Infrared radiation which belongs to the longer wavelength does not transmit to the outside as easily as the solar radiation transmits inside. This causes heat to be trapped inside. This is why when a driver or passenger opens the door of a vehicle parked under a sun for a long period of time, it is much hotter inside the cabin than it is outside.

The heat accumulation inside the cabin leads to thermal discomfort for the driver and passengers. Even when the AC is turned on, it takes a while for the cabin air and its surface temperatures to reach a comfortable temperature. Higher heat load inside the cabin means that the AC has to do more work to transfer that heat to the outside of the cabin, leading to lower fuel economy. Over long periods of time, solar radiation and heat may affect the durability of various materials and components found inside the vehicle cabin. Higher temperatures in the cabin also cause increases in VOCs, Volatile organic compounds and affect the overall cabin air quality.

1.2 Objective

With regards to heat transfer, a vehicle cabin acts as a storage unit for heat load. One of the forms of the first law of thermodynamics states that heat stored in a system equals mass times heat capacity times temperature gradient. By lowering the amount of mass inside the cabin or choosing a material with a lower heat capacity, the heat trapped inside the cabin will be reduced. If there is less mass, there is less of material to store the heat load; If the heat capacity of a material is lower, then the material will hold less energy. Thus, it will reach steady state at a lower temperature.

There is another approach in contrast to reducing the weight and heat capacity of the materials. This approach gets more focus in the project. If pre-emptive measures are taken, then the amount of heat load coming into the cabin can be reduced. A leading example of this is the insulation of fabric on the inside of the roof and the insulation of the carpet on the floor. Some new technologies are emerging for glass materials such as e-coatings for windshields which reduce the emissivity of the surface.

When these two approaches are combined, there are a lot of parameters which can affect the amount of heat load transferring inside the cabin, and once inside, soaking into the furniture such as the dashboard, steering wheel seats, etc. All these parameters are connected to each other. Changing one parameter affects the heat transfer in some other medium and source. Thus, it is difficult to do optimization using only one subsection such as just the roof, or just the windshield.

The objective of this project is to investigate main factors and pick out top factors which are most effective in reducing the temperatures of air and surfaces inside the cabin. Factors which will be investigated include different glass types, roof insulation, materials and their thicknesses, under body insulation and heat shielding, and exterior and interior colours

Highlighting the factors which have a significant effect on the temperature of the cabin will reduce heat stored in the cabin system. Less heat storage means improved fuel economy, better customer comfort, and improved durability of interior vehicle surfaces and components.

1.3 Methodology

A transient energy model is developed in MATLAB which can evaluate the total heat transfer. Thermal analysis is performed for both stationary soak conditions and engine idling condition. The system upon which the thermal analysis is conducted comprises of cabin air and a variety of surfaces either single layer or multilayer.

Thermal state of cabin air is modeled by the first law of thermodynamics. The first law of thermodynamics is in a format of ordinary differential equation as its derivative is only dependent on the derivative of time. The mass of air times the heat capacity of air times the temperature gradient of air equals the convection heat coming from all surfaces including inside surfaces of the roof, windshield, windows, under body, seats, and outside surfaces of the dashboard and instrument panel

Thermal state of surfaces at the boundary of the cabin and inside the cabin are modeled by the heat diffusion equation. The heat diffusion equation is in a format of partial differential equation meaning it is partially dependent on time and partially depended on thickness, width, length or all three. In this project, surfaces are only modeled in 1D space. For surface models, only thickness is considered as a dimension, width and length are assumed to be infinite for simplicity. The heat diffusion equation encompasses convection and radiation via boundary conditions.

The size of the surface is considered when the ordinary differential equation, (ODE) based on the first law of thermodynamics, is coupled with the partial differential equations (PDEs); one PDE is written for each surface. ODE takes surface area into account when it adds or subtracts the convective heat depending on the direction of the transfer. Temperatures of surfaces and the temperature of cabin air are dependent on each other as calculations cannot be completed without finding the temperature gradient. That is why 1 ODE and multiple PDEs are coupled and must be iterated to find the correct temperatures. The first iteration starts with initial conditions; each additional iteration utilizes results from previous iterations.

Performing the heat transfer simulation yields temperatures of the cabin air and each of the surfaces. The temperature of the cabin air is the solution of ODE, and the temperature of each surface is the solution of its corresponding PDE. A heat curve can be created for the air; this curve shows the amount of heat coming into the cabin air. The area underneath this curve shows the amount of heat accumulated inside the air. Heat curves can also be created for each of the surfaces. The sum of the amount of heat accumulated in the cabin air and the amount of heat accumulated inside each of the surfaces equals the total amount of heat trapped in the system. This is the number which needs to be optimized. By lowering the amount of heat trapped inside the system, the AC must perform less work to extract the heat.

The model developed in the MATLAB is verified using an extensive model previously created by FCA engineers in TAITherm, a leading 3D heat transfer analysis software. Model developed in MATLAB is much simpler but tailored for heat transfer in vehicle cabin.

A Design for Six Sigma (DFSS) study is performed to compare different parameters which can affect heat transfer to the cabin. The DFSS study incorporates different signal levels such as solar loads from the sun; it also incorporates different noise levels such as low and high exterior wind speeds, ambient temperature, and whether the engine is turned off or idling. Each parameter under investigation is treated as a control factor; each control factor has numerous alternatives known as control levels which could prove better or worse for the heat transfer into the cabin. An L18 matrix is made which has 18 different combinations based on the matching of different control levels. These 18 combinations are performed for 3 different signal levels and 2 different noise levels. That is a total of 108 simulations. The results of heat accumulation from 108 simulations help pick out parameters which have the most effect on the heat transfer despite the change in noise and signal levels.

CHAPTER 2

LITERATURE REVIEW

2.1 The Heat is On

An article by the Society of Automotive Engineers “The heat is on: Don’t leave your chocolate candy, kids or pets in a parked car” (Atkinson, & Hill, 2015) emphasises heat is able to accumulate inside the vehicle cabin and essentially make it an oven. The factors which contribute to the heat transfer are vehicle’s exterior and interior surface colours; the type, angle and size of the windows; and the size of the passenger compartment.

The increasing amount of glass on today’s modern vehicle has a major impact on vehicle’s interior surface temperatures. Even on cool days, temperature at breath level in vehicle can reach over 40°C in a closed vehicle. On hotter days, this temperature can reach over 65°C.

Heat stroke can occur when body temperature exceeds 40°C. An adult’s body may take longer to heat up, but a children’s or pet’s body reaches and exceeds this temperature much faster due to smaller mass. Even when making short trips, interior vehicle conditions may reach 43°C in a matter of minutes. This time may be as short as 6 minutes on a day with 30°C of exterior air temperature and high solar radiation.

Figure 3 shows a study which was performed to record breath temperatures in a vehicle during a typical 30°C day of running errands in Phoenix. The vehicle is a 4-door sedan with white exterior colour and tinted windows. The temperature profile shows that when the driver enters the vehicle and turns on the AC, temperature decreases to a comfortable temperature, and when the vehicle is parked, it rises again and reaches up to 50°C at one of the stops (Atkinson, & Hill, 2015).

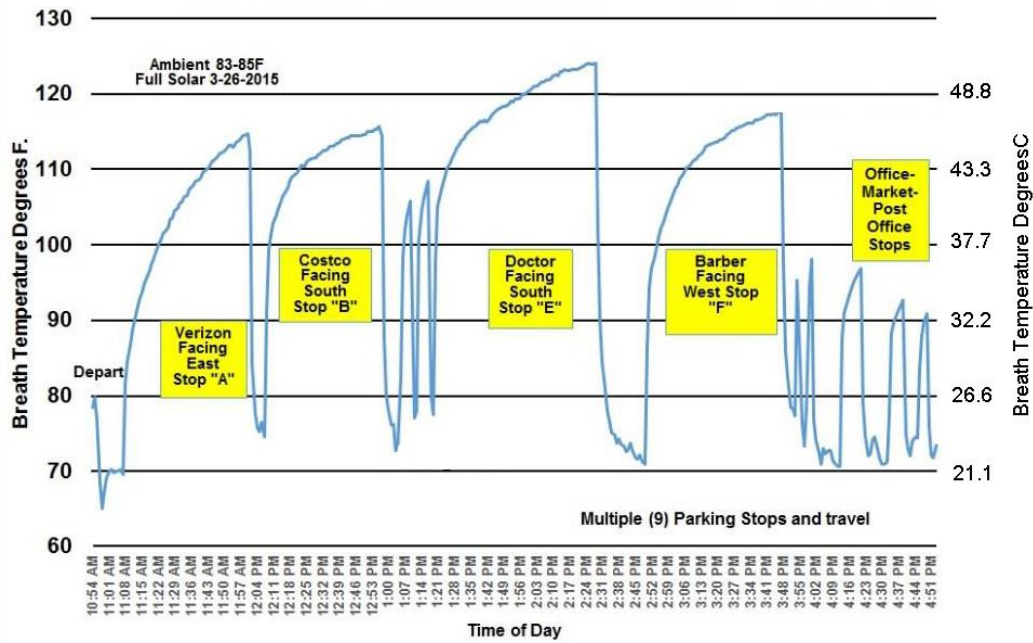


Figure 3: Vehicle breath temperature during a typical day trip schedule.

2.2 Volatile Organic Compounds

The paper “Measurement of Volatile Organic Compound inside Automobiles” (Fedoruk, & Kerger, 2003) dictates that studies have shown that fuel and exhaust related VOCs sometimes accumulate in a vehicle cabin two to fourfold higher than ambient outdoor air. VOCs are also associated with surfaces situated inside the vehicle cabin. These surfaces such as sealants, carpets, vinyl, leather, plastics, and foam cushions emit VOCs over an extended period of time due to off-gassing, compound breakdown due to age, and heating/cooling.

Figure 4 shows the concentration of total VOCs under static conditions during two heat levels. High heat is vehicle soak temperature between 43°C and 62°C whereas moderate heat is soak temperatures between 32°C and 42°C. The difference in the number of VOCs which are measured in micrograms is between fourfold to eightfold between moderate temperature and high heat temperature. These VOCs may affect the quality of cabin air (Fedoruk, & Kerger, 2003).

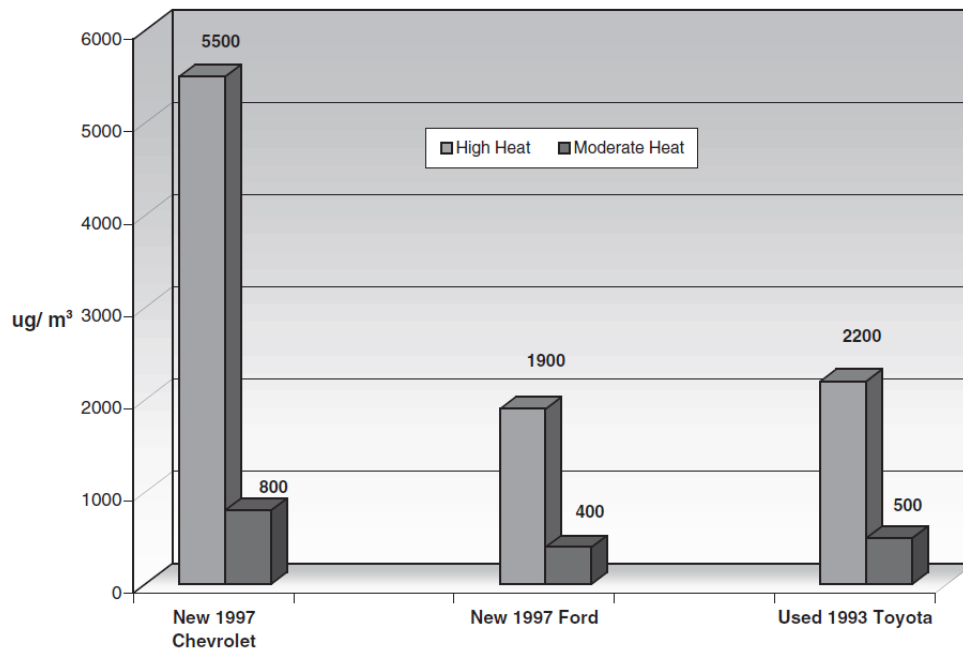


Figure 4: VOC concentration under static conditions for high and moderate heat

2.3 Climate Control Load Reduction

The paper “Climate control load reduction strategies for electric drive vehicle in warm weather” (Jeffers et al., 2015) tries to assess existing strategies for reducing load on AC systems and suggests some new ones. One existing strategy is insulating the headliner in the roof section of the vehicle. This strategy was evaluated by increasing the headliner insulation by a factor of ten. Figure 5 shows a simulation from a validated model prepared in TAITherm comparing a baseline case and an insulated headliner case. As can be seen in the insulated headliner case, the roof temperature is higher but the headliner temperature and essentially all other cabin temperatures are lower. The breath level air temperature is 2°C cooler with insulated headliner. There is a moderate impact on the headliner temperature but minimal impact on other cabin surfaces as most of solar radiation is still able to enter via glass surfaces.

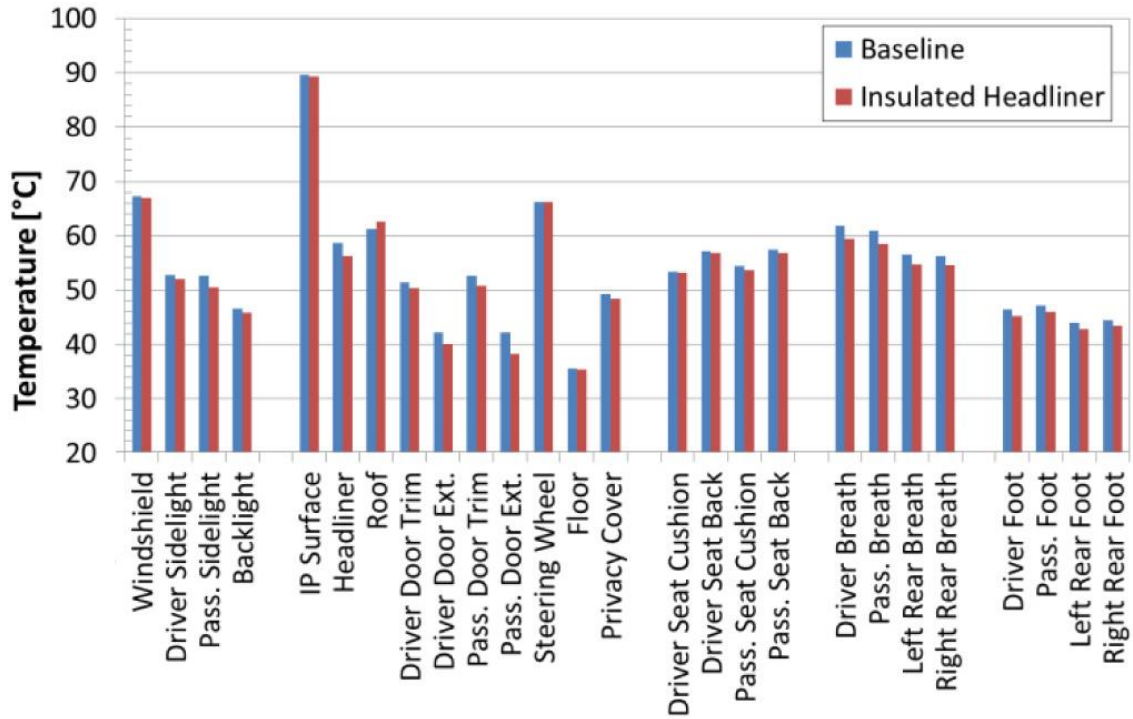


Figure 5: Comparison of soak temperatures between baseline and insulated case

Some other strategies are explored in the paper such as overhead temperature-controlled air ventilation. The idea behind ventilation is that when the interior temperature of the cabin exceeds the outside air temperature, a blower can ventilate fresh air from outside and relatively cool down the hot soaked surfaces of the cabin (Jeffers et al., 2015).

2.4 Solar Control PVB Glass

The paper “Impact of Solar Control PVB Glass on Vehicle Interior Temperature, Air-Conditioning Capacity, Fuel Consumption, and Vehicle Range” (Rugh et al., 2013) investigates the impact of a polyvinyl butyral windshield with regards to the thermal management of vehicle’s interior cabins.

Table 1: Windshield glass properties

| Config. | Glazing Type | Trans. | Abs. | Thick ness |
|-------------------------|--|--------------------------|--------------------------|---------------|
| | | Solar weighted (%) | Solar weighted (%) | (mm) |
| Baseline | Eastman Chemical baseline (standard PVB) | 53.61 | 39.49 | 5.5 |
| Solar Control PVB | Saflex solar control PVB | 39.23 | 54.32 | 5.5 |

Table 1 presents the properties of the baseline windshield glass and solar control PVB windshield glass. Baseline glass has lower absorptivity but much higher transmissivity; this means it lets 53 % of solar energy into the vehicle cabin because of its transparency. Figure 6 shows test data and analysis from TAITherm simulation. The results show increase in windshield temperature and reduction in essentially all other temperatures when solar control PVB glass is used. This is because PVB glass allows less solar radiation into the cabin as it has lower transmissivity and ultimately results in 4% reduction in AC power and increases fuel economy by 0.7% - 1.1% for conventional vehicles (Rugh et al., 2013).

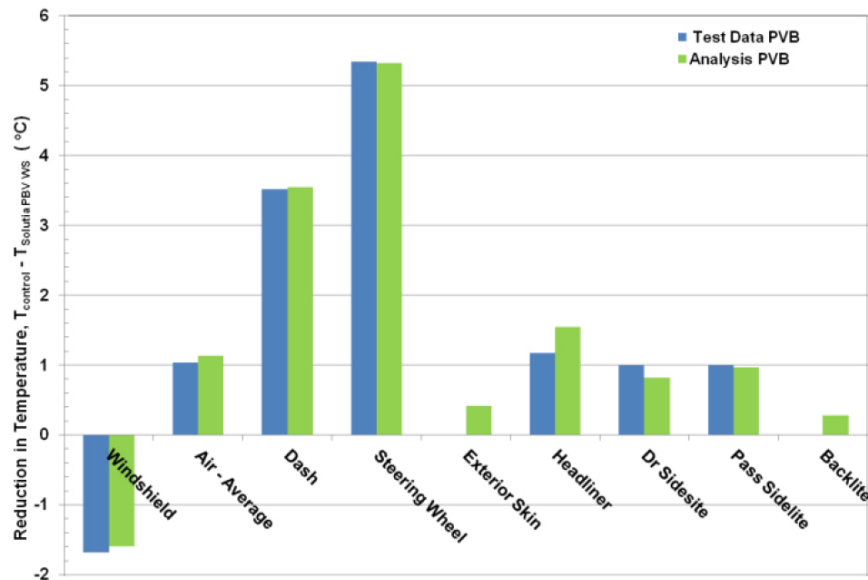


Figure 6: Reduction in temperature due to PVB glass as opposed to baseline glass

2.5 Impact of Vehicle AC on Fuel Economy

The conference paper “Impact of Vehicle Air-Conditioning on Fuel Economy, Tailpipe Emissions, and Electric Vehicle Range” (Farrington, & Rugh, 2000) discusses the potential improvement in fuel economy and reduction in emissions by reducing load on air conditioning systems. For some driving conditions, AC systems can increase the fuel consumption of fuel efficient vehicles by 50% and mid size vehicles by 20% while increasing NO_x and CO by 80% and 70% respectively. This paper also investigates the effects of advanced glazing for glass and recirculated air ventilation on thermal comfort and fuel economy.

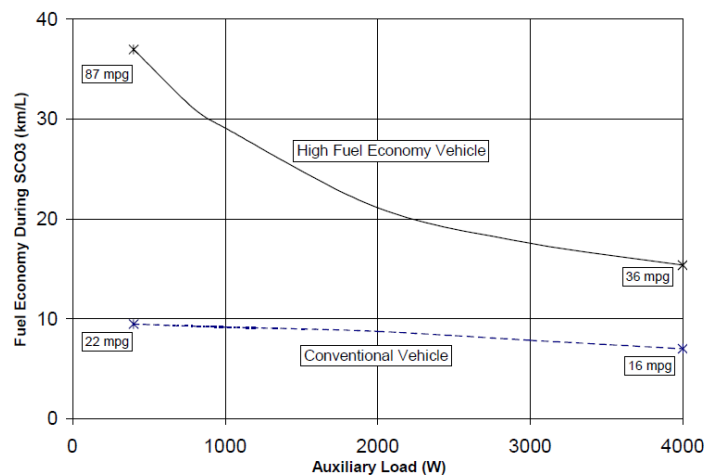


Figure 7: Fuel economy impacts of auxiliary loads

AC system is the largest auxiliary load on a vehicle; other loads such as headlights, electronics etc. are much smaller in magnitude. Figure 7 presents the impact of auxiliary load on the fuel economy of a conventional vehicle and a high fuel economy vehicle. These results were obtained from Advanced Vehicle Simulator. The conventional vehicle from Figure 7 is modeled with 1406 kg weight and 3.0 L spark ignition engine. The high fuel economy vehicle is modeled with a 907 kg weight, 1.3 L direct injection compression ignition engine, and parallel hybrid. A driving profile from an SC03 test procedure is used with air conditioning. ACs of today significantly reduce the fuel economy, and its effect is further evident for high fuel economy vehicles with smaller internal combustion engines (Farrington, & Rugh, 2000).

2.6 Fuel Used for Air Conditioning

The paper “Fuel Used for Vehicle Air Conditioning: A State-by-State Thermal Comfort-Based Approach” (Jonson, 2002) emphasises that the use of AC outweighs the loss of energy to rolling resistance, aerodynamic drag, or even driveline losses. Figure 8 shows the breakdown of energy losses for a conventional vehicle. An AC system can account for 7% of the energy produced and can be much higher for smaller engine vehicles with higher fuel economy. For a conventional vehicle, the AC compressor can add up to 5 kW peak power draw which is equivalent to a vehicle driving at a constant speed of 56 km/h.

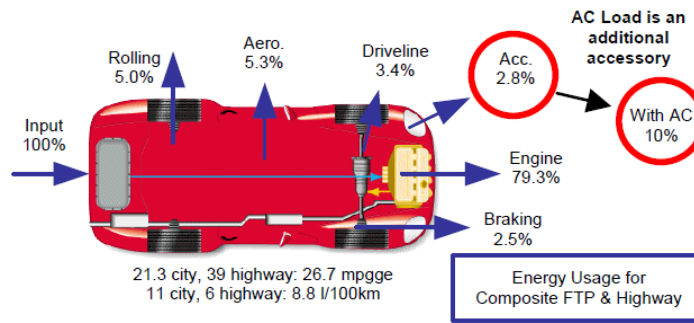


Figure 8: Energy Losses in a conventional vehicle

Figure 9 shows the yearly amount of additional fuel used by different states for operating the AC system. This totals to 7.14 billion gallons of gasoline which makes up 6% of domestic petroleum consumption and 10% of crude oil imports (Jonson, 2002).

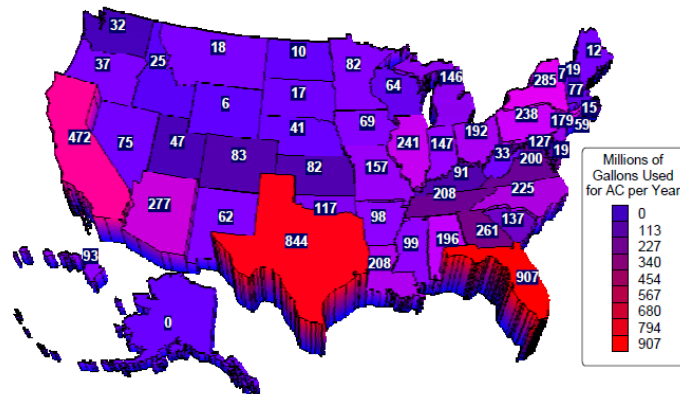


Figure 9: Fuel used by AC system for light duty vehicles in USA

CHAPTER 3
THEORETICAL FRAMEWORK

3.1 Conduction

Conduction is the transfer of energy from particles of a substance to the adjacent less energetic ones as a result of their interaction. Conduction can take place in solids, liquids, or gases. In solids, the conduction heat transfer is due to vibrations of molecules and energy transport of free electrons. In liquids and gases, conduction heat transfer is due to the collision and diffusion of molecules (Cengel, & Ghajar, 2015).

$$\dot{Q}_{cond} = -k A \frac{\Delta T}{\Delta x} \quad \text{Equation 3.1}$$

As shown above in the equation, conduction heat transfer depends on the geometry of the medium which is its thickness, material of the medium which is its thermal conductivity, the cross-section area, and the temperature gradient across the medium.

Conduction can take place in solids, liquids, or gases. Conduction can also take place between different states such as solid and gas, but most often the convective heat transfer coefficient overpowers the thermal conductivity; thus, the conductive heat transfer is assumed to be zero.

3.2 Convection

Convection is the transfer of energy between a solid surface and the adjacent liquid or gas that is in motion. It involves the combined effects of conduction and fluid motion; heat transfer due to fluid motion is referred to as advection. The faster the fluid flows, the greater the convective heat transfer. Convection can be divided into two scenarios; forced convection where the fluid flow over the surface is caused by an external means such as a fan; and free convection where the fluid motion over the surface is caused by buoyance forces which are induced by density differences due to the variation of temperature in the fluid (Cengel, & Ghajar, 2015).

$$\dot{Q}_{conv} = h A_s (T_s - T_{\infty}) \quad \text{Equation 3.2}$$

As shown above in the equation, convective heat transfer depends on the flow which is characterized by the convective heat transfer coefficient, area of the surface in contact, and temperature difference between the solid and the fluid. This equation is also known as Newton's law of cooling.

3.3 Radiation

Thermal radiation is the absorption of energy emitted by a matter due to its temperature. All bodies whether solid, liquid or gas emit thermal radiation at temperatures greater than absolute zero. Energy transfer by radiation is the fastest at the speed of light (Cengel, & Ghajar, 2015).

$$\dot{Q}_{rad} = \varepsilon \sigma A_s (T_s^4 - T_{surr}^4) \quad \text{Equation 3.3}$$

The equation above shows that radiative heat transfer depends on the emissivity of the surface absorbing the radiation, Stefan-Boltzmann constant, surface area, and the gradient of temperature raised to the power of 4. The emissivity in the equation is interchangeable with absorptivity of the surface; both emissivity and absorptivity are equal to each other under steady state conditions. For this project, analysis is performed under transient conditions, thus distinction is made when model equations are written.

3.4 Heat Transfer in Cabin

Heat transfer in the vehicle cabin is caused by various sources via different heat transfer modes. To describe heat transfer in the cabin, a system boundary must be first defined. As shown in Figure 10 below, a cabin system boundary includes the roof, windshield, firewall, under-body, and rear and side windows. The cabin system includes all the surfaces mentioned in the boundary and additionally all the furniture inside the cabin such as the dashboard, console, carpet, headliner, and seats.

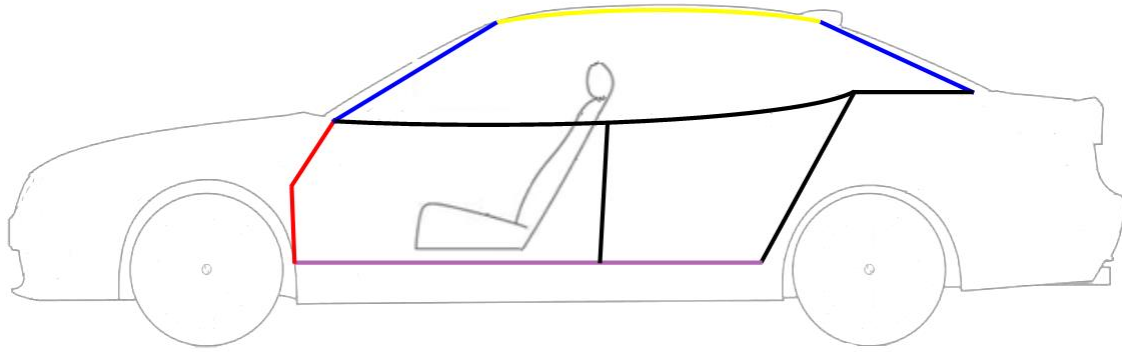


Figure 10: Cabin System Boundary

Surfaces at the boundary are exposed to both the exterior air and the interior cabin air, whereas the surfaces inside the cabin boundary are only in contact with the interior cabin air. Heat is added to the system from a variety of sources: solar radiation, convection from hotter exterior air, convection from hotter air and IR radiation from the engine bay and exhaust.

At all times, heat is being added and removed from the system simultaneously. At initial times, the net heat transfer is into the system. After some period, temperature inside the cabin increases to a point where heat coming into the system is equal to the heat leaving the system. This is referred to as the steady state. Before the steady state, the heat comes into the system via solar radiation and exterior air convection. After the steady state, heat comes in via solar radiation, and leaves via exterior air convection because the cabin air temperature is higher than the temperature outside.

Figure 11 below illustrates the breakdown of energy when it enters the system. The roof, windows, firewall, and floor are at the boundary of the system and are in contact with both the exterior air and cabin air. The dashboard and seats are inside the system and are only in contact with the cabin air. The surfaces inside the system behave differently compared to surfaces at the boundary.

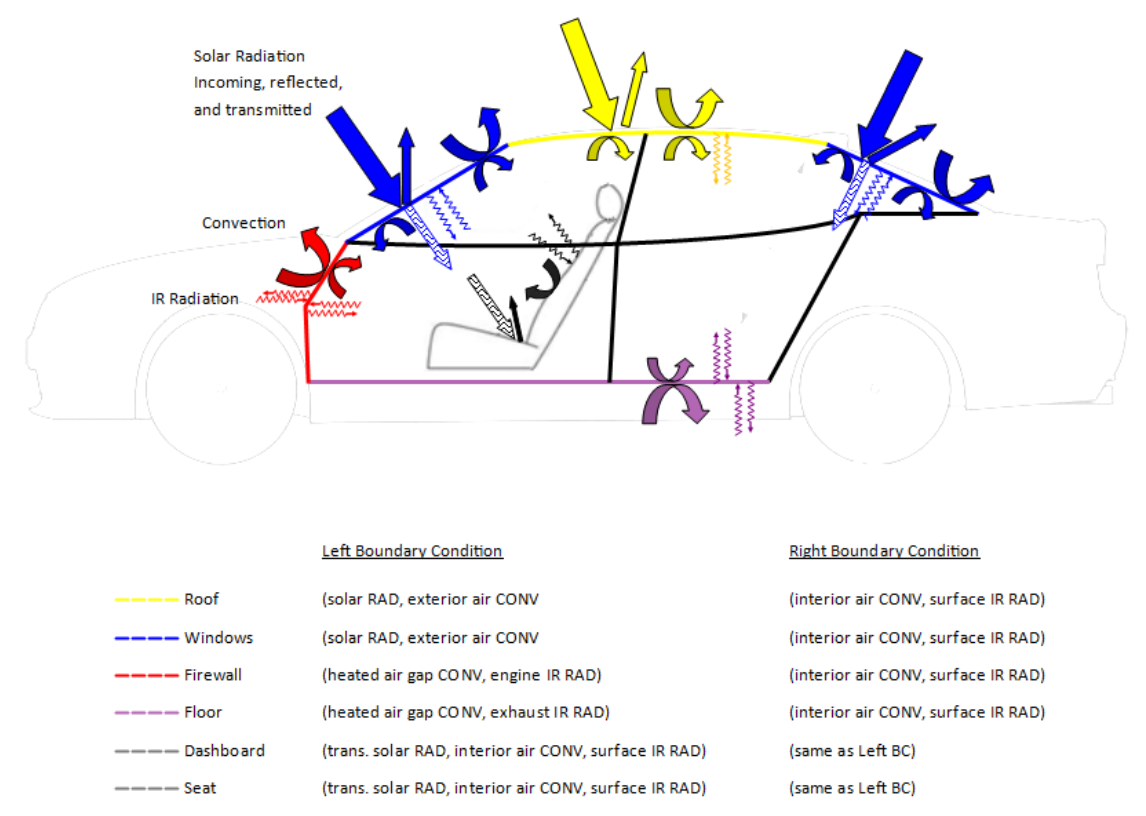


Figure 11: Breakdown of energy as it enters the system

When radiation strikes a surface, part of it is absorbed; part of it is reflected; and if the surface is not opaque, then part of it is transmitted. The large arrow in Figure 11 represents solar radiation coming from the sun. The smaller arrow right beside it represents reflected solar radiation. The patterned arrow represents transmitted solar radiation; this arrow is only present in the windows and not at the hood as it is an opaque surface. The curved arrow represents convective heat transfer. The very thin and squiggly arrow shows the IR radiation heat transfer; surfaces inside the system have IR radiation heat transfer with other surfaces inside the cabin and surfaces at the system boundary. Figure 11 also shows the description of the left and right boundary conditions. A block model of the same illustration can be seen in Figure 12; this block model shows how some of the surfaces are connected to each other.

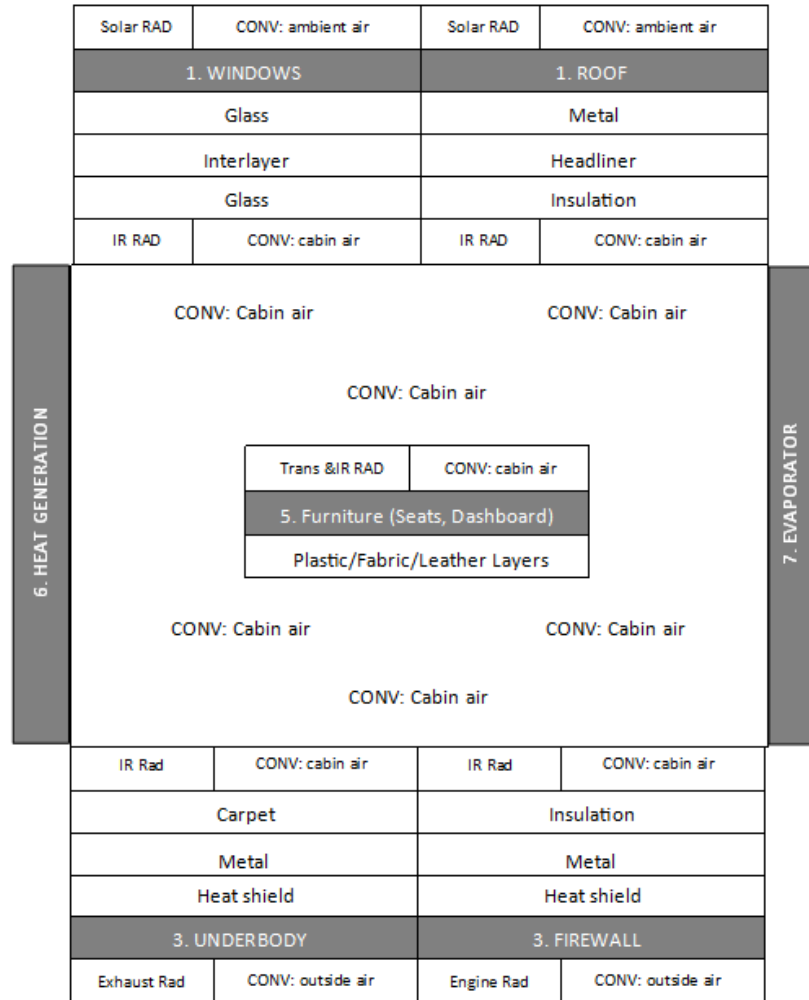


Figure 12: Block illustration of cabin model

The big block in the center is the cabin air. On the inside, the cabin air has different furniture items, and on the outside, the cabin air is surrounded by surfaces at the boundary such as the windows, roof, firewall, and under body. Figure 12 also breaks down the surfaces into possible material layers. Layers at the either end are exposed to their respective boundary conditions. The block illustration also includes the evaporator which will not be modelled but it is one of the players which removes the heat from the system when the AC is turned on. There could also be heat generated inside the system such as human occupants.

3.5 First Law of Thermodynamics

The first law of thermodynamics, which is also known as the conservation of energy principle, states that energy can neither be created and nor destroyed; It can only change forms. Thus, the first law of thermodynamics allows one to do an energy balance of the system. The conservation of energy principle states that the total energy of the system during a process is equal to the difference between the total energy entering and the total energy leaving the system during that process.

$$\Delta U = Q - W \quad \text{Equation 3.4}$$

$$\Delta U = m C \Delta T \quad \text{Equation 3.5}$$

The equation 3.4 above shows the energy balance for a stationary closed system. Closed system means that the mass is fixed in the system. Since the cabin air is not performing any work, the work done is zero. The equation 3.5 shows a stationary closed system with no work, and heat added to the system has been expanded to $mC\Delta T$: mass, specific heat, and temperature difference (Cengel, & Ghajar, 2015).

For this project application, the first law of thermodynamics is applied in two instances. For the first time, it is used to model just the cabin air and determine its temperature with respect to time. For the second instance, it is used to calculate the energy accumulation for the whole cabin system, including all surfaces in and around the cabin and the cabin air.

3.6 Heat Equation

Steady state conduction equation 3.1 cannot be used to calculate the temperatures of the surfaces. For example, if we consider a wall with ambient air temperature on either side; the conduction equation assumes the temperature gradient to be constant and not changing with time. The conduction equation also assumes that the whole body has the same temperature; for steady state this is true, but for transient analysis, for a period of time, there will be a distribution of temperature moving from either edge of the wall to the inside core of the wall. In the vehicle cabin, it is possible that the air outside the

vehicle stays at the same temperature, but the air inside the cabin must change in temperature.

The heat equation, also known as the heat diffusion equation, is a partial differential equation (PDE) which defines the variation of temperature in space over time. This means that the wall can have different temperatures across its thickness; there can be different ambient temperatures on either side of the wall, and these ambient temperatures can also change with time. The heat equation in this case would only model the wall, and it will have boundary conditions on either side which incorporates the ambient temperatures surrounding it.

$$\frac{\partial T}{\partial t} = \alpha \left(\frac{\partial^2 T}{\partial x^2} + \frac{\partial^2 T}{\partial y^2} + \frac{\partial^2 T}{\partial z^2} \right) \quad \text{Equation 3.6}$$

The equation 3.6 above shows the heat equation in 3D. The heat equation in 3D considers temperature variation with time for all three dimensions: thickness, width, and length. In the example of a wall, if the ambient temperatures on either side of the thickness are consistent along the height and the length of the wall, then 1D heat equation can be used to model a three-dimensional wall. It is being assumed that the height and the length of the wall are infinite, and temperature of wall varies only across the thickness.

The heat equation has three parts to it. The first part shows that temperature is partially dependent on time. The second part is the thermal diffusivity; which is thermal conductivity divided by density and specific heat capacity. The third part shows that the temperature is partially dependent on the three dimensions of space.

3.7 Parameters effecting extent of Heat Transfer

There are many parameters which effect the amount of heat coming into the system, leaving the system, and accumulating inside the system. The effect of these parameters is detailed below.

3.7.1 Mass

Heat energy trapped inside a material is the product of mass, heat capacity, and temperature difference. This is dictated by the first law of thermodynamics as shown below

$$\dot{Q} = m C \frac{dT}{dt} \qquad \text{Equation 3.7}$$

The more material there is, the more it weights thus trapping more heat. In a simple system with a singular mass, reducing mass of surfaces can lead to lower energy. In the case of a vehicle cabin, reducing mass can have a positive effect on the said surface, but a negative effect on the overall system.

Mass and other parameters which are related to mass have a varying effect on heat transfer. For example, consider the thickness of the roof insulation material; the headliner and insulation layer on the roof provide heat, vibration, and sound insulation to the cabin. On one hand, lower insulation thickness means lower mass, thus less heat accumulated inside the roof insulation layer. On the other hand, lower thickness might allow more heat to pass through the boundary to the system. Both aspects are important; when the AC is turned on, heat is extracted from the cabin air. However, recycled colder cabin air absorbs heat from the surfaces it encounters, whether those surfaces be on the boundary of the system or inside the system.

3.7.2 Thickness

Reduction of thickness will lead to lower volume and mass. This will lead to less energy trapped inside the object but not necessarily less energy inside the system.

3.7.3 Surface Area

Reduction of surface area will lead to lower volume and mass, thus lower heat accumulation in the object. Depending on the type and magnitude of boundary conditions on the surface of the object, an increase or decrease in the surface area will define its impact on heat transfer into the system. If the surface is transparent such as the windshield, surface area also determines how much of the heat energy gets transmitted into the system in addition to being absorbed at the surface.

3.7.4 Time

Since a transient model is being considered, time plays an important role in the temperature distribution of the system. If the transient analysis is run for a long duration, temperatures will reach a steady state. Steady state is the point where heat coming into the system is same as heat leaving the system, thus the energy and temperatures in the system do not rise.

A heat equation as presented in equation 3.6 is a partial differential heat equation which is dependent on both the progression of time and the dimensions of the surface. The first law of thermodynamics which may be used to define the temperature of the cabin air is an ordinary differential equation which is dependent on also time among other parameters.

In transient analysis, temperatures of objects at the boundary and inside the system start at room temperatures and approach their respective steady state temperature with the progression of time. Until steady state is reached, temperature is dependent on time. After steady state is reached, temperature will stay constant and will not be dependent on time.

3.7.5 Heat Capacity

Heat capacity represents how much energy a material stores per volume. Heat capacity is the product of density ρ and specific heat C . Specific heat, C , is the amount of heat per unit mass required to raise the temperature by 1 degree Celsius. Collectively, the product of density and specific heat is a ratio between the heat added or removed from the surface and the temperature increase or decrease due to the heat addition or removal. Given that mass and other parameters stay consistent, a material with a higher heat capacity would mean that it can store more heat energy (Cengel, & Ghajar, 2015).

3.7.6 Thermal Conductivity

Thermal conductivity, k , is a measure of the ability of a material to conduct heat. Thermal conductivity is a key parameter for surfaces at the boundary of the system (Cengel, & Ghajar, 2015). Surfaces which are located at the boundary shield the interior from exterior environmental conditions. Some of the objects around the vehicle cabin are made of multiple materials; e.g. the roof has multiple layers: metal sheet, air gap, polyurethane foam, and headliner cloth. Materials such as metal are high conductors of heat as compared to material like carpets and polyurethane foams. Thus, the reason why the layer of metal on the outside of vehicle structures is followed by materials which have lower thermal conductivity to insulate the interior air from heat.

3.7.7 Thermal Diffusivity

Thermal diffusivity, α , defines how fast heat diffuses through a material (Cengel, & Ghajar, 2015). As shown in the equation below, thermal diffusivity is thermal conductivity divided by heat capacity. A material with higher thermal conductivity and lower density and specific heat has higher thermal diffusivity.

$$\alpha = \frac{k}{\rho C} \qquad \text{Equation 3.8}$$

The thermal diffusivity parameter shows the ratio between heat conducted into the material and the heat stored inside the material per volume. A thermal diffusivity with larger value means faster heat propagation into the medium, smaller value means heat will mostly be absorbed by the material and small amount of heat will be conducted further. Metallic materials have higher thermal diffusivity values, whereas materials such as carpets and foams have lower values.

3.7.8 Convective Heat Transfer Coefficient

The convective heat transfer coefficient, h , in equation 3.2, is not a fluid property, rather an experimentally determined parameter whose value depends on factors influencing convection such as geometry, nature of fluid motion, and the properties and velocity of the fluid.

In the model, the convective heat transfer coefficient is utilized in convective boundary conditions for the ordinary differential equation based on the first law of thermodynamics which models interior air inside the cabin. Surfaces such as the windshield and roof, which are higher in temperature due to the solar radiation, heat the interior air via convective heat transfer.

In the model, convective heat transfer is also utilized when convective boundary conditions are applied to the heat diffusion equation on both sides of the surface. Consider the windshield as one of the surfaces being modeled in the system. Convective heat transfer is present on both sides of the windshield: on the exterior with outside ambient air; and on the interior of the cabin with interior air. The value of the convective heat transfer coefficient may be different for air flowing on the exterior and interior of the cabin. In this case, difference would be heavily influenced by the speed of the air.

3.7.9 Emissivity and Absorptivity

Emissivity is an effectiveness measurement for a material's surface to emit energy as thermal radiation. Absorptivity is an effectiveness measurement for a material's surface to absorb radiant energy. Values for emissivity and absorptivity range between 0 and 1, this value measures how closely a material's surface approximates a blackbody. A blackbody has both emissivity and absorptivity equal to 1 (Cengel, & Ghajar, 2015).

In the heat diffusion equation which models surfaces inside and around the cabin, emissivity and absorptivity values are used in the radiation boundary condition. Consider the windshield of a vehicle; radiation coming from the sun is transmitted, absorbed, and reflected. The amount of solar radiation absorbed by the windshield is related to the absorptivity factor of the material's surface. When the windshield heats up, it radiates its own energy based on the emissivity factor.

Kirchhoff's law of thermal radiation dictates that for an arbitrary body emitting and absorbing thermal radiation in thermodynamic equilibrium, the emissivity is equal to absorptivity. This may not hold true; firstly, because the analysis is transient and secondly, because Kirchhoff's law is true when incoming and outgoing radiation has similar wavelengths. Sunlight which is blackbody radiation at very high temperatures consists of mostly smaller wavelength radiation. When materials heat up, they produce their own infrared radiation; but it has a bigger wavelength due to very lower surface temperature.

3.7.10 Orientation/View Factor

Radiation heat transfer between two or more surfaces depends on the orientation of the surfaces relative to each other. If there are two infinitely long plates which are parallel to each other, view factor would be 1 as all the radiation leaving surface A would reach surface B. But if surfaces have different surface areas and if they are located at different angles, only part of radiation from one surface will reach the other surface. Consider 3 surfaces inside a cabin: the windshield, dashboard top surface, and passenger side glass window. Visually looking at the surfaces, it can be determined that part of the IR radiation generated by the windshield will go to the dashboard top surface and part of it will go the passenger side glass window.

$$A_1 F_{12} = A_2 F_{21} \qquad \text{Equation 3.9}$$

To take the orientation aspect into account, view factors are defined. View factor F is the fraction of radiation leaving surface A that strikes surface B directly. The equation above shows a reciprocity relation for view factors. View factors for some common geometries are available such as parallel plates, perpendicular plates, etc. If the areas of the plates are different, then the relation above can be used to find the relative view factor for the other surface. In the model, the surfaces are too complex to make these calculations by hand; a third-party software may be used to calculate view factors for each of the surface relative to other surfaces.

CHAPTER 4

MATLAB MODEL DEVELOPMENT

4.1 Use of MATLAB

MATLAB is used to model the transient equations of the vehicle cabin system. This software has built-in standard functions, but they are difficult to adapt to a specific scenario. For example, the built-in function which can solve for heat equation can only accept a fixed boundary condition. In the case of the vehicle cabin, the boundary condition such as the cabin air temperature is continuously changing. Thus, custom functions are made to solve the heat equations from scratch by discretizing the space, marching in time, and using LU – Lower Upper factorization to solve the system of equations in the matrix.

There are many other programs which allow transient heat transfer analysis without having to write the differential equations. TAITherm is one such software which allows complex 3D models to undergo steady state or transient analysis, but its complexity and long computation time does not allow for exhaustive analysis. TAITherm is also used by the automotive industry to simulate the heat up and transient cool down to design the air conditioning system.

TAITherm is used for verifying the MATLAB model. After a successful verification, the MATLAB model is then used for performing an extensive DFSS study for optimization.

4.2 Partial Differential Equation

When heat is introduced onto the surface via boundary conditions, it conducts/diffuses through the material. The equation derived from the same principle is often referred to as the heat conduction equation when considering a steady state scenario or a heat diffusion equation when considering a transient analysis.

Heat diffusion means conduction of heat varies in the space and changes with time. When heat is introduced at a surface, it diffuses from one end to the other in all three spaces. In the analysis, most of the surfaces such as the windshield, roof etc. are flat and have much higher lengths and widths as compared to the thicknesses. It is assumed that boundary conditions are consistent in the length and the width of the surface; thus, heat will only diffuse into the depth of the material. Due to this, space is only discretized in the thickness of the material.

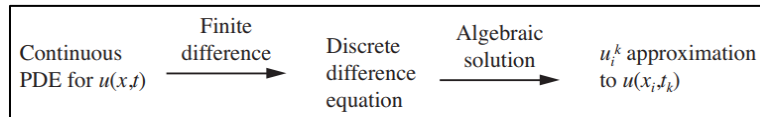
$$\frac{\partial T}{\partial t} = \alpha \left(\frac{\partial^2 T}{\partial x^2} \right)$$

$$u_t = \alpha u_{xx} \qquad \text{Equation 4.1}$$

The equation 4.1 above shows that the heat diffusion equation is partially dependent on time and partially dependent on space, but only in the x-axis, the thickness. It is assumed that there is no change in temperature with respect to change in space of the y-axis and z-axis.

4.2.1 Solution of Partial Differential Equation

Finite difference approximation is used to find solutions for the partial differential heat equation. The space in the x-axis can be discretized into “n” number of nodes. This results in “n” number of ordinary differential equations: one ordinary differential equation for each node, where differential of temperature is now only dependent on differential of time. Each of these ordinary differential equations can be marched forward in time. This results in a system of equations which can then be solved algebraically. Methodology of achieving a solution from partial differential equation as described above is illustrated below.



There are many methods of performing finite differencing. FTCS, abbreviated for forward time central space, method is conditionally stable. It uses forward differencing at time t_n to march in time and second order central differencing to discretize space. BTCS,

abbreviated for backward time central space, method is unconditionally stable. It uses backward differencing at time t_{n+1} to march in time and second order central differencing to discretize space. CN, abbreviated for Crank Nicolson, scheme is unconditionally stable. It uses central differencing at $t_{n+0.5}$ to march in time and second order central differencing to discretize space. In comparison, Crank Nicolson scheme is more accurate for smaller time steps, unconditionally stable for any size of time or space steps, but more numerically intensive.

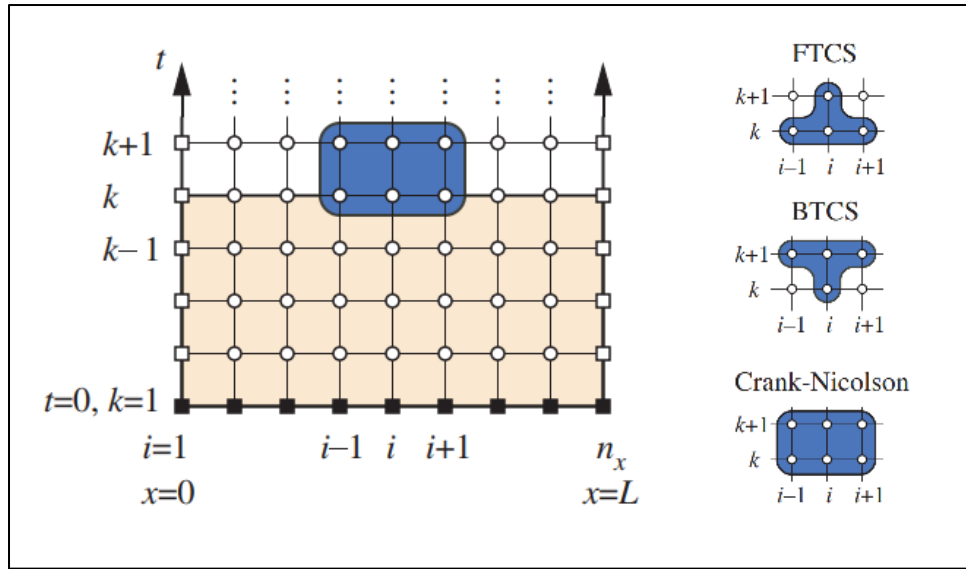


Figure 13: Visual representation of CN scheme

Figure 13 (Recktenwald, 2014) above illustrates space discretizing and time marching. The left side of the figure demonstrates space divided into 9 nodes shown horizontally starting from distance of zero at $i = 1$ to distance equal to the length of material thickness at $i = 9$. All these nodes then march forward in time shown vertically starting from time of 0 at $k = 1$. Time marches forward as much as necessary for transient analysis.

The right side of the figure shows the comparison between the three schemes. The very bottom row which is at $t = 0$ is the initial condition, which is known. Using these initial values, calculations are made to find the solution to the time step above it. The FTCS scheme uses the values from the 3 nodes at the previous time step to calculate the solution for the node in consideration. The BTCS scheme uses the value from a singular

node to calculate the solutions for 3 nodes in consideration which are in the next time step. The CN scheme uses values from 3 nodes at the previous time step to calculate the solutions for the 3 nodes in the next time step.

The FTCS scheme is easier to implement, but only conditionally stable. It is only stable when k/h^2 is less than or equal to half, where k is the time step Δt and h is the distance between the nodes Δx . The Solution for the BTCS scheme is complex but unconditionally stable. For the CN scheme, the solution is a bit more complex compared to BTCS, and like BTCS, its solution is also unconditionally stable. The CN scheme provides better time accuracy compared to the other two schemes. Only the CN scheme is used in calculations for partial differential equations of this model.

$$\frac{\partial u}{\partial t} = \alpha \frac{\partial^2 u}{\partial x^2}$$

$$\left. \frac{\partial u}{\partial t} \right|_{t_k, x_i} \approx \frac{u_i^{k+1} - u_i^k}{\Delta t}$$

$$\left. \frac{\partial^2 u}{\partial x^2} \right|_{t_k, x_i} \approx \theta \left[\frac{u_{i-1}^{k+1} - 2u_i^{k+1} + u_{i+1}^{k+1}}{\Delta x^2} \right] + (1 - \theta) \left[\frac{u_{i-1}^k - 2u_i^k + u_{i+1}^k}{\Delta x^2} \right]$$

$$\frac{u_i^{k+1} - u_i^k}{\Delta t} = \alpha \theta \left[\frac{u_{i-1}^{k+1} - 2u_i^{k+1} + u_{i+1}^{k+1}}{\Delta x^2} \right] + \alpha(1 - \theta) \left[\frac{u_{i-1}^k - 2u_i^k + u_{i+1}^k}{\Delta x^2} \right]$$

where $\left. \begin{array}{l} \theta = 0 \iff \text{FTCS} \\ 0 \leq \theta \leq 1 \\ \theta = 1 \iff \text{BTCS} \end{array} \right\}$

Figure 14: CN scheme applied to heat diffusion equation

Figure 14 (Recktenwald, 2014) above shows how the CN scheme is applied to the heat equation. The left side of the heat equation has the partial differential of temperature “u” dependent on the partial differential of time. The left side is evaluated by marching forward in time; going from time point of “k” to “k+1” in the elapsed time which is equal to Δt . The right side of the heat equation has the second order partial differential of temperature dependent on the second order partial differential of distance in x-axis. The right side is evaluated by performing central differencing around point “i” at both time

steps “k” and “k+1”. The CN scheme is utilized because central differencing is performed at both time steps, thus Θ is 0.5. If Θ was 0, the scheme would be purely FTCS as it would perform central differencing at the current time step and march forward in time, if Θ was 1, the scheme would be purely BTCS as it would march forward in time and perform central differencing at the next time step. Central differencing is found by calculating the temperature difference between the node “i-1” and “i”. In addition to the temperature difference between the node “i+1” and “i”, this central differencing term is then divided by the product of distances between two sets of nodes; in this case, the space in x-axis is discretized at a consistent distance between the nodes, thus Δx is the same between both sets of nodes.

$$\begin{aligned}
 &-\frac{\alpha}{2\Delta x^2}u_{i-1}^{k+1} + \left(\frac{1}{\Delta t} + \frac{\alpha}{\Delta x^2}\right)u_i^{k+1} - \frac{\alpha}{2\Delta x^2}u_{i+1}^{k+1} = \frac{\alpha}{2\Delta x^2}u_{i-1}^k + \left(\frac{1}{\Delta t} - \frac{\alpha}{\Delta x^2}\right)u_i^k + \frac{\alpha}{2\Delta x^2}u_{i+1}^k \\
 &\begin{bmatrix} a_1 & b_1 & 0 & 0 & 0 & 0 \\ c_2 & a_2 & b_2 & 0 & 0 & 0 \\ 0 & c_3 & a_3 & b_3 & 0 & 0 \\ 0 & 0 & \ddots & \ddots & \ddots & 0 \\ 0 & 0 & 0 & c_{n_x-1} & a_{n_x-1} & b_{n_x-1} \\ 0 & 0 & 0 & 0 & c_{n_x} & a_{n_x} \end{bmatrix} \begin{bmatrix} u_1^{k+1} \\ u_2^{k+1} \\ u_3^{k+1} \\ \vdots \\ u_{n_x-1}^{k+1} \\ u_{n_x}^{k+1} \end{bmatrix} = \begin{bmatrix} d_1 \\ d_2 \\ d_3 \\ \vdots \\ d_{n_x-1} \\ d_{n_x} \end{bmatrix} \\
 &: \\
 &a_i = 1/\Delta t + \alpha/\Delta x^2 = 1/\Delta t - (b_i + c_i) \\
 &b_i = c_i = -\alpha/(2\Delta x^2) \\
 &d_i = -c_i u_{i-1}^k + (1/\Delta t + b_i + c_i) u_i^k - b_i u_{i+1}^k
 \end{aligned}$$

Figure 15: System of equations for temperature at each node throughout thickness

Figure 15 (Recktenwald, 2014) above shows the equation which has been organized; temperatures from the next time step which are unknown are present on the left side of the equation, and temperatures from the current time step which are known are located on the right side of the equation. This equation is for a specific “i” value. Equations need to be written for $i=2, 3, 4 \dots N-1$. An equation does not need to be written for $i=1$ and $i=N$ because they are covered in the central differencing of $i=2$ and $i=N-1$ respectively. This will lead to a system of equations with N number of equations and N number of unknowns. This system of equations can be written in a matrix format such as

$[A][u] = [B]$; where matrix $[u]$ contains the unknown temperatures at the next time step. Looking at the structure of matrix $[A]$, it can be realized that it is a tridiagonal matrix, meaning there are three collections of numbers which run diagonal across the matrix: sub-diagonal, main-diagonal, and super-diagonal; the rest of the values outside these diagonal collections are all zero. The LU factorization method is then used to solve the system of equations.

All equations in the model are initial value problems. Temperatures of surfaces at the initial time of $t=0$ are known. The process explained in the previous paragraph is to march forward only in one time step. Starting from $k=0$, the temperature can be found for all nodes at time step $k=1$. The above process can be performed as many times as necessary depending on the total run time for transient analysis (Recktenwald, 2014).

4.2.2 Surface Layers

Each surface is made of multiple layers. Consider the roof as an example; it has a metal panel, air gap, polyurethane foam, and headliner fabric. Each heat equation models a single surface. If each equation was modeling a single layer, then the conduction boundary conditions would need to be applied, and in the case of the roof, 4 equations with boundary conditions would make up one surface. For simplicity, only one equation is used for all layers which make up a surface together. Thus, the coefficients a_n , b_n , and c_n in matrix $[A]$ need to use different diffusivity values depending on the nodes which may correspond to different layers.

Considering the seat surface as an example, it is composed of nylon fabric which is 2mm thick and fiberglass wool which is 48mm thick. If one divides the total thickness into 50 nodes, then for the first 2 nodes, a_n , b_n , and c_n coefficients in matrix $[A]$ will use diffusivity of nylon fabric to calculate its values, and for the last 48 nodes, a_n , b_n , and c_n coefficients will use diffusivity of fiberglass wool.

4.2.3 Types of Boundary Conditions

When solving a heat equation, boundary conditions take the environment around the surface into consideration. Figure 16 below shows an example surface which is modeling the roof. Solar radiation is coming from the sun and convective heat is incoming from the ambient air and leaving from the exterior surface of the roof, this heat then diffuses through the material. On the other side of the surface, convective heat is incoming from the cabin air and leaving from the interior surface of the roof, and IR radiation is incoming from other surfaces of the cabin and leaving the interior surface of the roof. Heat accumulated on the interior surface of the roof diffuses towards the exterior of the surface. These are various factors which either cause increase or decrease in the temperature. Solar radiation coming in from the sun will cause an increase in temperature; this would be considered a boundary condition for flux. Air surrounding the surface would either provide heat energy or take heat energy depending on positive or negative difference; this would be considered a boundary condition for convective heat. IR radiation generated by surfaces in the surrounding provides heat energy, but at the same time, the surface in question also emits radiation thus removing heat energy; this would be considered a boundary condition for radiation.

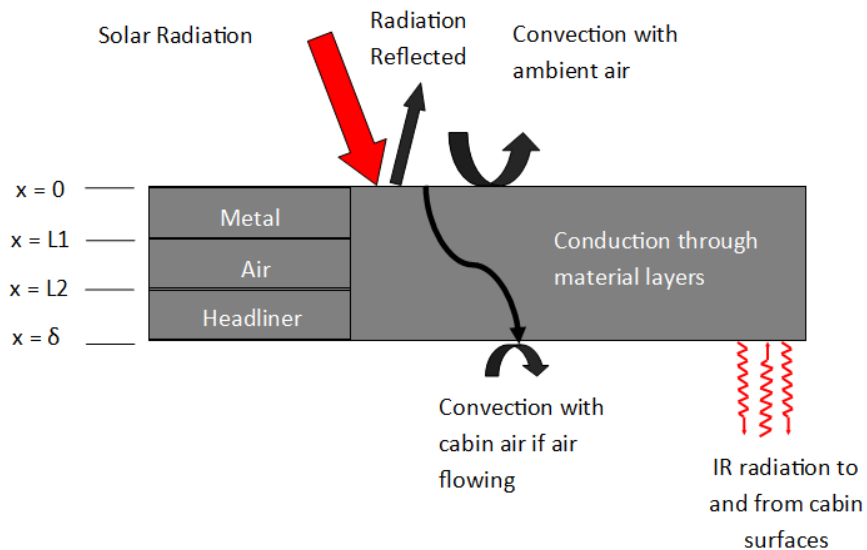


Figure 16: Breakdown of layers and boundary conditions for roof surface

There are three broad classes of boundary conditions which can be modified and used in the application: Dirichlet, Neuman, and Robin boundary conditions.

Dirichlet Boundary Condition: $u = g_1$ *Equation 4.2*

In the Dirichlet boundary condition, the value of the dependent variable is specified on the boundary. This means that a temperature value is assigned to the nodes at the boundary of the surface; this is useful in a case where it is known that one side of the surface will stay at a consistent temperature. In the model, there is no such case which requires a fixed temperature at the boundary of a surface. (Arendt, & Warma, 2003)

Neuman Boundary Condition: $\frac{\partial u}{\partial x} = g_2$ *Equation 4.3*

In the Neuman boundary condition, the normal derivative of the dependent variable is specified on the boundary. This means that a derivative value is assigned to all the nodes at the boundary; this is useful in a case when a consistent amount of energy is being added to the surface, such as solar radiation which will stay consistent regardless of the temperature of the surface being modeled (Arendt, & Warma, 2003).

Robin Boundary Condition: $a u + b \frac{\partial u}{\partial x} = g_3$

$$\frac{\partial u}{\partial x} = \frac{g_3}{b} - \frac{a u}{b}$$

$$\frac{\partial u}{\partial x} = g_o + h_o u$$
 Equation 4.4

The Robin boundary condition is often referred to as a boundary condition of the third type and uses Newton's law of cooling. The Robin boundary condition is a weighted combination of the Dirichlet and Neuman boundary condition. Thus, a linear combination of a dependent variable and a normal derivative of the dependent variable is specified on the boundary; this case is useful for convective heat transfer at the surface.

Only the Robin boundary condition structure is used in the model as it covers all aspects of the Neuman boundary condition. It is used in applying flux and convective boundary conditions at both ends of a surface.

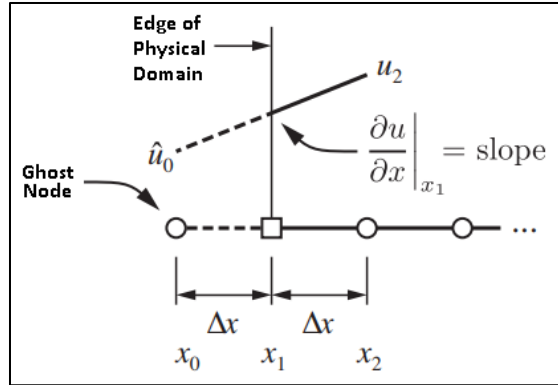


Figure 17: Introduction of ghost node to apply boundary condition

The structure of the Robin boundary condition has to be modified before it can be used with the CN scheme. As illustrated in the Figure 17 above (Recktenwald, 2014), a ghost node must be introduced on both sides of the surface. Considering the boundary on the left side, the ghost node is located outside the surface domain, and placed Δx to the left of the first node. The equations below show the derivation for the temperature of the ghost node. Central differencing is performed at first node x_1 . The equation is then rearranged for u_0 —the temperature of the ghost node. Values from flux, convective, and radiative heat transfer will be written in terms of g_o and $h_o u$.

$$\text{Robin Boundary Condition} \quad \frac{\partial u}{\partial x} = g_o + h_o u$$

$$\text{Central Differencing at node 1} \quad \frac{u_2 - u_0}{2 \Delta x} = g_o + h_o u$$

$$\text{Temperature of Ghost node} \quad u_0 = u_2 - 2 \Delta x (g_o + h_o u) \quad \text{Equation 4.5}$$

When central differencing is performed at the first node, it takes the temperature of the ghost node into the CN solution. If there was no boundary condition, then for CN scheme, central differencing would be performed for node numbers from $n = 2$ to $n = N - 1$; this is done since central differencing at $n=2$ calculates temperature difference between the two nodes on its either side. But if there is boundary condition, due to the addition of the ghost node, central differencing has to be performed for node numbers from $n = 1$ to $n = N$ to take g_o and $h_o u$ into the solution system.

When the CN scheme marches forward in time, the temperature value of the ghost node is calculated from the previous time step; but this is not what is desired. The ghost node temperature value is overwritten with the same temperature from the initial time step. The values of g_o and $h_o u$ at the ghost node are usually kept consistent as time progresses unless environment change needs to be simulated. For example, if, in the simulation, the ambient temperature of air, or the solar flux coming from the sun changes with time, then their time appropriated values can be imposed at the ghost node accordingly (Recktenwald, 2014).

4.2.4 Flux Boundary Condition

In the analysis, solar radiation is referred to as flux because of its constant value. Although the value of flux can change, such as between dawn and dusk when the Sun changes its position relative to the earth. The amount of flux is constantly changing with time, and possibly dependent on the density and cover of clouds, but it does not change based on the temperature of the surface. Since the value of solar radiation is independent of the surface temperature, it is referred to as a flux. Solar radiation flux can be measured using pyranometers. Nominal values for solar radiation flux range between $650\text{W}/\text{m}^2$ and $1200\text{W}/\text{m}^2$; for typical analysis, a value of $1000\text{W}/\text{m}^2$ is used. The boundary condition for such a typical case would appear as follows:

$$\frac{\partial u}{\partial x} = g_o = 1000 \text{ W}/\text{m}^2 \quad \text{Equation 4.6}$$

4.2.5 Convection Boundary Condition

Convective heat transfer is equal to $h A (T - T_\infty)$. Since the analysis is only in 1D and the length and width of the surface are assumed to be infinite, the boundary condition is considered as a rate of heat per area. If the convective heat transfer expression is expanded, there are two components. The first component is hT : convective heat transfer coefficient times the surface temperature; this is the amount of heat per area that leaves a surface and absorbed by the ambient air. The second component is $-hT_\infty$: convective heat transfer coefficient times the ambient air temperature; this is the amount of heat per area that leaves the ambient air and is absorbed by the surface. The first component, hT , is dependent on the surface temperature and thus, h is equal to h_o . The second component, $-hT_\infty$, is not dependent on the surface temperature and thus, the whole component can be treated as a flux. The difference between the two components determines the direction of net heat transfer. The convective boundary condition for such a case can be written as follows:

$$Q = h A (T - T_\infty)$$

$$Q/A = h T - h T_\infty$$

$$\frac{\partial u}{\partial x} = h_o u + g$$

$$\text{Where } h_o = h, \quad u = T, \quad g = -hT_\infty \qquad \text{Equation 4.7}$$

4.2.6 IR Radiation Boundary Condition

IR radiation should technically be treated as a robin boundary condition because the magnitude of radiative heat transfer has the unknown temperature term which is being solved for. But for simplicity, IR radiation is calculated outside of the boundary condition using temperature values from previous iteration and added as a flux using Dirichlet boundary condition. If enough iterations are performed, the result between two consecutive iterations will be same, at which point, the flux for IR radiation flux will be accurate.

4.2.7 Sample Heat Equation with Boundary Conditions

The application of the previously described boundary condition is illustrated below for two surfaces; the windshield and the top surface of the dash board. This application illustrates a sample scenario. The windshield and the dashboard cover different setups in the model. The windshield is located at the boundary of the model and is exposed to ambient air on one side and cabin air on the other; It receives direct solar radiation, some of which passes through depending on the transmissive property of the windshield glass. The windshield exchanges IR radiation with the top surface of the dashboard. The dashboard surface is divided into two virtual surfaces in the model. The example illustrated below only shows the boundary conditions for the top surface. The dashboard surface is exposed to interior cabin air on both sides. It receives IR radiation generated by the hot surface of the windshield and solar radiation from sun which transmits through the windshield. Some variables which are used in the sample boundary conditions are listed below:

Sample Heat Equation for Windshield

$$\frac{\partial T_{wd}}{\partial t} = \frac{k}{\rho c} \frac{\partial^2 T_{wd}}{\partial x^2} \quad \text{Equation 4.8}$$

Sample Left Boundary Conditions for Windshield

Left Boundary Condition @ x = 0

Solar RAD + exterior air CONV = COND

$$Q_{solar} + Q_{conv} = -\frac{dT_{wd}}{dx}$$

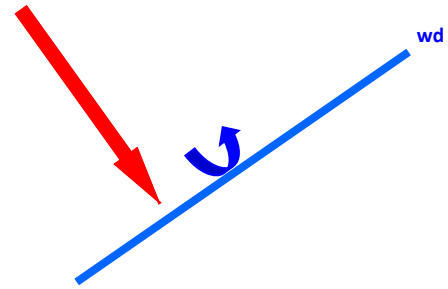
$$(load_{solar})\alpha_{wd} + h_{air}(T_{\infty} - T_{wd}) = -\frac{dT_{wd}}{dx}$$

$$load_{solar}\alpha_{wd} + h_{air}T_{\infty} - h_{air}T_{wd} = -\frac{dT_{wd}}{dx}$$

$$[load_{solar}\alpha_{wd} + h_{air}T_{\infty}] - [h_{air}T_{wd}] = -\frac{dT_{wd}}{dx}$$

$$[load_{solar}\alpha_{wd} + h_{air}T_{\infty}] - [h_{air}]T_{wd} = -\frac{dT_{wd}}{dx}$$

$$\frac{dT_{wd}}{dx} = [h_{air}]T_{wd} - [load_{solar}\alpha_{wd} + h_{air}T_{\infty}]$$



$$\frac{du}{dx} = hu + g$$

Where

$$u = T_{wdo}, \quad h = [h_{air}], \quad g = -[load_{solar}\alpha_{wd} + h_{air}T_{\infty}]$$

Sample Right Boundary Conditions for Windshield

Right Boundary Condition @ $x = \delta$

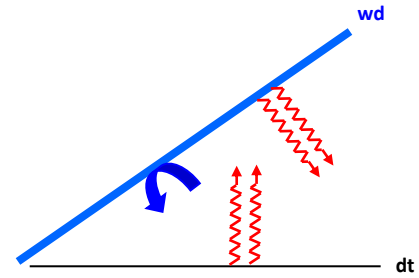
COND = interior air CONV + surface IR RAD

$$-\frac{dT_{wd}}{dx} = Q_{conv} + Q_{wd IR} - Q_{dt IR}$$

$$-\frac{dT_{wd}}{dx} = h_{air}(T_{wd} - T_{cair}) + Q_{net IR}$$

$$-\frac{dT_{wd}}{dx} = [h_{air}T_{wd}] - [h_{air}T_{cair} + Q_{wd IR}]$$

$$\frac{dT_{wd}}{dx} = -[h_{air}]T_{wd} + [h_{air}T_{cair} + Q_{net IR}]$$



$$\frac{du}{dx} = hu + g$$

Where

$$u = T_{wd\delta}, \quad h = -[h_{air}], \quad g = [h_{air}T_{cair} + Q_{net IR}]$$

Sample Heat Equation for Dashboard

$$\frac{\partial T_{dt}}{\partial t} = \frac{k}{\rho c} \frac{\partial^2 T_{dt}}{\partial x^2} \quad \text{Equation 4.9}$$

Sample Left Boundary Conditions for Dashboard Surface

Left Boundary Condition @ x = 0

Transmitted solar RAD + interior air CONV + surface IR RAD = COND

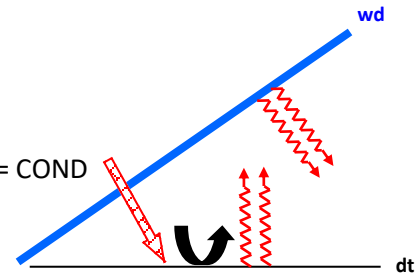
$$Q_{trans.solar} + Q_{conv} + Q_{wd IR} - Q_{dt IR} = - \frac{dT_{dt}}{dx}$$

$$(load_{solar} \tau_{wd}) \alpha_{dt} + h_{air} (T_{cair} - T_{dt}) + Q_{net IR} = - \frac{dT_{dt}}{dx}$$

$$load_{solar} \tau_{wd} \alpha_{dt} + h_{air} T_{cair} - h_{air} T_{dt} + Q_{net IR} = - \frac{dT_{wd}}{dx}$$

$$- [h_{air} T_{dt}] + [load_{solar} \tau_{wd} \alpha_{dt} + h_{air} T_{cair} + Q_{net IR}] = - \frac{dT_{dt}}{dx}$$

$$\frac{dT_{dt}}{dx} = [h_{air}] T_{dt} - [load_{solar} \tau_{wd} \alpha_{dt} + h_{air} T_{cair} + Q_{net IR}]$$



$$\frac{du}{dx} = hu + g$$

Where

$$u = T_{dto}, \quad h = [h_{air}], \quad g = -[load_{solar} \tau_{wd} \alpha_{dt} + Q_{net IR}]$$

Sample Right Boundary Conditions for Dashboard Surface

Right Boundary Condition @ $x = \delta$

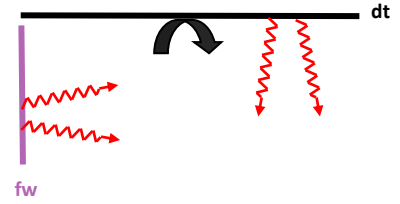
COND = interior air CONV + surface IR RAD

$$-\frac{dT_{dt}}{dx} = Q_{conv} + Q_{IR}$$

$$-\frac{dT_{dt}}{dx} = h_{air}(T_{dt} - T_{cair}) + Q_{net IR}$$

$$-\frac{dT_{dt}}{dx} = [h_{air}T_{dt}] - [h_{air}T_{cair} + Q_{net IR}]$$

$$\frac{dT_{dt}}{dx} = -[h_{air}]T_{dt} + [h_{air}T_{cair} + Q_{net IR}]$$



$$\frac{du}{dx} = hu + g$$

Where

$$u = T_{dt\delta}, \quad h = -[h_{air}], \quad g = [h_{air}T_{cair} + Q_{net IR}]$$

4.3 Ordinary Differential Equation

When heat is introduced into a material that is considered lumped, usually an ordinary differential equation can be used to determine the temperature of the material given that the heat input and output are known. In the model, cabin air is taken as a lumped mass. For materials such as aluminum, copper, or any other material with such high thermal diffusivity, heat transfers from one end of material to the other in a very short time. Thus, in a lumped mass, there is no need to discretize mass in space as the temperature diffuses from one boundary to another in a such a small fraction of time that all mass is practically at the same temperature.

Air does not have high diffusivity; thus, it can not be considered a lumped mass in a general situation. The Biot number is used to determine whether mass should be discretized into space or lumped all together. The Biot number is the ratio of heat transfer resistance through the mass to the heat transfer resistance at the surface. A ratio much smaller than 1 is considered thermally simple and does not require space to be discretized as the temperature diffuses at a very fast rate and stays consistent throughout space. Although air does not fall in this category, there are few factors such as density and buoyancy which cause air to behave in a different way when compared to conventional stationary masses.

Surfaces inside the cabin heat up due to incidental solar radiation. In return, these surfaces heat up the cabin air via convective heat transfer. As the air gets hotter, its density changes locally and it becomes lighter. Air around the surface which is lighter will rise above the heavier air. Due to the gravitational field, there is a net force which pushes the lighter, hot air upwards through the heavier air, this force is called buoyancy force. This overall movement of air is called the natural convection current. This movement sets the mass of air apart from other masses. By this movement, air is consistently moving and mixing. It is important to note that in the absence of air movement, there would not be any convective heat transfer. If air was still and immobile, then there would only be conduction between the surface and the air. In an immobile scenario, it would not be accurate to model the air as a lumped mass (Bahrami, n.d.).

Since there is air movement which causes continuous flow, air is modeled as a lumped mass. This drastically simplifies the differential equation to a simple energy balance. The difference between the incoming energy and outgoing energy results in the increase of the cabin air temperature.

$$\sum Q_{in} - Q_{out} = m C \frac{\partial T}{\partial t} \quad \text{Equation 4.10}$$

According to the equation above which is based on the first law of thermodynamics, the sum of the incoming heat from various surfaces around the cabin minus the sum of the heat outgoing from air to the surfaces equals the product of mass of air, specific heat capacity of air, and difference in temperature of air with respect to difference of time. This equation represents the energy balance of the cabin air. If incoming heat is more than the leaving heat, then temperature of cabin air will rise.

This equation is solved using built-in MATLAB functions such as ode45. In this equation, the differential of temperature is only dependent on the differential of time; thus, it is a simple ordinary differential equation. MATLAB has a wide variety of solvers dedicated to solving ordinary differential equations of which ode45 is just one. Different solvers require different amount of computing resources to provide different levels of accuracy. Each of these solvers automatically determine the time step used for marching forward in time to achieve a balance between speed of calculation and accuracy. As these solvers do not allow the user to pick a time step manually, the output solution from the solver will have different Δt steps. Thus, interpolation is used to generate temperatures at time steps which are consistent with the solution of partial differential heat equation. Having temperatures of all surfaces and cabin air at consistent time steps allows for easier coupling of all partial and ordinary differential equations.

Sample Energy Balance for Interior Cabin Air

$$mc \frac{dT}{dt} = h_{\text{c}air} A_{wd} (T_{wd\delta} - T) + h_{\text{c}air} A_{dt} (T_{dto} - T) + h_{\text{c}air} A_{fw} (T_{fw\delta} - T) + \dots \text{other surfaces} \quad \text{Equation 4.11}$$

The term on the left side is the amount of total net energy that cabin air gains in each time step. The terms on the right are convective heat transfer terms from each of the surface surrounding the cabin air which causes the heat to either come in or leave the cabin air. All surfaces do not heat up at the same rate, e.g. the top surface of the dashboard will heat up much faster than the front fascia of the dashboard due to the difference in the incident solar radiation; there will be cases wherein cabin air temperature will gain heat from the top surface of the dashboard and will lose heat to the front of the dashboard surface.

4.4 View Factors and The Greenhouse Effect

Radiation is one of the main components in this model. There are two types of radiation: solar and infrared. Solar radiation is treated as a flux and it is independent of the temperature of the incident surface. Solar radiation makes up the majority of the heat coming into the system, whereas IR radiation is emitted from a surface only when the surface gets higher in temperature due to the incident solar radiation.

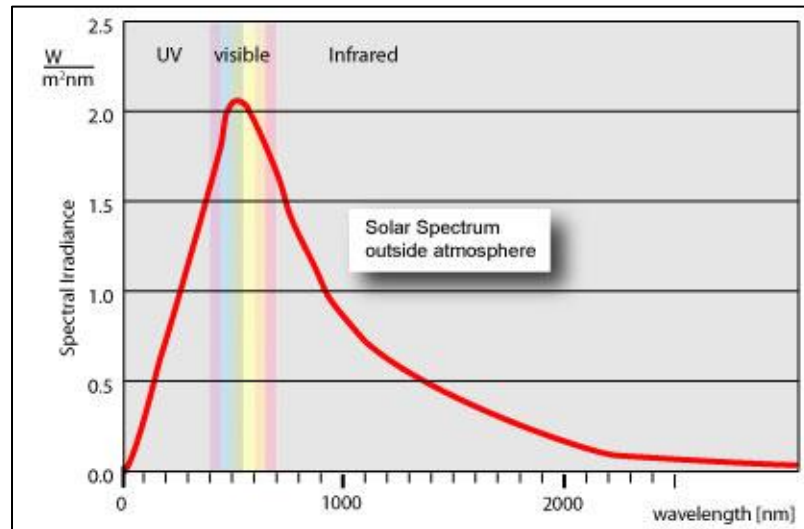


Figure 18: Spectrum of solar radiation

Within the electromagnetic spectrum, solar radiation spans a wide range, including three different classes: ultra violet, visible, and infrared. As seen in the Figure 18 above (Green Rhino Energy, 2016), the peak of solar radiation falls in the visible region of the spectrum. Ultraviolet, visible, and infrared radiation differ from each other

based on their wavelength. Within the thermal spectrum of the electromagnetic range, shorter wavelengths have higher energy. Since ultraviolet rays have a much shorter wavelength than infrared rays, this gives them higher energy. The surface temperature of the sun is around 5500°F; thus, its radiation peaks around 0.5 μm of wavelength which is falls in the visible spectrum. When broken down, roughly 5% falls in the ultraviolet range, 45% in the visible range, and 50% in the near infrared range. Infrared covers a very wide range; thus, it is divided into near-infrared and infrared. Near-infrared rays have wavelengths very close to visible rays, but they are not visible. The solar radiation that makes it to the earth's surface after passing through the ozone layer and the atmosphere is largely visible rays.

Any material above the temperature of absolute zero emits IR radiation. When surfaces located inside the cabin are exposed to the solar radiation, they absorb a percentage of this heat and start emitting radiation of their own. There is a vast difference between radiation emitted from the sun and the surface inside the vehicle cabin. The source temperature of the surface inside the vehicle cabin is miniscule compared to the surface temperature of the sun; thus, the emitted radiation from surfaces in the vehicle cabin fall in the very high wavelength region of infrared rays.

Since IR radiation cannot pass through most transparent glasses, vehicle cabin systems exhibit the greenhouse effect. Solar radiation which mostly falls in the visible range of the spectrum has higher energy content and it can transmit through the transparent surfaces at the boundary of the cabin such as the windshield, and rear and side windows. IR radiation generated by the vehicle cabin surfaces is not able to transmit through any of the surfaces located at the boundary of the system. Due to such an arrangement, solar radiation is able to get into the system, but infrared radiation is not able to exit the system. This is the reason why, on a hot and clear sunny day, the interior cabin air and surfaces are much hotter than the outside temperatures. IR radiation generated by surfaces inside the cabin do however heat other surfaces within the cabin. Radiation generated by interior surfaces is divided based on view factors and applied to the recipient surfaces. The surfaces which receive a lot of solar radiation such as the top surface of the dashboard heat up other surfaces across the cabin via IR radiation.

4.5 Coupling and Iterations

Each of the partial differential and ordinary differential equations which are initial value problems depend on each other. These equations cannot be solved in a conventional sense, as some of the dependent variables are unknown until all equations have been solved. Take the windshield and the cabin air for example: The boundary condition for the windshield heat equation requires the temperature of cabin air at the next time step, which is unknown until the cabin air ordinary differential equation has been solved. On the other hand, the cabin air ordinary differential equation requires the temperature of windshield at the next time step, which is unknown until the windshield heat equation is solved.

Thus, the unknown temperatures must be guessed before solving the equations. In this model, the guessed value is the initial value. The solution to the two uncoupled equations generated after solving all the equations for the first time would lie between the initial value and the accurate solution; this process is the first iteration of the solution. All equations are solved again, but this time, the guess is the results from the first iteration rather than the initial value. The process of using the results from previous iteration to substitute for unknown temperatures couples all of the equations. The solution is iterated until there is very little difference left between the unknown temperatures among the two consecutive iterations. Once two consecutive iterations yield the same results, this demonstrates that the solution in the previous iteration was already the accurate solution. In this model, it takes between 15 and 30 iterations to achieve an accurate solution.

4.6 Output of the Model

After each iteration of the ordinary differential equation and multiple partial differential equations, the model outputs temperatures. Solution to the ordinary differential equation yields the cabin air temperature. The cabin air temperature values are available for each time step. The solution for each of the partial differential equations yields the temperature for materials located in and around the cabin system boundary. Material temperature values are available at different thicknesses for each time step.

Temperature values are the basic outputs of this model; these can not easily be used for making comparisons among different material and thickness selections. It is possible that changing one material causes lower temperature in that material but unintentionally increases the temperature of another material. An easier approach is to compare the amount of heat that the whole system is entrapping. At each time step, the net temperature difference from a reference initial temperature multiplied by mass and specific heat capacity yields the amount of additional heat that was entrapped in the material. If this heat is plotted with time, the area under the curve is the additional energy that has entered the system in the given time span.

The following charts are outputs of this model. The values used in this simulation are representative of a generic sedan-sized vehicle. In Figures 19 and 20, the cabin system is exposed to an exterior air temperature of 43°C and solar radiation of 1000 W/m². The initial temperature for cabin air and all materials in the system at time of zero have a temperature of 20°C. These figures show temperature profiles at the first and final iterations. The multiple lines in the subplots are temperature profiles at different thicknesses; the profile with the higher temperature is the one exposed to solar radiation or hotter, exterior air; as opposed to the profile with the lower temperature which is the interior side of the material. The temperature gap between profiles is very large in the first iteration as compared to the last iteration. This is due to the fact that the guesses used for the unknown values in the first iteration are initial value temperatures; thus, the surface side which is not exposed to solar radiation is not experiencing any heat transfer because the temperature difference is zero, and the temperature at the unexposed side is only rising due to the conduction from the exposed side of the surface. Guesses for the unknown values get more accurate as iterations progress. Thus, later iterations have a lower temperature gap between the two sides of the surface as they are using guesses for unknown values which are not initial value temperatures, but values that are closer to the accurate temperatures.

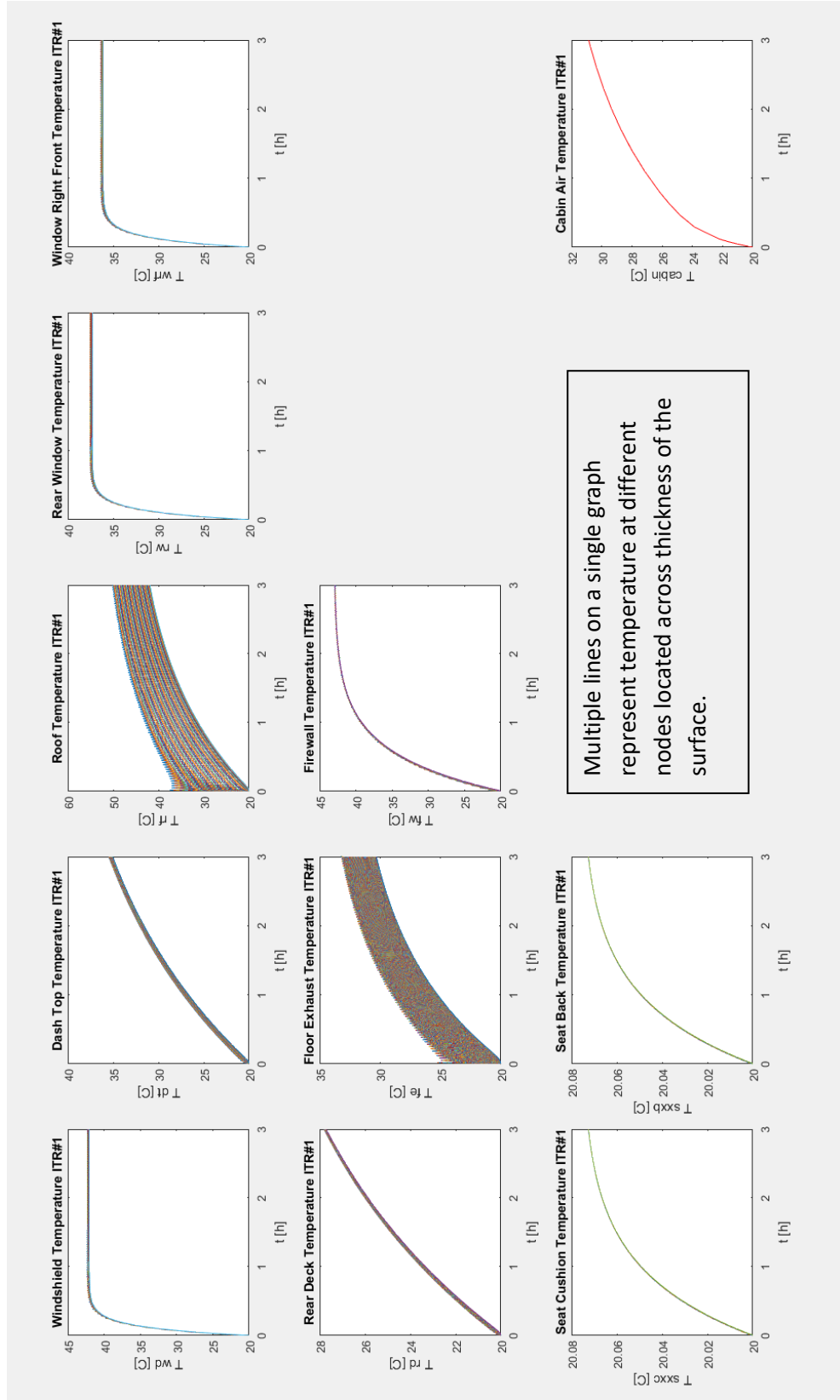


Figure 19: Temperature profile from 1st iteration of MATLAB simulation

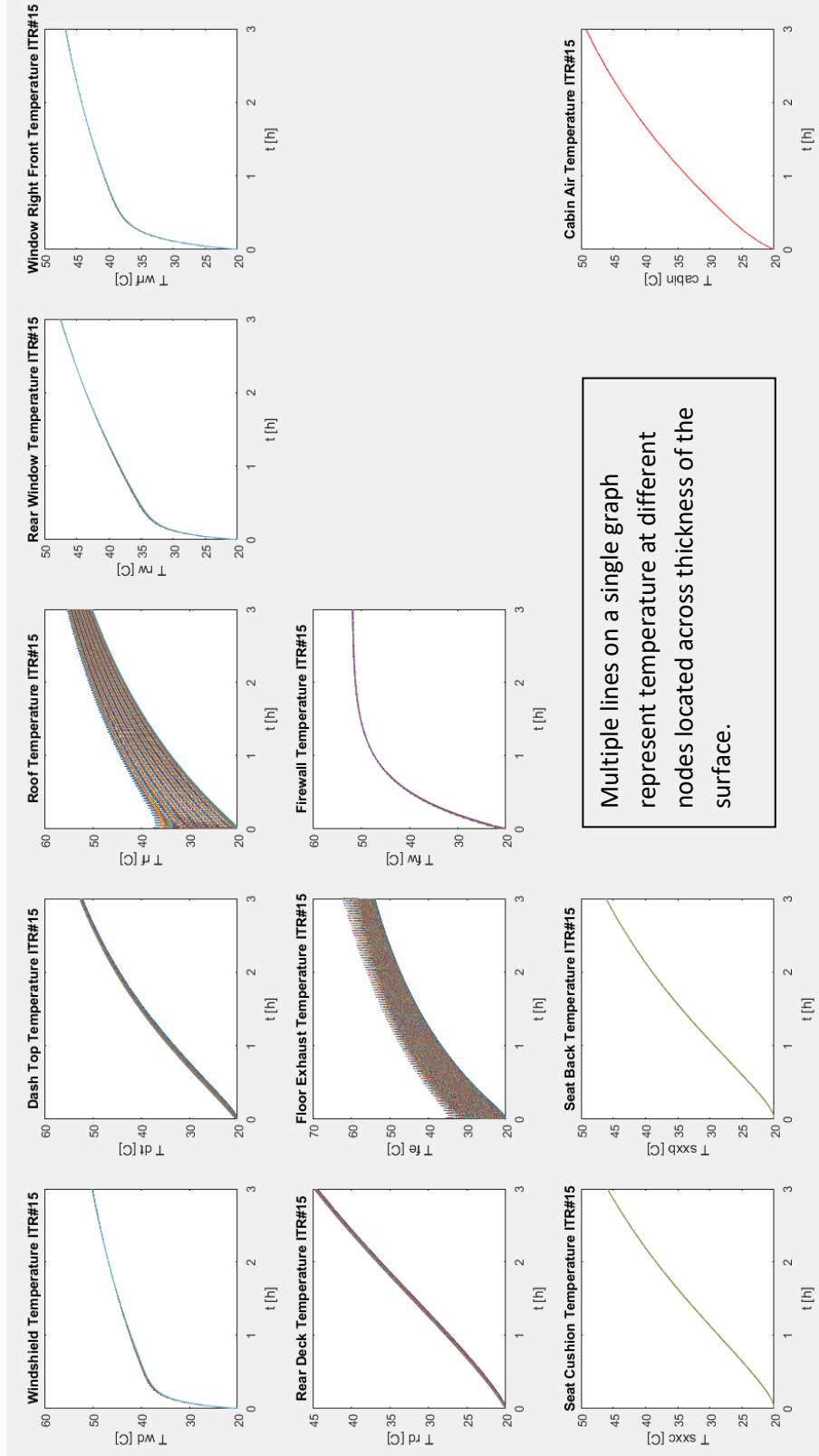


Figure 20: Temperature profile from 15th and final iteration of MATLAB simulation

It can be seen that the temperature curves in Figure 19 and Figure 20 follow one of three shapes. The first shape is quite evident in the windshield temperature curve, located in the upper left graph; it can be divided into two parts, the first part where the temperature increases rapidly at a much faster rate, and second part where temperature increases at a much slower rate. If the windshield temperature is considered from the first iteration, the first part is similar to where the temperature increases rapidly at a fast rate, but the second part is different from the final iteration, as there is no increase in temperature, the temperature has reached its maximum limit and is at a steady state. In the final iteration however, the second part is not at steady state, rather the temperature is increasing at a very low rate due to an increase in cabin air temperature. This shape of the curve can also be seen on other glass surfaces which are located at the boundary of the cabin. The surfaces which exhibit this shape are highly dependent on solar radiation and exterior air temperature.

The second shape is quite evident in the dashtop temperature curve, located in the top row second graph. The rate of temperature increase is comparatively constant. This shape can also be seen on other surfaces which are located inside the cabin, such as the rear deck at seat surfaces. The surfaces which exhibit this shape are highly dependent on transmitted solar radiation and interior air temperature.

The third shape is evident in the roof temperature curve, located in the top row third graph. The characteristics of the curves are different depending on which side of the surface is being considered. Since the roof is heavily insulated, the temperature curve of the metal surface located on the outside of the vehicle is different from the temperature curve of the interior headliner surface located on the inside of the cabin. This shape can also be seen in the floor temperature curves. The surfaces which exhibit this shape have many material layers with different properties which are designed to provide insulation.

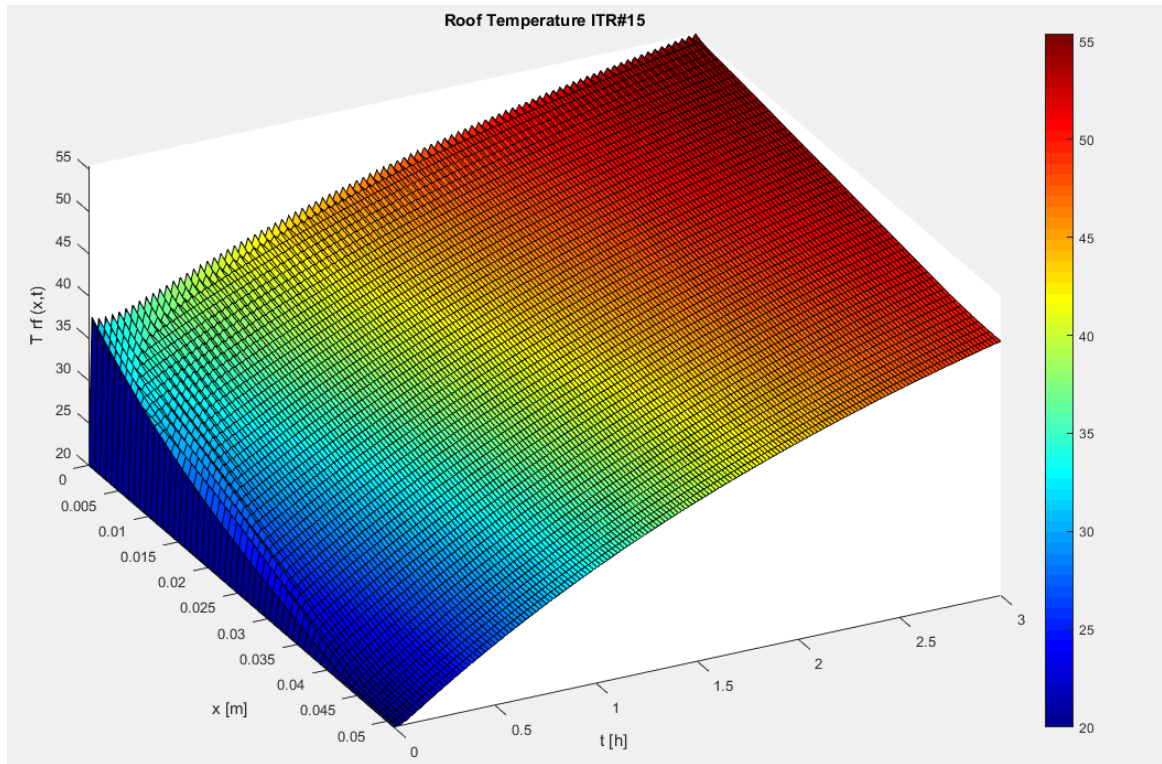


Figure 21: Temperature of Roof plotted across surface thickness and time

Figure 21 shows the temperature profile of the roof over time and material thickness. The chart has a total of 3 axes; the x-axis represents time in hours; the y-axis represents the thickness of the material spanning 8mm divided into 110 nodes; and the z-axis represents temperatures of material at each time step and each node. At the end of the 3-hour simulation, the surface exposed to the solar radiation is at a temperature of 55°C and the surface which is only exposed to cabin air on the opposite side of the material is at a temperature of 50°C.

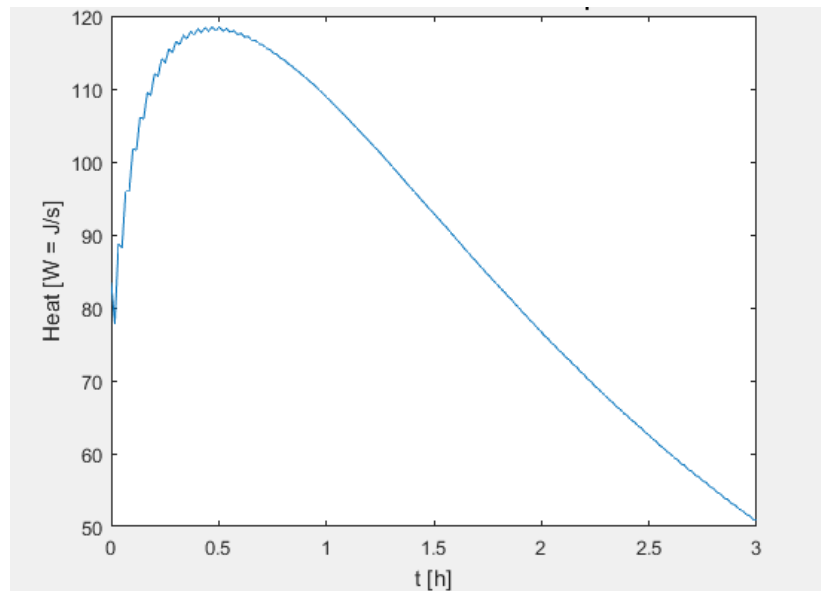


Figure 22: Heat accumulation inside dashboard surface

Figure 22 shows the heat curve for the dashboard material. Heat is plotted in the unit of watts across 3 hours. This chart shows the amount of net heat coming into the material. At time of zero, the amount of heat coming into the material spikes due to the exposure of solar radiation. As time progresses, the temperature of the material rises, and then it starts losing heat to the surrounding cabin air. Towards the end of the time period, net heat coming into the material is still positive, but much lower compared to the start of time period. This can also be seen in the Figure 21 on the last page; the temperature rises at a faster rate for the first half hour, then it rises at a much lower rate. The area underneath this heat curve in Figure 22 is 320.846 kJ which would be the total amount of additional heat entrapped in the roof material for the duration of 3 hours. This amount can also be represented as 89.129 W of energy averaged over a 3-hour period.

CHAPTER 5

MATLAB MODEL VERIFICATION

TAITherm is used to verify the model developed in MATLAB. TAITherm is time proven and used across the automotive industry for heat transfer analysis. It has a graphical interface which allows the user to create 3D objects or import previously meshed geometry. There is a vast library of thermal properties which can be applied to the object and new custom properties can be created.

TAITherm is an excellent choice to verify the model developed in MATLAB since it has been developed by engineers who are professionals in heat transfer, and it specializes in the automotive application. FCA group also uses this software and has created various models of their vehicles which help them determine the size their AC system and predict the surface and air temperatures after a cool down from extremely hot conditions.

Since the MATLAB model was developed from scratch, multiple partial verifications were performed to test the progress. The model was developed in stages; the first milestone was to model a single layer surface with a convective heat transfer with a fixed air temperature. There are many third-party proprietary software programs which can solve such a simple scenario with ease. EES software, which stands for Engineering Equation Solver, was used as a reference to make sure that the heat equation modeled in MATLAB was responding accordingly. The second milestone was to model the air. This was tested against an example model available in the MATLAB Simulink extension. The example Simulink model was used as a reference to check if the air modeled in MATLAB was behaving as it was supposed to. The next milestone was to couple each of the surfaces and the air. The exterior ambient air causes the surfaces at the boundary of the cabin to increase in temperature, and the solar radiation causes all exposed surfaces to increase in temperature. The cabin air increases in temperature via free convection with surfaces. The cabin air also acts as an equalizer as it takes heat from surfaces which are much hotter and loses heat to the surfaces which are relatively colder. After the model was completely developed, a final verification was performed.

5.1 Final Verification

Specification from a Fiat 500L were used to verify the final version of the MATLAB model. Fiat 500L model already existed in the TAItherm which had previously been created and validated by FCA engineers. Thermal properties were extracted from the TAItherm model to recreate the same simulation conditions in the MATLAB.

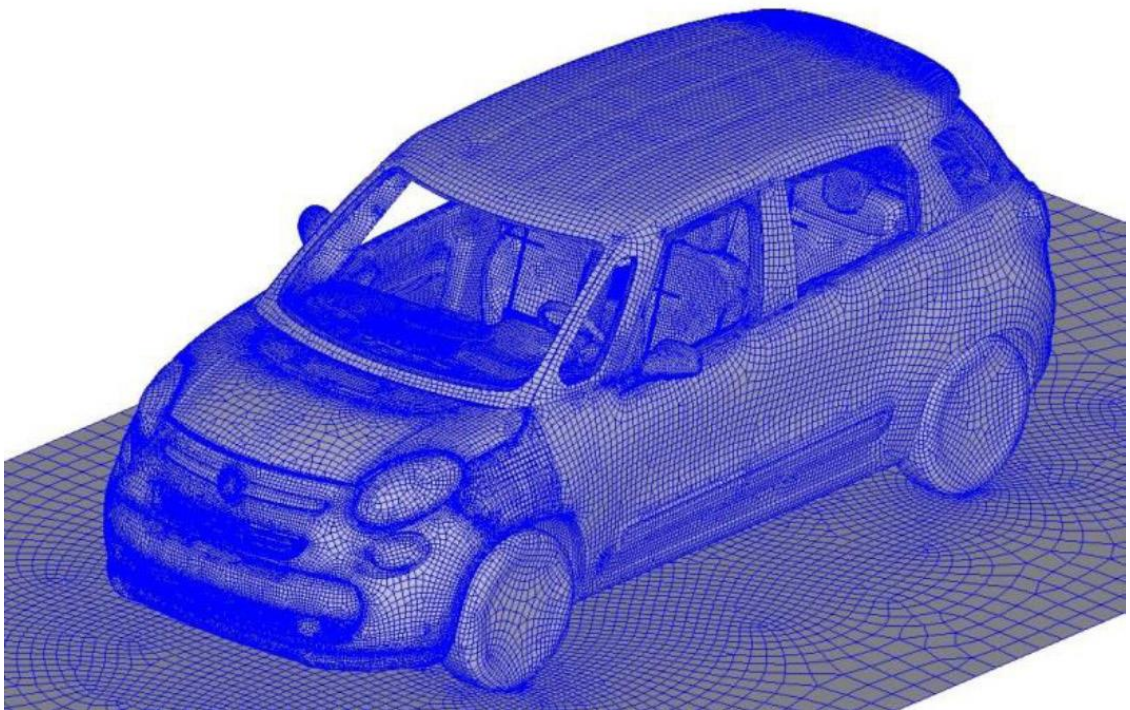


Figure 23: Exterior view of Fiat 500L modeled in TAItherm

Figure 23 (Piovano et al., 2016) above shows a meshed 3D model of the Fiat 500L in TAItherm. Figure 24 (Piovano et al., 2016) below shows the interior of the model. It can be seen that the model is very detailed. The vehicle is structured with shell elements, but it has multilayer properties to represent all the material layers present in the real vehicle.

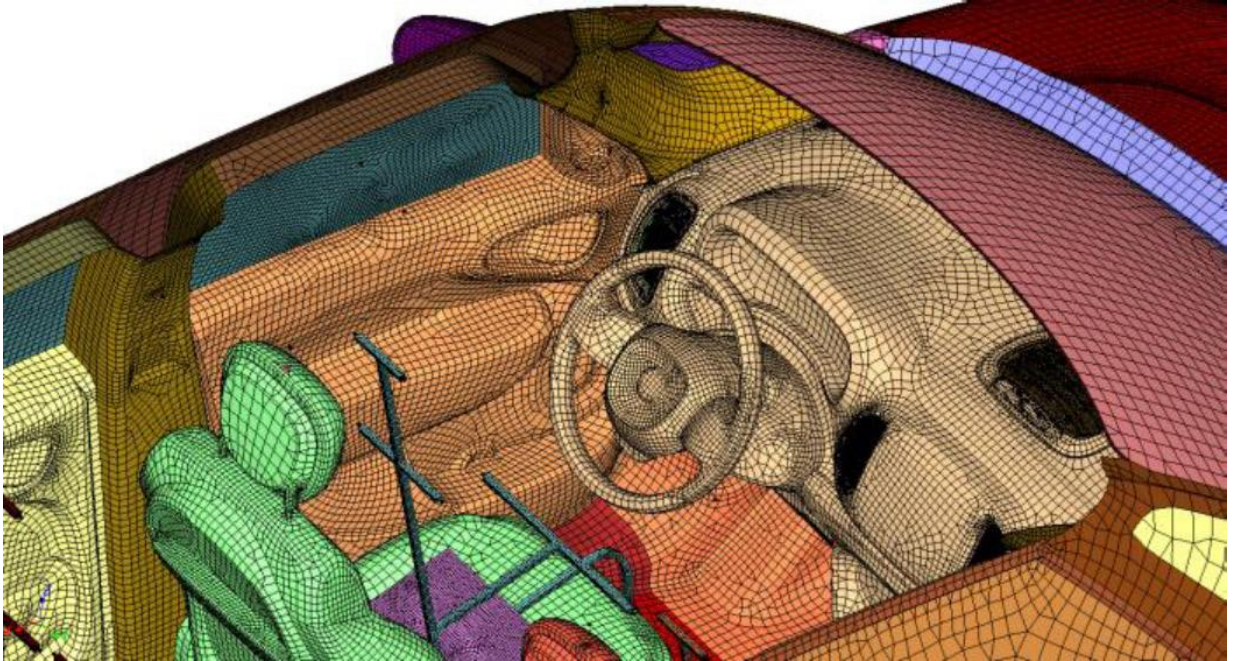


Figure 24: Interior view of Fiat 500LTAItherm model

5.1.1 Model Similarities and Differences

The MATLAB model previously presented in Chapter 4 has the same objective as the Fiat 500L model in TAItherm. Both are simulating the same vehicle dimensions, environmental conditions, and thermal properties; but there are still many differences which set both models apart. The MATLAB simulation offers some clear advantages because it has been developed for a specific application. The TAItherm simulation on the other hand is a generic software which requires a lot of effort to setup a specific scenario.

The MATLAB model has a very small setup time. For example, if an engineer was to run a simulation on a new vehicle, it would only take a few hours to input all the parameters in a single file which contains everything from vehicle dimensions to thermal properties. Performing a similar simulation in that new vehicle, it would take few days to import CAD model to a third-party software, create a mesh to make shell elements, import to TAItherm, create thermal links between surfaces, and apply environmental and thermal properties.

MATLAB also has a very small simulation run time since it is not a 3D model. The MATLAB model only has one dimensional space, which is the thickness of the material. The length and width of the material are assumed to be infinite in the differential equations. The area of the surface and the view factors give this model partial second and third dimensions.

Some similarities between the two models are as follows:

- Vehicle dimensions, environmental conditions, and thermal properties
- Interior air modeled as a single fluid node rather than a mesh

Some differences between the two models are as follows:

- The TAItherm model uses three dimensions for computation of material temperatures as opposed to the MATLAB model which uses one dimension
- TAItherm models every single surface whether exterior or interior down to air ducts behind the dashboard panel. MATLAB only models select surfaces located at the boundary and on the inside.

5.1.2 Model Environment

Environmental conditions of the models are as follows:

- Ambient air around the vehicle has an assigned temperature of 43°C. External ambient air is able to lose or gain energy from the cabin but its temperature does not decrease or increase from the transfer of energy.
- Cabin air inside the vehicle cabin and surfaces located in and around the vehicle cabin have an initial temperature of 20°C. Cabin air and all of the cabin surfaces are modeled with equations and thus their temperature changes with time.
- In TAItherm, solar radiation is modeled as if it is coming from a solar lamp board. Thus, the solar load is higher at the centre of the vehicle. Solar radiation is fixed at an intensity of 1000 W/m² at a central node on the roof.

5.1.3 Thermal Properties

Table 2 lists the surfaces which are being modeled in the system along with their corresponding surface area and convective heat transfer coefficients for the left and right boundary conditions.

Table 2: Surface areas and heat transfer coefficient

| Surface | Area | LBC | RBC |
|-------------------|-------------------|----------------------|----------------------|
| | [m ²] | [W/m ² K] | [W/m ² K] |
| Windshield | 0.92 | 12.5 | 5 |
| Dash | 1.83 | 5 | 1 |
| Roof | 2.99 | 10.3 | 5 |
| Rear Window | 0.38 | 8.6 | 5 |
| Rear Deck | 0.59 | 5 | 0 |
| Underbody | 3.06 | 6.7 | 5 |
| Firewall | 1.15 | 8 | 0 |
| Side Windows (x6) | 1.35 | 8.6 | 5 |
| Front Seats (x1) | 1.89 | 5 | 0 |
| Rear Seat (x1) | 1.81 | 5 | 0 |

Table A1 in the appendix lists all the materials used in the model and their respective thermal properties such as conductivity, density, specific heat, and diffusivity. Table A2 in the appendix lists different types of glass and their reflectivity and transmissivity. Table A3 in the appendix lists different surface conditions and their absorptivity and emissivity. Table A4 in the appendix lists view factors for all surfaces with respect to every other surface; for example, the view factor from the windshield to the dashboard is 0.35 and the view factor from the dashboard to the windshield is 0.52. These view factors have surface areas already factored in.

Table 3 on the next page lists the number of layers for each surface, and its corresponding material, thickness, and surface condition. Surface condition is only available for the first and last layer. Some surfaces have air gaps; these air gaps are modeled just like any other material: with the heat diffusion equation. No convection is considered for these air gaps as they are not large enough to generate air flow.

Table 3: Surface layers, materials, thicknesses, and conditions

| Surface | Variables | Layer 1 | Layer 2 | Layer 3 | Layer 4 | Layer 5 | Layer 6 | Layer 7 |
|------------------|-------------------|----------------------------|-----------------|-------------------|-----------------|-------------------|--------------|-----------------|
| Windshield | Material | Glass Conventional | | | | | | |
| | Thickness [m] | 0.0046 | | | | | | |
| | Surface Condition | Glass Window | | | | | | |
| Dash | Material | Polypropylene | Polypropylene | Air | Polypropylene | | | |
| | Thickness [m] | 0.0035 | 0.0025 | 0.002 | 0.003 | | | |
| | Surface Condition | Default Surface | - | - | Default Surface | | | |
| Roof | Material | Steel Mild | Air | Steel Mild | Air | Polyurethane | ABS | Cotton |
| | Thickness [m] | 0.0003 | 0.0386 | 0.0003 | 0.002 | 0.007 | 0.002 | 0.001 |
| | Surface Condition | Paint White | - | - | - | - | - | Default Surface |
| Rear Window | Material | Glass Conventional | | | | | | |
| | Thickness [m] | 0.0038 | | | | | | |
| | Surface Condition | Glass Window | | | | | | |
| Rear Deck | Material | Woodstock | Air | Woodstock | | | | |
| | Thickness [m] | 0.0037 | 0.0093 | 0.001 | | | | |
| | Surface Condition | Plastic Black Polyurethane | | Default Surface | | | | |
| Underbody | Material | Steel Mild | Air | Steel Mild | Air | Polyurethane Foam | Polyurethane | Carpet 16oz |
| | Thickness [m] | 0.0004 | 0.01946 | 0.0004 | 0.002 | 0.02 | 0.003 | 0.001 |
| | Surface Condition | Steel Oxidized | - | - | - | - | - | Fiberglass Dark |
| Firewall | Material | Aluminum | TNT | | | | | |
| | Thickness [m] | 0.0003 | 0.01 | | | | | |
| | Surface Condition | Aluminum Galvanized | Paint Black | | | | | |
| Side Windows(x6) | Material | Glass Conventional | | | | | | |
| | Thickness [m] | 0.0038 | | | | | | |
| | Surface Condition | Glass Window | | | | | | |
| Front Seats(x4) | Material | Nylon Bonded | Fiberglass Wool | | | | | |
| | Thickness [m] | 0.003 | 0.0065 | | | | | |
| | Surface Condition | Default Surface | Fiberglass Dark | | | | | |
| Rear Seat(x1) | Material | Nylon Bonded | Fiberglass Wool | Steel Mild | | | | |
| | Thickness [m] | 0.003 | 0.0065 | 0.002 | | | | |
| | Surface Condition | Default Surface | - | Steel As Received | | | | |

5.1.4 Results and Comparison

Table 4: Temperatures at the end of 3-hour soak

| Part | Temp | Temp | Temp |
|---------------|--------|----------|------------|
| | (°C) | (°C) | (°C) |
| | MATLAB | TAItherm | Difference |
| Interior Air | 44.45 | 44.54 | 0.1 |
| Windshield | 47.80 | 46.31 | 1.5 |
| Dash | 48.36 | 52.54 | 4.2 |
| Roof | 50.77 | 46.11 | 4.7 |
| Rear Windows | 45.13 | 40.64 | 4.5 |
| Under Body | 38.46 | 38.98 | 0.5 |
| Firewall | 43.05 | 45.05 | 2.0 |
| Front Windows | 45.01 | 39.91 | 5.1 |
| Seats | 42.14 | 43.12 | 1.0 |

Table 4 and Figure 25 show the temperatures from both simulations at the end of a 3-hour soak. Some temperatures are very accurate, whereas others have a marginal difference; all within 5 degrees.

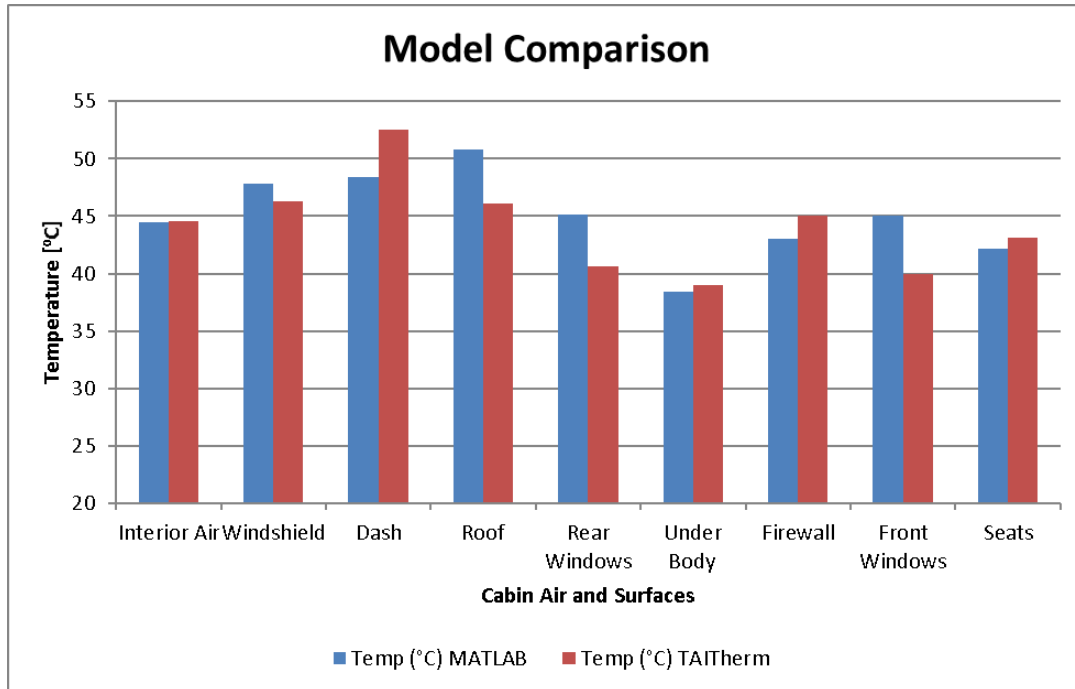


Figure 25: Temperature comparison between two models at the end of 3-hour soak

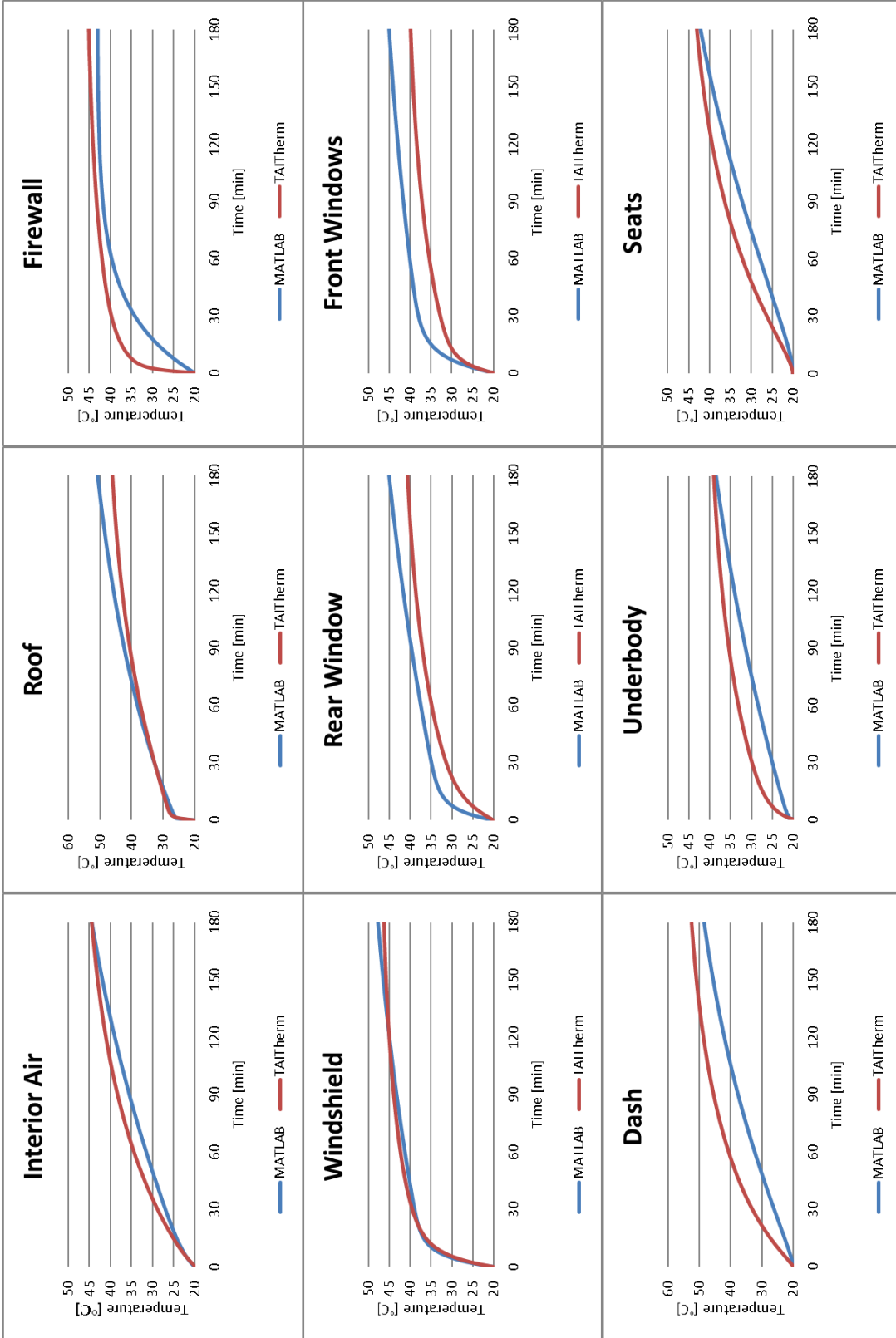


Figure 26: Temperature profile comparison for both models

Figure 26 on the previous page shows the temperature profile from both simulations with respect to time. The General shape of the curve is similar for each respective temperature subplot. Both models share the exact same thermal properties. The major difference in setup is that TAItherm is considering a complete 3D model, whereas MATLAB is only a 1D model. The MATLAB model compensates for the other two dimensions by incorporating surface areas and view factors to give it a 3D functionality.

For some surfaces, temperature is overpredicted and for some it is underpredicted. This difference may be due to the fact that conduction between two adjacent components is not considered in the MATLAB model. For example, there is no conduction heat transfer modeled between the dashboard and frame of the vehicle or the A pillars. Nonetheless, it can be seen that both models are comparable. The MATLAB model does however capture the correct behaviour of the temperature curves.

For rear and front side window, the difference is 4.5°C and 5.1°C respectively, but the behaviour of the curves is identical. For the firewall, underbody, dashboard, and seat temperatures, temperatures curves from MATLAB model have a slower rate of increase. This difference may be caused by the aforementioned reasons: the fact that TAItherm is based on a 3D model and TAItherm models items such as the hood, rims, tires etc. which are not modeled in the MATLAB model. For interior air, roof, and windshield temperatures, the temperature curves are nearly identical.

For the purposes of performing a detailed study and weighing which factors have the most effect in minimizing heat accumulation inside the cabin, the MATLAB model seems very suitable. To perform the same simulation with similar computing power, TAItherm takes between 16-18 hours whereas MATLAB takes a couple of minutes.

CHAPTER 6

DESIGN FOR SIX SIGMA STUDY

6.1 Need for DFSS

There are a lot of factors which affect how much heat is accumulated inside the vehicle cabin. It is very difficult to single out factors whose variations would lead to improvement in all conditions. Throughout the year, day, and hour, conditions are continuously changing; for example, solar radiation, ambient exterior temperature, and wind speed all change throughout the day. It would not be accurate to assume a condition set it might yield improvement, but a different condition set might result in a downgrade.

Design for Six Sigma, DFSS, is a management method for Six Sigma. DFSS separates the condition set into input signals and noise factors. It organizes different parameters into control factors and the possible variations of each parameter are given their level within the control factor.

The purpose of DFSS is to single out control factors which make the design robust. A design is robust when it is insensitive to noise variation. For example, if a parameter in a design is changed, it should not cater to a single noise level but instead bring improvement to the variation of that noise level.

The DFSS study is performed to optimize the vehicle cabin for lower heat accumulation by determining the parameters which lead to a robust design regardless of the noise level. This optimization will rank control factors in order of the effect they have on the design. High ranking control factors will be verified via individual testing and determining the percent improvement.

6.2 DFSS Setup for Optimization

Figure 27 illustrates how a DFSS study is set up. DFSS is setup around a function whose input is the solar radiation load, and output response is the energy accumulated which is being optimized. Factors which can be controlled by an engineer in the design of cabin are listed under the heading “control factors.” Factors which cannot be controlled by an engineer such as the weather conditions are listed under the heading “noise factors.” All of these factors collectively affect the function in determining how much of the solar radiation from an input signal is able to transfer to the interior of the cabin.

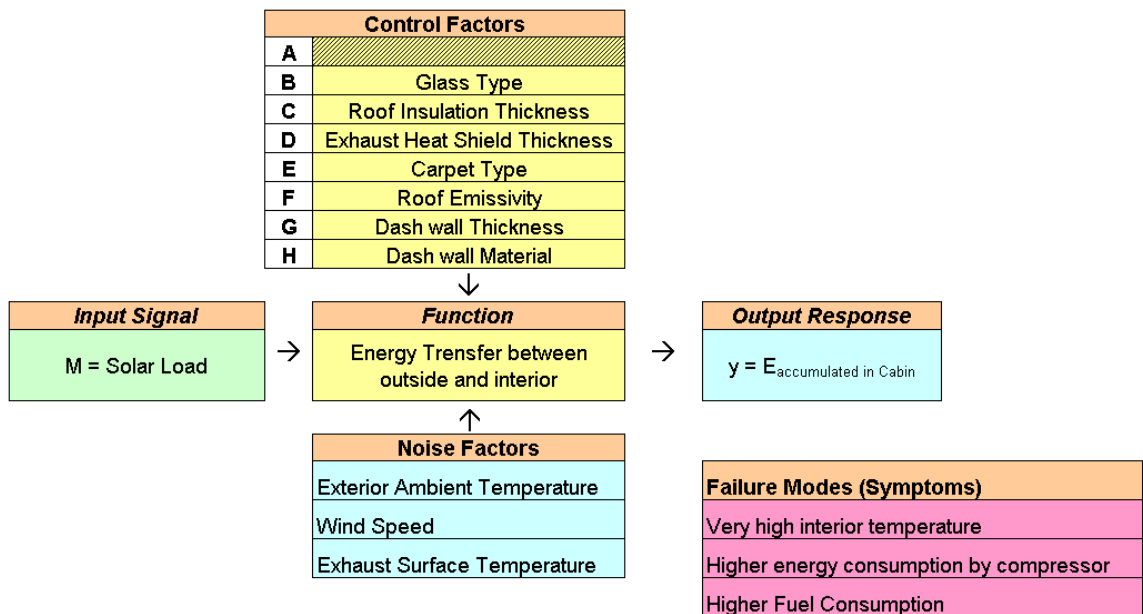


Figure 27: Parameter diagram for a DFSS study setup

6.2.1 Signal Input

An input signal differs from noise factors such that an increase in the input signal will result in linear increase in output response. Solar load is a definitive source of energy into the cabin system. Three levels are selected for the solar load; $M_1 = 750 \text{ W/m}^2$, $M_2 = 1000 \text{ W/m}^2$, and $M_3 = 1250 \text{ W/m}^2$. Input signal 2, 1000 W/m^2 is considered a peak load from an average summer day. Input signal 1 and 3 represent a lenient and extreme case respectively.

6.2.2 Noise Factors

Factors which are not a definitive source of energy into the system are considered under noise factors. Table 5 shows 3 noise factors which are considered; the exterior ambient air temperature, the speed of wind, and the temperature of exhaust.

Table 5: Compounded Noise Strategy

| Noise Factor Levels for N₁ | |
|---|-----------------|
| Noise conditions when the response tends to be lower | |
| Noise Factor | Level |
| Low Ambient Temperature | 20 °C (68 °F) |
| High Wind Speed | 32 km/h (20mph) |
| Low Exhaust Temperature | 20 °C (68 °F) |
| | |
| Noise Factor Levels for N₂ | |
| Noise conditions when the response tends to be higher | |
| Noise Factor | Level |
| High Ambient Temperature | 43 °C (110 °F) |
| Low Wind Speed | 3.2 km/h (2mph) |
| High Exhaust Temperature | 120 °C (248 °F) |

Since it is difficult to incorporate all noise levels into the study, only the best and worst-case noise levels are considered. Noise levels which lead to less or no heat accumulation into the vehicle cabin are listed under the heading N1. Noise levels which lead to higher heat accumulation into the vehicle cabin are listed under the heading N2.

A lower exterior air temperature, which if equal to the initial vehicle cabin temperature, will not add any heat energy to the vehicle cabin. In fact, when the temperature inside the vehicle rises, lower exterior air temperature will help cool down the cabin via convection. On the other hand, a higher exterior air temperature will add heat to the cabin air. Wind speed accelerates the affect of the exterior air temperature. The higher the wind speed, the higher the heat transfer coefficient which will aid in more convective heat transfer. If the engine of the vehicle is turned off, then the exhaust manifold and pipe temperatures will be same as the ambient air temperature. If the engine is idling, then heat energy from the exhaust will be transferred to the vehicle cabin.

6.2.3 Control Factors

Control factors are a list of parameters that are thought to be influential in determining how much energy gets into the vehicle cabin system and accumulates. There are an excessive number of parameters which can be chosen to perform the study, but a limited number of parameters must be picked which can be easily changed by an engineer in a design process. These selective parameters are called control factors. Each control factor has multiple levels where the value for the parameter can be varied.

Control factor A only has two levels and has been left blank where no changes are made. Control factors B to H have 3 levels each. For example, there are three different types of glass from which an engineer can select. A conventional glass has higher transmissivity whereas reflective and absorptive glass have lower transmissivity. Properties for these materials are available in Table A1, Table A2, and Table A3 in the appendix. Consider another example, an engineer can vary the thickness of the roof insulation; here, the last three layers: polyurethane, abs, and cotton are either left default, doubled, or tripled.

Table 6: L-18 Control Factors and Levels

| Control Factors | Level 1 | Level 2 | Level 3 | |
|-----------------|-------------------------------|-----------------------|-------------------------------------|-------------------------------------|
| A | | | | |
| B | Glass Type | Conventional | Reflective Glass with low e coating | Absorptive Glass with low e coating |
| C | Roof Insulation Thickness | Last 3 layers doubled | Default | Last 3 layers tripled |
| D | Exhaust Heat Shield Thickness | 0 mm | 2 mm | 7 mm |
| E | Carpet Type | Cut Pile 16oz | Polyurethane Foam | Nylon |
| F | Roof Emissivity | Black | Green | White |
| G | Dash wall Thickness | Last layer halved | Default | Last layer doubled |
| H | Dash wall Material | Aluminum | Aluminum + Polyurethane Foam | Aluminum + tnt |

There are several other factors, each of which are varied either in material or thickness choice. The DFSS study will analyze these factors and determine which factors' variation affects the amount of heat accumulated in the vehicle cabin.

6.2.4 L-18 Matrix

Table 7 shows the combinations of different levels of control factors to make 18 different simulation cases. The first column shows the simulation case number; the first row shows the Control Factors; and the numbers ranging between 1 and 3 is the selected level from that column's control factor. For example, simulation case 9 has a combination of first level from control factor A, third level from control factor B and C, first level from control factor D, and so on. This matrix mixes and matches a different level from each of the control factors. Each of the combinations are unique and output a different response. The signal to noise ratio and slope of the output response will distinguish relevant factors from these sets of combinations.

Table 7: L18 Matrix grouping

| L18 Case # | Control Factor-Level Combination | | | | | | | |
|------------|----------------------------------|---|---|---|---|---|---|---|
| | A | B | C | D | E | F | G | H |
| 1. | 1 | 1 | 1 | 1 | 1 | 1 | 1 | 1 |
| 2. | 1 | 1 | 2 | 2 | 2 | 2 | 2 | 2 |
| 3. | 1 | 1 | 3 | 3 | 3 | 3 | 3 | 3 |
| 4. | 1 | 2 | 1 | 1 | 2 | 2 | 3 | 3 |
| 5. | 1 | 2 | 2 | 2 | 3 | 3 | 1 | 1 |
| 6. | 1 | 2 | 3 | 3 | 1 | 1 | 2 | 2 |
| 7. | 1 | 3 | 1 | 2 | 1 | 3 | 2 | 3 |
| 8. | 1 | 3 | 2 | 3 | 2 | 1 | 3 | 1 |
| 9. | 1 | 3 | 3 | 1 | 3 | 2 | 1 | 2 |
| 10. | 2 | 1 | 1 | 3 | 3 | 2 | 2 | 1 |
| 11. | 2 | 1 | 2 | 1 | 1 | 3 | 3 | 2 |
| 12. | 2 | 1 | 3 | 2 | 2 | 1 | 1 | 3 |
| 13. | 2 | 2 | 1 | 2 | 3 | 1 | 3 | 2 |
| 14. | 2 | 2 | 2 | 3 | 1 | 2 | 1 | 3 |
| 15. | 2 | 2 | 3 | 1 | 2 | 3 | 2 | 1 |
| 16. | 2 | 3 | 1 | 3 | 2 | 3 | 1 | 2 |
| 17. | 2 | 3 | 2 | 1 | 3 | 1 | 2 | 3 |
| 18. | 2 | 3 | 3 | 2 | 1 | 2 | 3 | 1 |

These 18 combinations are simulated in the MATLAB model with three different signal levels and two different noise levels. This equates to 108 different simulations which are run in the MATLAB model.

6.3 DFSS Results

Table 8 shows the results from 108 MATLAB model simulations. The first column shows the simulation combinations. The last 6 columns show the amount of total net power being transferred inside the vehicle cabin in kilowatts for two noise levels and three input signal levels. Table A5 in the appendix shows the same results but in different units: megajoules. The results in Table A5 represent the amount of heat accumulated over the duration of a 3-hour period. The total heat accumulated in the vehicle cabin is the sum of the heat accumulated inside the interior air, and heat accumulated inside every other surface in or around the boundary of the vehicle cabin. For Table 8, the heat accumulated over a 3-hour period (kJ) has been converted to the rate of energy transfer into the cabin (kW.) The resulting values in Table 8 with units of kW are not dependent on the duration of the simulated period. These values show the amount of net energy transferred into the vehicle cabin per unit time.

Table 8: L18 Matrix results in kW

| L18 Case # | Control Factor-Level Combination | | | | | | | | Energy Accumulation [kW] | | | | | |
|------------|----------------------------------|---|---|---|---|---|---|---|--------------------------|------------------------|------------------------|-----------------------|------------------------|------------------------|
| | | | | | | | | | N1 | | | N2 | | |
| | A | B | C | D | E | F | G | H | M ₁ 750 | M ₂ 1000 | M ₃ 1250 | M ₁ 750 | M ₂ 1000 | M ₃ 1250 |
| 1. | 1 | 1 | 1 | 1 | 1 | 1 | 1 | 1 | 0.3241 | 0.4314 | 0.5383 | 0.6976 | 0.8110 | 0.9242 |
| 2. | 1 | 1 | 2 | 2 | 2 | 2 | 2 | 2 | 0.2130 | 0.2834 | 0.3537 | 0.5812 | 0.6565 | 0.7306 |
| 3. | 1 | 1 | 3 | 3 | 3 | 3 | 3 | 3 | 0.1503 | 0.2000 | 0.2498 | 0.5344 | 0.5884 | 0.6421 |
| 4. | 1 | 2 | 1 | 1 | 2 | 2 | 3 | 3 | 0.1776 | 0.2366 | 0.2953 | 0.5319 | 0.5935 | 0.6550 |
| 5. | 1 | 2 | 2 | 2 | 3 | 3 | 1 | 1 | 0.1165 | 0.1551 | 0.1939 | 0.4648 | 0.5063 | 0.5478 |
| 6. | 1 | 2 | 3 | 3 | 1 | 1 | 2 | 2 | 0.2802 | 0.3731 | 0.4656 | 0.6555 | 0.7513 | 0.8470 |
| 7. | 1 | 3 | 1 | 2 | 1 | 3 | 2 | 3 | 0.1313 | 0.1752 | 0.2184 | 0.5068 | 0.5529 | 0.5989 |
| 8. | 1 | 3 | 2 | 3 | 2 | 1 | 3 | 1 | 0.3012 | 0.4013 | 0.5008 | 0.6350 | 0.7385 | 0.8418 |
| 9. | 1 | 3 | 3 | 1 | 3 | 2 | 1 | 2 | 0.1996 | 0.2660 | 0.3320 | 0.5697 | 0.6385 | 0.7074 |
| 10. | 2 | 1 | 1 | 3 | 3 | 2 | 2 | 1 | 0.2259 | 0.3006 | 0.3755 | 0.5928 | 0.6728 | 0.7530 |
| 11. | 2 | 1 | 2 | 1 | 1 | 3 | 3 | 2 | 0.1517 | 0.2019 | 0.2519 | 0.5394 | 0.5936 | 0.6480 |
| 12. | 2 | 1 | 3 | 2 | 2 | 1 | 1 | 3 | 0.3057 | 0.4066 | 0.5071 | 0.6762 | 0.7820 | 0.8875 |
| 13. | 2 | 2 | 1 | 2 | 3 | 1 | 3 | 2 | 0.2791 | 0.3716 | 0.4637 | 0.6497 | 0.7451 | 0.8403 |
| 14. | 2 | 2 | 2 | 3 | 1 | 2 | 1 | 3 | 0.1818 | 0.2421 | 0.3024 | 0.5574 | 0.6204 | 0.6834 |
| 15. | 2 | 2 | 3 | 1 | 2 | 3 | 2 | 1 | 0.1142 | 0.1521 | 0.1901 | 0.4465 | 0.4872 | 0.5274 |
| 16. | 2 | 3 | 1 | 3 | 2 | 3 | 1 | 2 | 0.1283 | 0.1709 | 0.2132 | 0.4811 | 0.5263 | 0.5712 |
| 17. | 2 | 3 | 2 | 1 | 3 | 1 | 2 | 3 | 0.2966 | 0.3950 | 0.4927 | 0.6686 | 0.7698 | 0.8708 |
| 18. | 2 | 3 | 3 | 2 | 1 | 2 | 3 | 1 | 0.2082 | 0.2776 | 0.3466 | 0.5623 | 0.6345 | 0.7067 |

Figure 28 shows the results from Table 8 in two axes to depict the trend energy transfer values. The x-axis shows the 108 DFSS cases. The space of 0 to 20 on the x-axis shows the L18 cases from noise level N1 and signal input M1, followed by two empty spaces, space of 20 to 40 shows L18 cases from noise level N1 and signal input M2.

The data set from each column is represented as a different series in the graph. The first and last three data sets have same noise level but a different signal input. It can be observed that as the signal input increases at either noise level, the amplitude changes but the trend remains exactly the same. If each set of 18 cases were averaged, this fixed average at noise level 1 and 2 seems to change linearly with input level 1, 2, and 3. Additionally, it can be observed that as the noise level changes at either signal input, there are subtle changes in the trend; for example, L4 behaves significantly different between noise level 1 and 2.

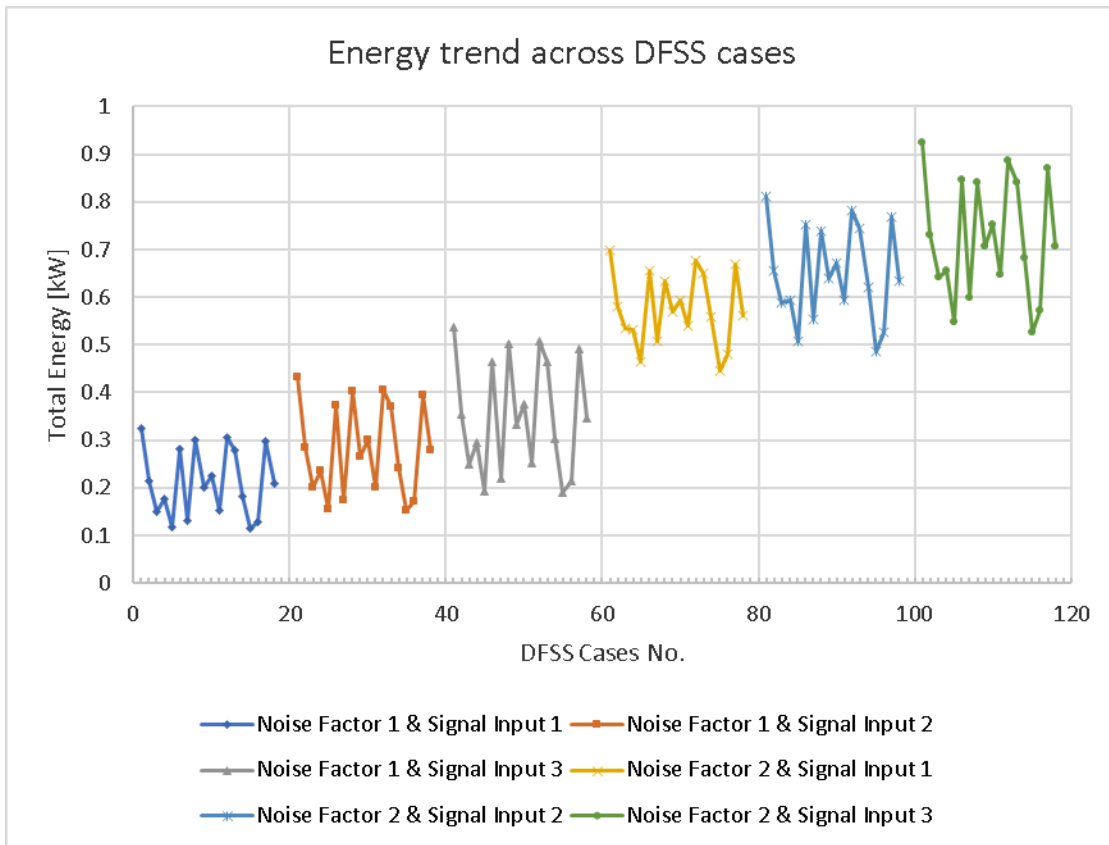


Figure 28: Energy trend across DFSS cases

Table 9: Control factor ranking for signal to noise ratio and slope

| | Signal to Noise | | | | | | | |
|----------|-----------------|-----------------|----------|----------|----------|-----------------|----------|----------|
| | A | B | C | D | E | F | G | H |
| 1 | -53.40 | -53.07 | -53.42 | -53.43 | -53.44 | -51.20 | -53.51 | -53.17 |
| 2 | -53.41 | -53.85 | -53.38 | -53.44 | -53.35 | -53.46 | -53.42 | -53.47 |
| 3 | | -53.28 | -53.41 | -53.33 | -53.41 | -55.54 | -53.27 | -53.57 |
| Δ | 0.01 | 0.78 | 0.04 | 0.12 | 0.08 | 4.34 | 0.24 | 0.40 |
| Rank | 8 | 2 | 7 | 5 | 6 | 1 | 4 | 3 |
| | | | | | | | | |
| | β | | | | | | | |
| | A | B | C | D | E | F | G | H |
| 1 | 0.000457 | 0.000487 | 0.000458 | 0.000458 | 0.000465 | 0.000574 | 0.000456 | 0.000457 |
| 2 | 0.000457 | 0.000429 | 0.000456 | 0.000455 | 0.000446 | 0.000445 | 0.000457 | 0.000457 |
| 3 | | 0.000455 | 0.000456 | 0.000458 | 0.000460 | 0.000352 | 0.000458 | 0.000456 |
| Δ | 0.000000 | 0.000058 | 0.000003 | 0.000003 | 0.000019 | 0.000222 | 0.000002 | 0.000001 |
| Rank | 8 | 2 | 5 | 4 | 3 | 1 | 6 | 7 |

Table 9 above processes the data from the simulations and ranks the control factors based on signal to noise ratio and slope. Figure 29 on the next page graphically represents the same information. Since the signal input has units of W/m^2 and the simulation output has units of kW, the numbers in Table 9 are in a different range as compared to the generic convention of electrical signal to noise ratio. The signal to noise ratio represents the noise sensitivity for each control level on the output response. The slope represents the effect of each control factor on the output response.

Looking at Table 9, the signal to noise difference between the levels of control factors is the highest for control factor **F: roof emissivity**, followed by **B: glass type**. The slope difference is also the highest for control factor F followed by B. Similar deltas can be seen in Figure 29, with control level F3 and B2 showing the lowest values.

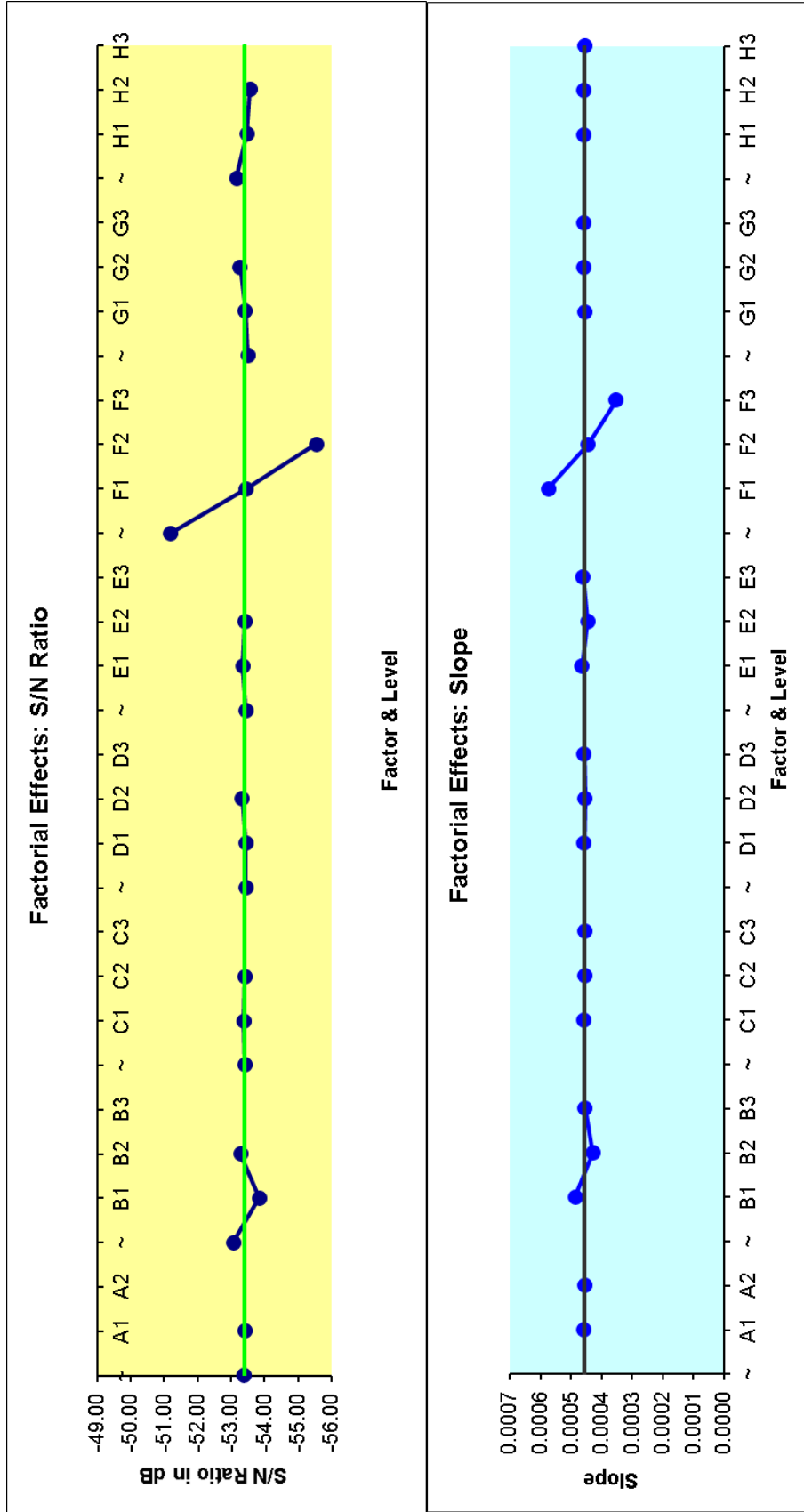


Figure 29: Signal to noise ratio and slope for control factors and its levels

6.4 Verification

The higher-ranking control factors: roof emissivity, glass type, and carpet type are further analyzed to determine the magnitude of change in heat accumulation. It is also verified that improvement happens at both noise levels, thus, confirming robustness. A lower ranking control factor such as roof insulation is also tested to distinguish whether it results in any improvement whatsoever. Each of the above listed control factors were analyzed separately. Only the thermal properties of the control factor in question are varied; all other properties are left to their default values. The simulation is run at a single input signal of $M_2 = 1000\text{W/m}^2$ and both noise levels N1 and N2.

6.4.1 High Ranking Control Factor

Table 10 shows the reduction of energy transfer into the vehicle cabin when varying the high-ranking control factors. Having a white coloured roof as opposed to a black coloured roof will reduce the energy accumulation in the vehicle cabin by 44% at noise level 1 and 30% at noise level 2. Having a reflective glass with soft e coating as opposed to conventional glass will reduce the energy accumulation in the vehicle cabin by 32% at noise level 1 and 11% at noise level 2. Having polyurethane foam as opposed to cut pile carpet will reduce the energy accumulation in the vehicle cabin by 2% at noise level 1 and 5% at noise level 2. In the case of carpet type, the reduction is higher at noise level 2 which is not the case for roof emissivity and glass type.

Table 10: Percent change for high ranking control factors

| Control Factors and Levels | N1 | N2 | N1 Change | N2 Change |
|--|--------|--------|-----------|-----------|
| | [kW] | [kW] | [%] | [%] |
| F1: Black Colour Roof | 0.2511 | 0.8564 | | |
| F2: Green Colour Roof | 0.1862 | 0.7075 | -25.87 | -17.39 |
| F3: White Colour Roof | 0.1407 | 0.6022 | -43.96 | -29.69 |
| B1: Conventional Glass | 0.1412 | 0.6084 | | |
| B2: Reflective Glass with e coating | 0.0963 | 0.5387 | -31.84 | -11.46 |
| B3: Absorptive Glass with e coating | 0.1186 | 0.5655 | -16.00 | -7.05 |
| E1: Cut Pile 16oz Carpet | 0.1407 | 0.6022 | | |
| E2: Polyurethane Foam | 0.1375 | 0.5742 | -2.33 | -4.64 |
| E3: Nylon Carpet | 0.1397 | 0.5965 | -0.75 | -0.94 |

Figure A1 to A4 in the appendix show the 3-hour temperature profile for the control levels F1 vs F3 and B1 vs B2 at both noise levels.

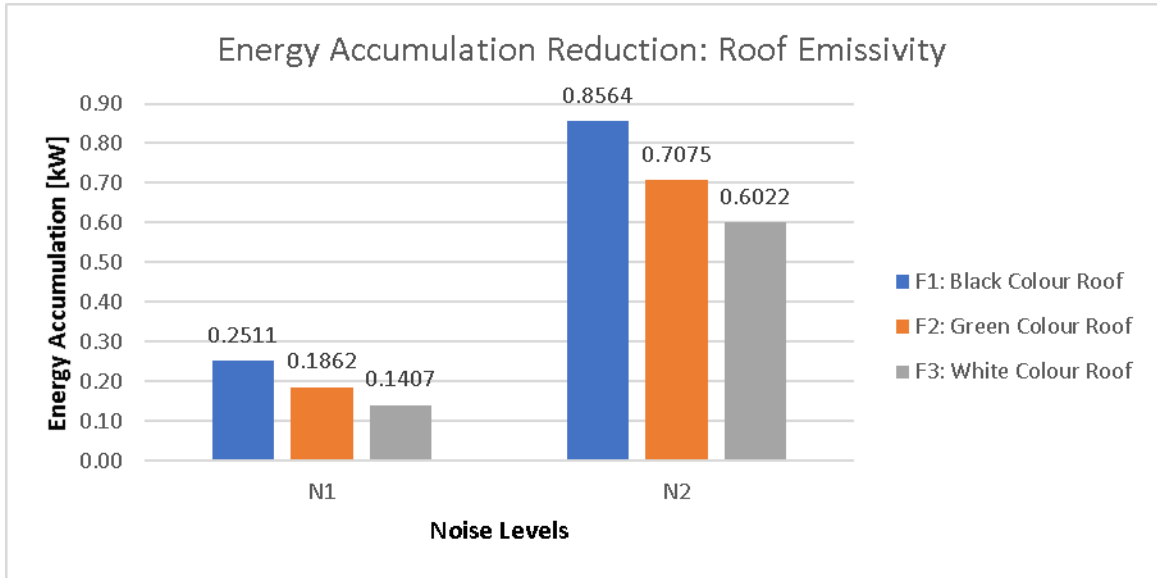


Figure 30: Reduction of energy transfer into cabin due to roof colour

Figure 30 and 31 visually represent the of reduction in energy for control factor F: roof emissivity, and B: glass type. It can be seen that control level **F3: White Colour Roof** and **B2: Reflective Glass with e coating** yield the most improvement.

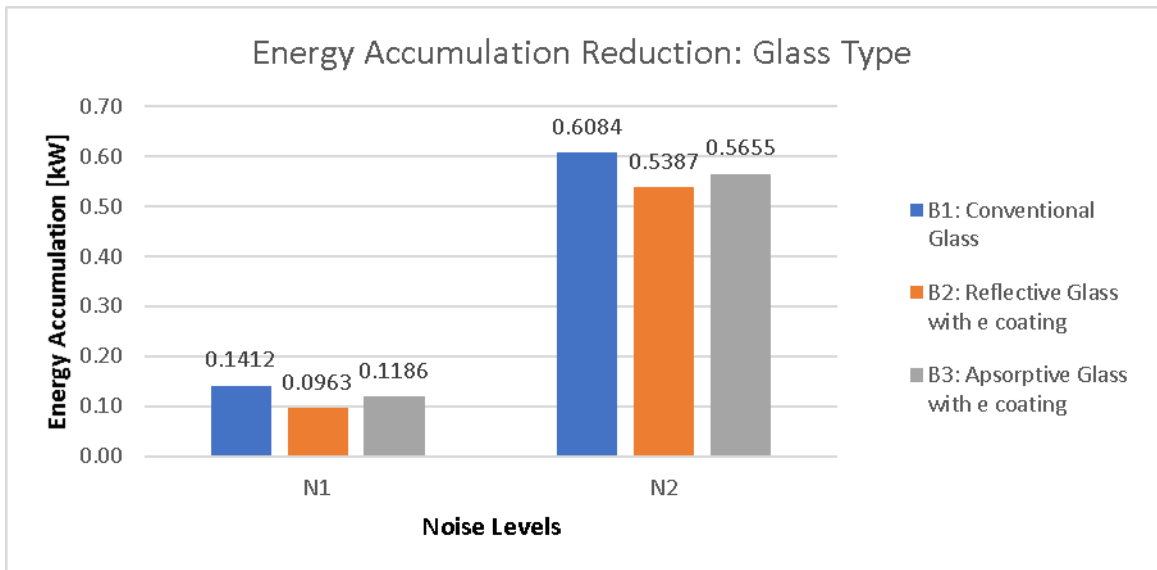


Figure 31: Reduction of energy transfer into cabin due to glass type

6.4.2 Low Ranking Control Factor

Table 11 shows the effect increasing the thickness of roof insulation. This has a negative affect on the heat accumulating inside the vehicle cabin. More insulation results in higher energy accumulation due to increase in mass.

Table 11: Percent change for low ranking control factor

| Control Factors and Levels | N1 | N2 | N1 Change | N2 Change |
|-----------------------------|--------|--------|-----------|-----------|
| | [kW] | [kW] | [%] | [%] |
| C2: Default roof insulation | 0.1407 | 0.6022 | | |
| C1: Last 3 layers doubled | 0.1611 | 0.6409 | 14.43 | 6.43 |
| C3: Last 3 layers tripled | 0.1708 | 0.6569 | 21.38 | 9.09 |

Table A5, A6 and A7 show the temperature profiles for a case with no roof insulation vs default insulation, default insulation vs doubled insulation, and default insulation vs tripled insulation respectively. It can be seen that there is a significant decrease in the temperature of the roof and a smaller decrease in the interior air and other temperatures when thickness is incrementally increased. Thus, roof insulation may slightly improve the thermal comfort, but it negatively affects the amount of heat transferring into the vehicle cabin. The decrease in temperature is not able to outdo the increase in mass resulting from the increased thickness. In this case, even though the roof temperature is significantly lowered, the system accumulates more energy since it is trapped in more mass.

This also verifies that the DFSS study has accurately ranked the control factors which reduce the heat accumulation inside the vehicle cabin. High ranking control factors have a positive effect; whereas lower ranking control factors have a negative effect on the heat accumulation.

6.5 Potential Improvements

The DFSS study is geared towards reducing the heat accumulation inside the vehicle cabin in order to increase the fuel economy. High ranking control factors achieve improvement in both fuel economy and thermal comfort. Low ranking control factors may result in improvement for either the fuel economy or the thermal comfort.

6.5.1 Fuel Economy

Since the noise level and signal input vary throughout the day and vary with location of the city, it is difficult to determine how lenient or harsh the conditions may be. Thus, it must be noted that exact values for improvement in fuel economy are impossible to determine. It is however possible to anticipate a range for improvement.

Table 12: Recapture of reduction in heat accumulation

| Control Factors and Levels | N1 Change | N2 Change |
|-------------------------------------|--------------|--------------|
| | [%] | [%] |
| F1: Black Colour Roof | | |
| F3: White Colour Roof | -43.96 | -29.69 |
| B1: Conventional Glass | | |
| B2: Reflective Glass with e coating | -31.84 | -11.46 |
| E1: Cut Pile 16oz Carpet | | |
| E2: Polyurethane Foam | -2.33 | -4.64 |

Table 12 recaps the percent reduction in heat accumulation due to high ranking control factors. Figure 32 (Rugh et al., 2013) plots the fuel economy of a conventional vehicle with respect to the percent reduction in AC load. Figure 33 (Rugh et al., 2013) plots the range of an electrical vehicle with respect to the percent reduction in AC load. Both of these plots have been produced by the NREL, The National Renewable Energy Laboratory, using a validated FASTSim model.

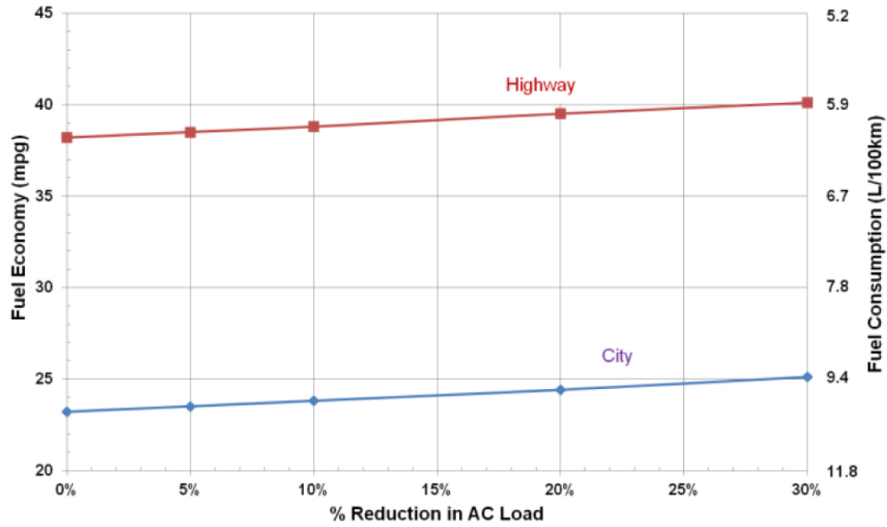


Figure 32: Impact of AC load reduction on fuel economy of a conventional vehicle

Considering a singular case as an example, the reduction of heat accumulation between black and white roof colours at noise level 2 is 30% which would also reduce the amount of load on the AC system by 30%, potentially resulting in fuel economy improvement of 0.93 L/100km (2 mpg) in both city and highway conditions. If the vehicle was electric, this would result in increasing the driving range by 11.6 km (7 miles) for city usage and 7.3 km (5 miles) for highway usage.

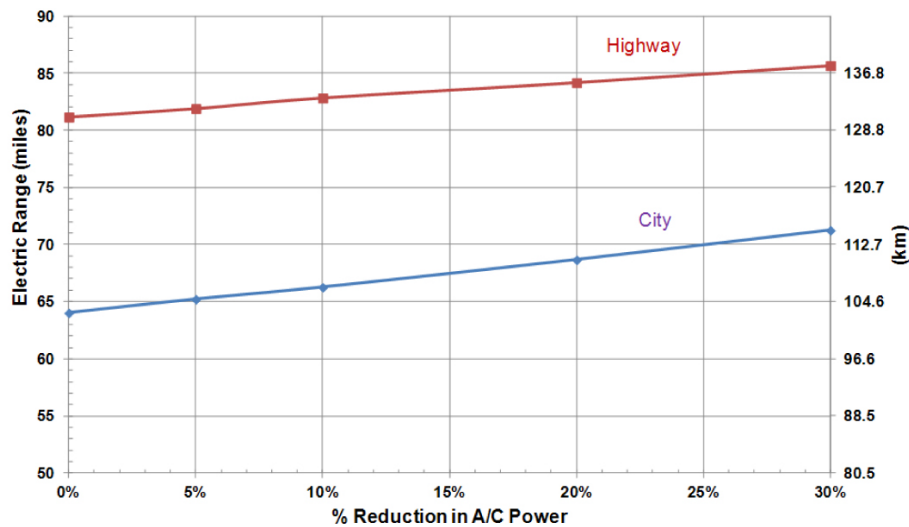


Figure 33: Impact of AC load reduction on the range of an electric vehicle

6.5.2 Thermal Comfort

Table 13 shows the effect of control factors on improvement in thermal comfort. Table A6 in the appendix shows the same table but with actual temperatures instead of improvements. Only surfaces which come in direct contact with the driver are considered for thermal comfort. Control factor F: roof emissivity and B: glass type result in definite improvement in thermal comfort. At noise level 2, F3: white color roof yields a 10.2°C, 11.0°C, and 4.2°C reduction in temperatures of interior air, seat, and dash respectively. Also, at noise level 2, B2: reflective glass with e coating yields a 3.7°C, 3.6°C, and 5.0°C reduction in temperatures of interior air, seat, and dash respectively. Thermal comfort is improved more at noise level 2; in contrast, fuel economy is improved more at noise level 1. For lower ranking control factors such as carpet type, only some cases experience improvement; when they do experience improvement, it is very minute.

Table 13: Improvement in thermal comfort

| Difference in Temperature at 3 hr [°C] | Interior Air | | Seat | | Dash | |
|---|--------------|--------|-------|--------|-------|-------|
| | N1 | N2 | N1 | N2 | N1 | N2 |
| F1: Black Colour Roof | | | | | | |
| F2: Green Colour Roof | -2.53 | -6.05 | -2.73 | -6.52 | -0.96 | -2.52 |
| F3: White Colour Roof | -4.30 | -10.28 | -4.61 | -10.97 | -1.62 | -4.23 |
| B1: Conventional Glass | | | | | | |
| B2: Reflective Glass | -2.42 | -3.76 | -1.88 | -3.67 | -5.87 | -8.43 |
| B3: Absorptive Glass | -1.23 | -2.35 | -0.97 | -2.58 | -2.52 | -5.04 |
| E1: Cut Pile 16oz Carpet | | | | | | |
| E2: Polyurethane Foam | 0.03 | -0.67 | 0.01 | -0.52 | 0.01 | -0.34 |
| E3: Nylon Carpet | 0.02 | 0.19 | 0.01 | 0.14 | 0.01 | 0.10 |
| C2: Default Roof Insulation | | | | | | |
| C1: Last 3 layers doubled | -0.71 | 0.57 | -0.81 | 0.52 | -0.35 | 0.34 |
| C3: Last 3 layers tripled | -1.18 | 0.86 | -1.30 | 0.66 | -0.54 | 0.44 |

CHAPTER 7

CONCLUSIONS

The fundamental purpose of this research was to analyze and optimize the thermal management of a vehicle in a heat soak condition. A heat soak condition represents a vehicle parked directly under the sunlight. Best-case and worst-case noise levels were considered which were comprised of wind speed, ambient air and exhaust temperatures. Three signal levels were considered to encompass a variation of solar radiation which may be affected by cloud cover.

The transient energy model which was developed in MATLAB to perform thermal analysis captures the correct thermal responses caused by heat soaking input conditions. MATLAB model was verified against a model previously prepared by FCA engineers in TAITherm. The MATLAB model was further utilized to perform a DFSS—Design for Six Sigma optimization study. The outcome of the optimization was geared towards reducing the heat load inside a vehicle cabin. The primary objective was to distinguish factors which yield significant improvement in fuel economy. Improvement in thermal comfort is equally important, but for the purpose of performing optimization, its objective is secondary.

The DFSS study identified top ranking factors whose thermal properties, when modified, yielded a significant heat load reduction inside the vehicle cabin, thus reducing the amount of work that the AC system needs to perform. Top ranking factors are as follows: roof emissivity, glass type, and carpet type. Considering the noise level 2 with exterior ambient air temperature of 43°C and signal level 2 with 100W/m² of solar radiation, change in colour can affect the fuel economy by 0.93 L/100km (2 mpg), and change in glass type can affect the fuel economy by 0.33 L/100km (0.75 mpg.) Reduction of heat load inside the vehicle also results in improved thermal comfort. Changing the roof colour could yield reduction in the final temperatures by 10.3°C, 11°C, and 4.2°C for interior air, seat, and dash materials respectively at noise level 2. Changing the glass type yields reduction in the final temperatures by 3.8°C, 3.7°C, and 8.4°C for interior air, seat, and dash materials respectively at noise level 2.

The aforementioned improvements in fuel economy and thermal comfort are potential gains and cannot be guaranteed for all conditions. Solar radiation characterised by signal levels may change between morning, noon, and evening, and vary significantly with cloud cover. The wind speed and exterior ambient air temperature characterised by noise levels may change with the weather and time of day. Different signal and noise levels will yield a different magnitude of improvement; but the DFSS optimization study ensures that the control factors which are ranked at the top yield some level of improvement under all conditions, regardless of the signal or noise level. Optimizing the top-ranking control factors yields a different magnitude but consistent improvement in a variety of signal and noise conditions, which leads to a robust design.

Additionally, this research provides a concise direction in which engineers can improve their material selection. For example, increasing insulation in the roof will only improve thermal comfort in some select conditions and not in others. At the same time, it will negatively affect the heat load for the air conditioner system as there is more mass from which the AC system must extract the heat. On the other hand, a change in the exterior roof colour or glass type will result in a significant improvement in both the fuel economy and thermal comfort under all signal and noise level conditions. Considering this, automakers can provide a wider selection of exterior paint colours which have lower absorptivity. Automakers can also invest in solar control glass technologies and make them more cost efficient. The MATLAB model which was developed for performing DFSS simulations can essentially be used as a design tool for material choices.

There are a few aspects of this research which can be further explored. First, the impact of colour in the interior of the vehicle can be vital. Most vehicles today come with very dark interiors. It would be interesting to see the effect of lighter interior colours on the heat load accumulation inside the cabin. Secondly, the thermal comfort and customer satisfaction is almost as important as improvement in fuel economy. It would be interesting to see a DFSS optimization study based on thermal comfort rather than heat accumulations. A DFSS study geared towards thermal comfort may highlight different factors which may favour the surfaces and materials which a driver is more likely to come in contact with.

REFERENCES/BIBLIOGRAPHY

- Arendt, W., & Warma, M. (2003). Dirichlet and Neumann boundary conditions: What is in between? *Nonlinear Evolution Equations and Related Topics*, 119-135
- Atkinson, W., & Hill, W. (2015). The heat is on: Don't leave your chocolate candy, kids or pets in a parked car. SAE International.
- Bahrami, M. (n.d.). Natural Convection. Lecture. Retrieved from <https://www.sfu.ca/~mbahrami/ENSC 388/Notes/Natural Convection.pdf>
- Cengel, Y. A., Dr., & Ghajar, A. J. (2015). *Heat and Mass Transfer: Fundamentals and Applications*. New York, NY: McGraw Hill Education.
- Farrington, R., & Rugh, J. (2000). Impact of Vehicle Air-Conditioning on Fuel Economy, Tailpipe Emissions, and Electric Vehicle Range. National Renewable Energy Laboratory.
- Fedoruk, M. J., & Kerger, B. D. (2003). Measurement of volatile organic compounds inside automobiles†. *Journal of Exposure Science & Environmental Epidemiology*.
- Green Rhino Energy. (2016). Solar Spectrum. Retrieved from <http://www.greenrhinoenergy.com/solar/radiation/characteristics.php>
- Jeffers, M. A., Chaney, L., & Rugh, J. P. (2015). Climate Control Load Reduction Strategies for Electric Drive Vehicles in Warm Weather. SAE Technical Paper Series.
- Johnson, V. H. (2002). Fuel Used for Vehicle Air Conditioning: A State-by-State Thermal Comfort-Based Approach. SAE Technical Paper Series.

Natural Resources Canada. (2016). Air conditioning and its effect on fuel consumption. Retrieved from <http://www.nrcan.gc.ca/node/16740>

Osborn, L. (n.d.). Hottest Cities in United States. Retrieved from <https://www.currentresults.com/Weather-Extremes/US/hottest-cities.php>

Piovano, A., Loreface, L., & Scantamburlo, G. (2016.). Modelling of Car Cabin Thermal Behaviour during Cool Down, Using an Advanced CFD/Thermal Approach. SAE Technical Paper Series.

Recktenwald, G. (2014.). Crank Nicolson Solution to the Heat Equation. Lecture. Retrieved from <http://web.cecs.pdx.edu/~gerry/class/ME448/notes/>

Recktenwald, G. (2014.). Alternative Boundary Condition Implementations for Crank Nicolson Solution to the Heat Equation. Lecture. Retrieved from <http://web.cecs.pdx.edu/~gerry/class/ME448/notes/>

Rugh, J., Chaney, L., Ramroth, L., Venson, T., & Rose, M. (2013). Impact of Solar Control PVB Glass on Vehicle Interior Temperatures, Air-Conditioning Capacity, Fuel Consumption, and Vehicle Range. SAE Technical Paper Series.

US Department of Commerce, & NOAA. (2018). 2017 Climate Year in Review. Retrieved from https://www.weather.gov/psr/Year_in_Review_2017

Vanos, J. K., Middel, A., Mckercher, G. R., Kuras, E. R., & Ruddell, B. L. (2016). Hot playgrounds and childrens health: A multiscale analysis of surface temperatures in Arizona, USA. *Landscape and Urban Planning*, 146, 29-42.

APPENDICES

Appendix A

Table A1: Thermal properties for various materials

| Material | Conductivity K | Density ρ | Specific Heat C_p | Diffusivity |
|----------------------|----------------|----------------------|---------------------|---------------------|
| | [W/mk] | [kg/m ³] | [J/kgK] | [m ² /s] |
| Glass Conventional | 1.1717 | 2529.60 | 754.04 | 6.14E-07 |
| Glass Reflective | 1.1717 | 2529.60 | 754.04 | 6.14E-07 |
| Glass IR Reflective | 1.1717 | 2529.60 | 754.04 | 6.14E-07 |
| Glass IR Absorptive | 1.1717 | 2529.60 | 754.04 | 6.14E-07 |
| ABS | 0.1660 | 996.35 | 1464.00 | 1.14E-07 |
| Steel Mild | 52.0190 | 7768.98 | 460.97 | 1.45E-05 |
| Fiberglass Composite | 0.2994 | 1320.04 | 1502.22 | 1.51E-07 |
| Fiberglass Wool | 0.2900 | 200.00 | 660.00 | 2.20E-06 |
| Leather | 0.1350 | 860.00 | 1500.00 | 1.05E-07 |
| Nylon Bonded | 0.2994 | 930.03 | 1502.22 | 2.14E-07 |
| Nylon Unbonded | 0.2994 | 740.02 | 1502.22 | 2.69E-07 |
| Polyethylene | 0.3950 | 913.05 | 2301.00 | 1.88E-07 |
| Polypropylene | 0.2600 | 908.25 | 1882.80 | 1.52E-07 |
| Polystyrene | 0.2200 | 1038.00 | 1339.00 | 1.58E-07 |
| Polyurethane | 0.3200 | 1200.00 | 2090.00 | 1.28E-07 |
| Polyurethane Foam | 0.0389 | 32.00 | 2090.00 | 5.82E-07 |
| Stainless Steel 430 | 26.9900 | 7700.00 | 460.24 | 7.62E-06 |
| Titanium | 22.0000 | 4540.00 | 523.00 | 9.27E-06 |
| Rubber Foam | 0.0900 | 500.00 | 1670.00 | 1.08E-07 |
| Cotton | 0.0590 | 81.00 | 1150.00 | 6.33E-07 |
| Woodstock | 0.1500 | 802.00 | 2250.00 | 8.31E-08 |
| TNT | 0.0370 | 87.00 | 660.00 | 6.44E-07 |
| Carpet 16z | 0.2942 | 1601.85 | 1465.38 | 1.25E-07 |
| Aluminum | 201.0730 | 2770.09 | 884.25 | 8.21E-05 |

Table A2: Glass properties

| Material | Thickness [mm] | Reflectance | Transmissivity |
|---------------------|-----------------------|--------------------|-----------------------|
| Glass Conventional | 5.2 | 0.08 | 0.76 |
| Glass Reflective | 5.2 | 0.45 | 0.34 |
| Glass IR Reflective | 5.2 | 0.37 | 0.52 |
| Glass IR Absorptive | 5.2 | 0.06 | 0.53 |

Table A3: Surface condition properties

| Surfaces | Emissivity | Absorptivity |
|----------------------------|-------------------|---------------------|
| Default | 0.9 | 0.7 |
| Window | 0.95 | 0.05 |
| Window Low E Hard Coat | 0.15 | 0.05 |
| Window Low E Soft Coat | 0.1 | 0.05 |
| Paint Black | 0.91 | 0.98 |
| Paint Green | 0.89 | 0.57 |
| Paint White | 0.87 | 0.28 |
| Paint Yellow | 0.9 | 0.38 |
| Carpet | 0.95 | 0.6 |
| Exhaust | 1 | 0.9 |
| Fiberglass Dark | 0.95 | 0.9 |
| Nylon Cloth | 0.77 | 0.13 |
| Plastic Black Polyethylene | 0.92 | 0.93 |
| Plastic Dark PVC | 0.95 | 0.9 |
| Plastic White PVC | 0.95 | 0.25 |
| Steel Oxidized | 0.8 | 0.74 |
| Aluminum Galvanized | 0.22 | 0.49 |
| Steel As Received | 0.74 | 0.74 |

Table A4: View Factor between surfaces

| | wd | dt | rf | rw | rd | fe | fw | sfc | sfb | src | srb | dtF |
|-----|------|------|------|------|------|------|------|------|------|------|------|------|
| | 1 | 2 | 3 | 4 | 5 | 6 | 7 | 8 | 9 | 10 | 11 | 12 |
| wd | 0.00 | 0.35 | 0.05 | 0.02 | 0.01 | 0.05 | 0.08 | 0.09 | 0.19 | 0.03 | 0.08 | 0.04 |
| dt | 0.52 | 0.00 | 0.04 | 0.00 | 0.00 | 0.02 | 0.24 | 0.04 | 0.03 | 0.00 | 0.01 | 0.09 |
| rf | 0.03 | 0.03 | 0.00 | 0.02 | 0.25 | 0.10 | 0.12 | 0.13 | 0.09 | 0.13 | 0.10 | 0.00 |
| rw | 0.04 | 0.00 | 0.10 | 0.00 | 0.45 | 0.04 | 0.08 | 0.03 | 0.18 | 0.07 | 0.00 | 0.00 |
| rd | 0.01 | 0.00 | 0.52 | 0.30 | 0.00 | 0.00 | 0.00 | 0.00 | 0.03 | 0.00 | 0.14 | 0.00 |
| fe | 0.10 | 0.03 | 0.40 | 0.04 | 0.00 | 0.00 | 0.04 | 0.00 | 0.33 | 0.00 | 0.06 | 0.00 |
| fw | 0.09 | 0.17 | 0.23 | 0.05 | 0.00 | 0.02 | 0.00 | 0.00 | 0.21 | 0.00 | 0.11 | 0.12 |
| sfc | 0.17 | 0.04 | 0.48 | 0.03 | 0.00 | 0.00 | 0.00 | 0.00 | 0.23 | 0.00 | 0.04 | 0.00 |
| sfb | 0.17 | 0.02 | 0.06 | 0.06 | 0.02 | 0.11 | 0.17 | 0.11 | 0.00 | 0.03 | 0.19 | 0.06 |
| src | 0.05 | 0.01 | 0.57 | 0.07 | 0.00 | 0.00 | 0.00 | 0.00 | 0.10 | 0.00 | 0.19 | 0.00 |
| srb | 0.08 | 0.01 | 0.27 | 0.00 | 0.11 | 0.03 | 0.10 | 0.02 | 0.29 | 0.10 | 0.00 | 0.00 |
| dtF | 0.13 | 0.19 | 0.00 | 0.00 | 0.01 | 0.00 | 0.38 | 0.00 | 0.29 | 0.00 | 0.00 | 0.00 |

Table A5: L18 Matrix results in MJ

| | Heat Accumulation during 3hr period [MJ] | | | | | |
|-----|--|---------|--------|--------|---------|--------|
| | N1 | | | N2 | | |
| | M1 750 | M2 1000 | M31250 | M1 750 | M2 1000 | M31250 |
| 1. | 1.1667 | 1.5532 | 1.9380 | 2.5114 | 2.9195 | 3.3272 |
| 2. | 0.7670 | 1.0204 | 1.2732 | 2.0922 | 2.3635 | 2.6303 |
| 3. | 0.5412 | 0.7201 | 0.8992 | 1.9239 | 2.1182 | 2.3114 |
| 4. | 0.6395 | 0.8518 | 1.0631 | 1.9147 | 2.1366 | 2.3581 |
| 5. | 0.4193 | 0.5585 | 0.6982 | 1.6732 | 1.8226 | 1.9720 |
| 6. | 1.0087 | 1.3432 | 1.6763 | 2.3598 | 2.7047 | 3.0492 |
| 7. | 0.4728 | 0.6308 | 0.7864 | 1.8243 | 1.9905 | 2.1559 |
| 8. | 1.0844 | 1.4447 | 1.8030 | 2.2858 | 2.6584 | 3.0305 |
| 9. | 0.7186 | 0.9577 | 1.1953 | 2.0510 | 2.2987 | 2.5466 |
| 10. | 0.8134 | 1.0823 | 1.3519 | 2.1340 | 2.4222 | 2.7109 |
| 11. | 0.5462 | 0.7268 | 0.9069 | 1.9420 | 2.1369 | 2.3329 |
| 12. | 1.1006 | 1.4637 | 1.8255 | 2.4344 | 2.8151 | 3.1951 |
| 13. | 1.0048 | 1.3378 | 1.6694 | 2.3389 | 2.6824 | 3.0252 |
| 14. | 0.6544 | 0.8714 | 1.0885 | 2.0068 | 2.2334 | 2.4603 |
| 15. | 0.4112 | 0.5475 | 0.6843 | 1.6073 | 1.7538 | 1.8985 |
| 16. | 0.4618 | 0.6152 | 0.7677 | 1.7320 | 1.8945 | 2.0563 |
| 17. | 1.0678 | 1.4221 | 1.7737 | 2.4068 | 2.7713 | 3.1349 |
| 18. | 0.7495 | 0.9993 | 1.2477 | 2.0244 | 2.2842 | 2.5442 |

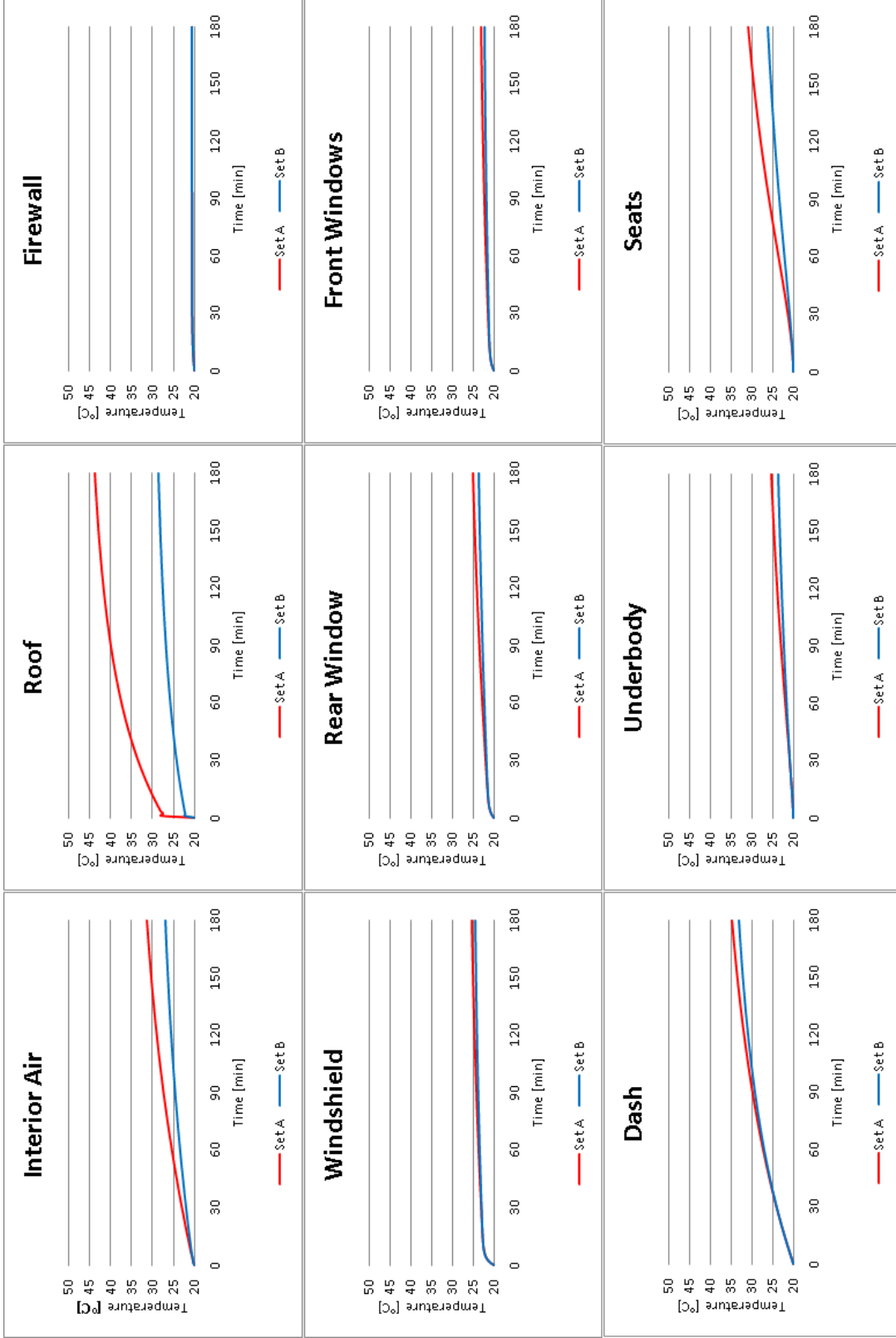


Figure A1: Roof-emissivity at N1. Data set A = F1-black, Data Set B = F3-white

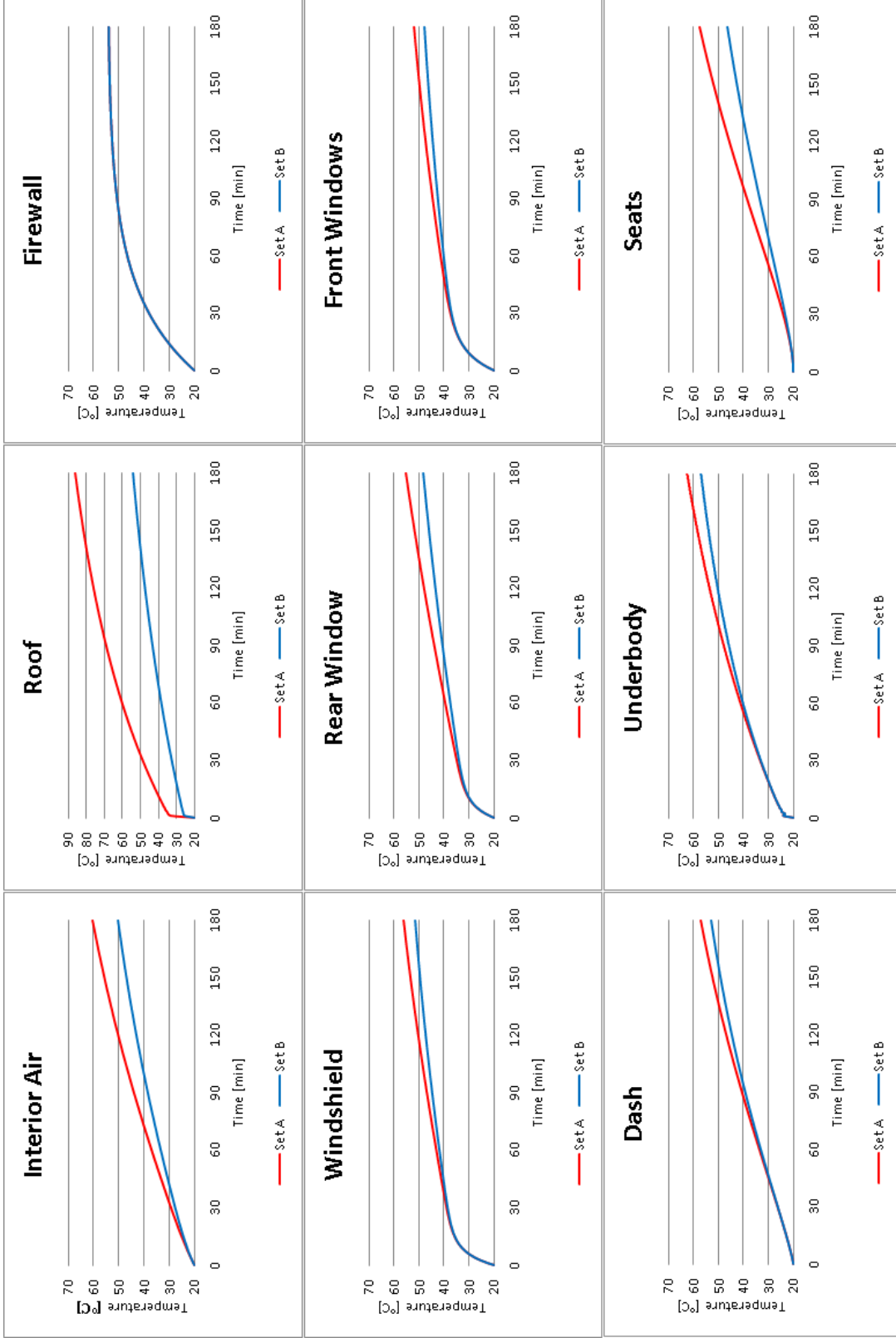


Figure A2: Roof-emissivity at N2. Data set A = F1-black, Data Set B = F3-white

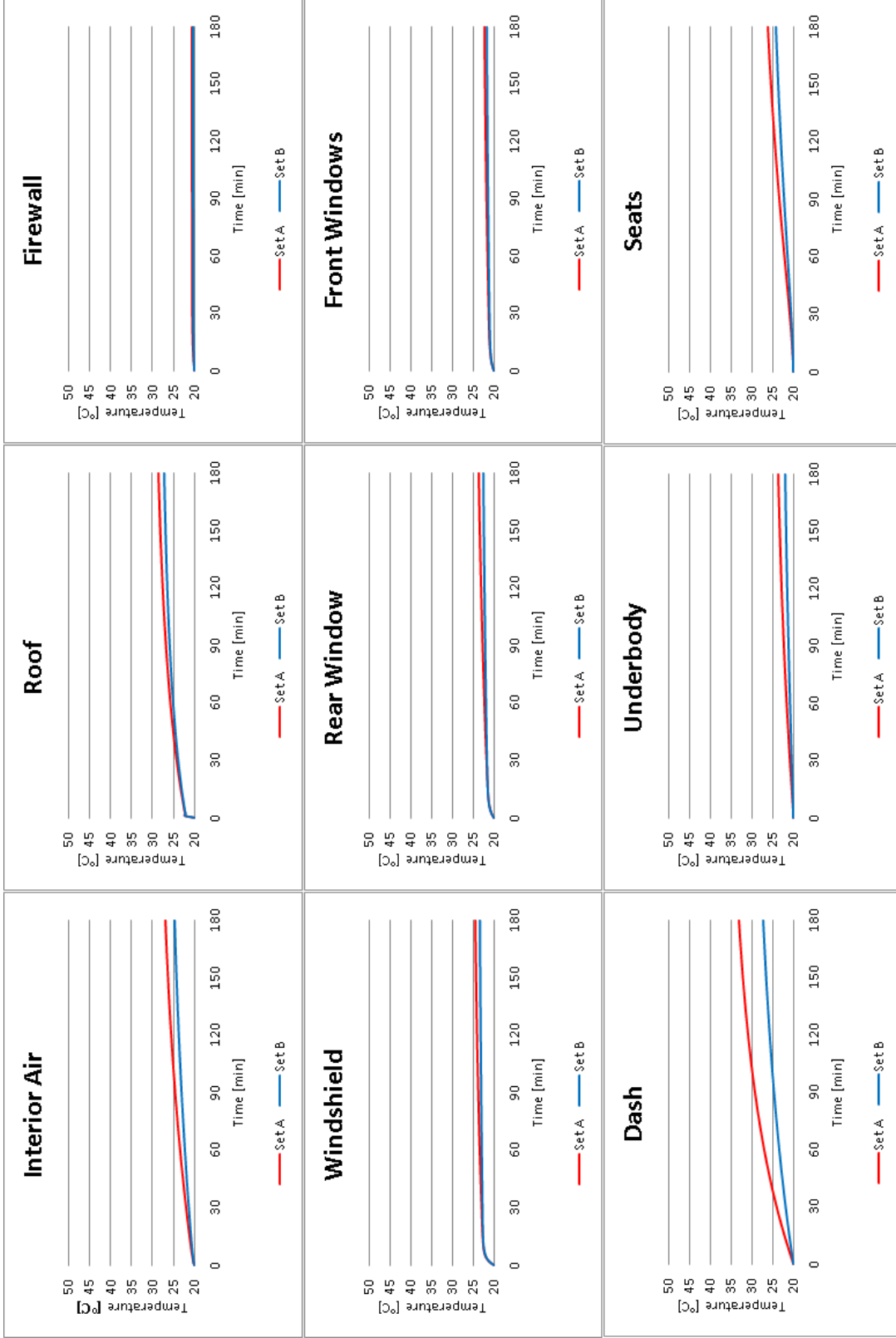


Figure A3: Glass-type at N 1. Data set A = B1-conventional, Data set B = B2-reflective

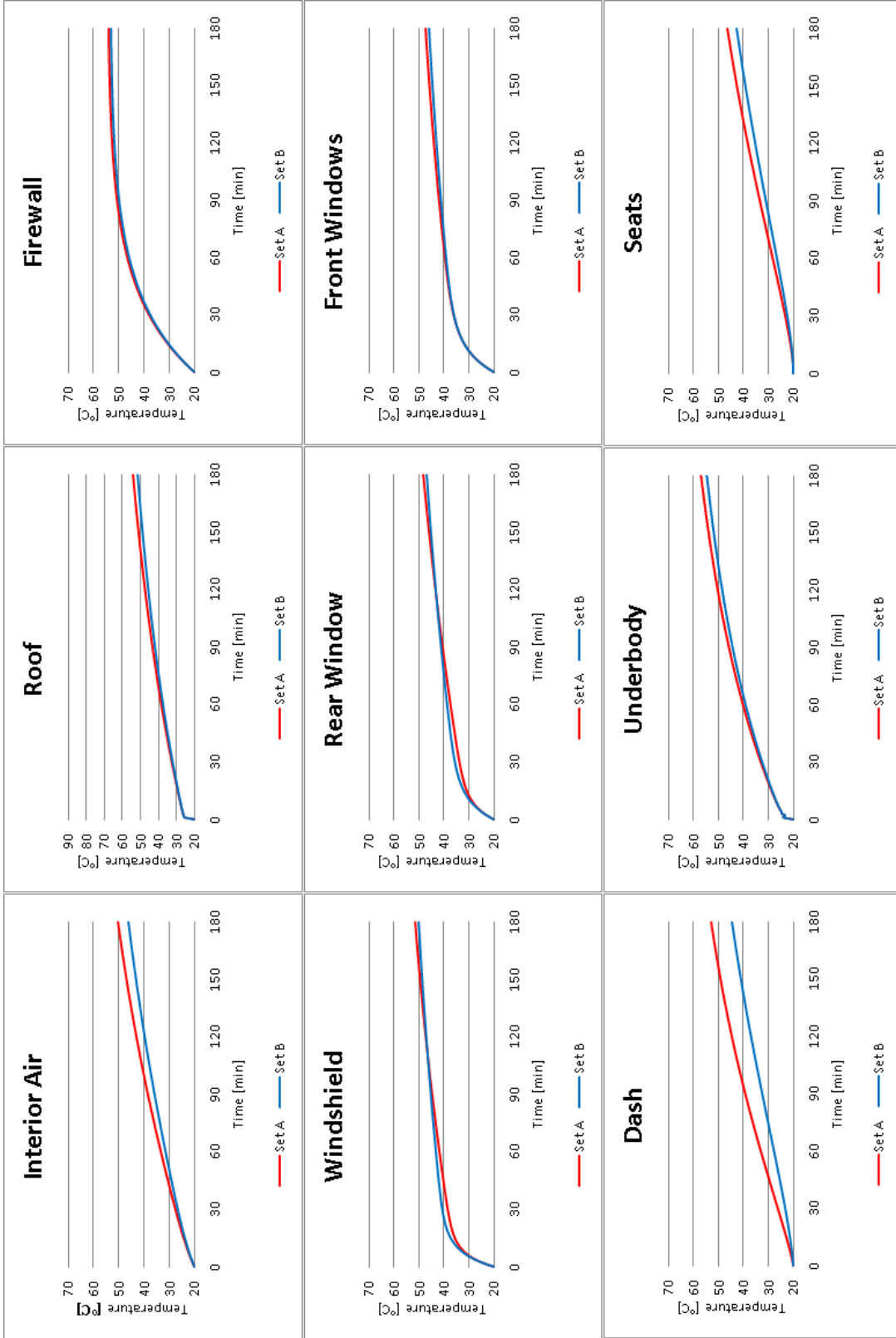


Figure A4: Glass-type at N2. Data set A = B1-conventional, Data set B = B2-reflective

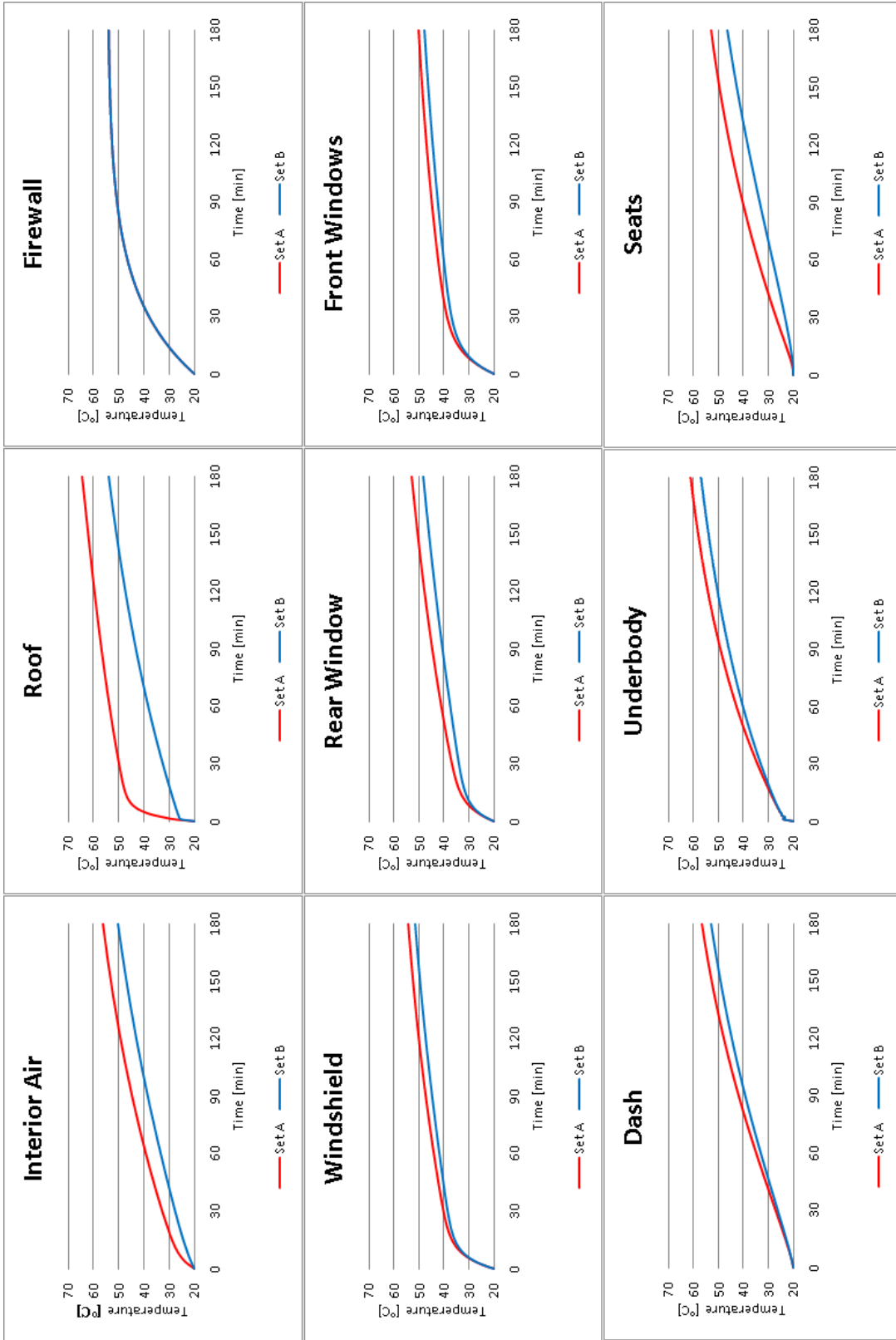


Figure A5: Roof-insulation at N2. Data set A = none, Data set B = C2-default

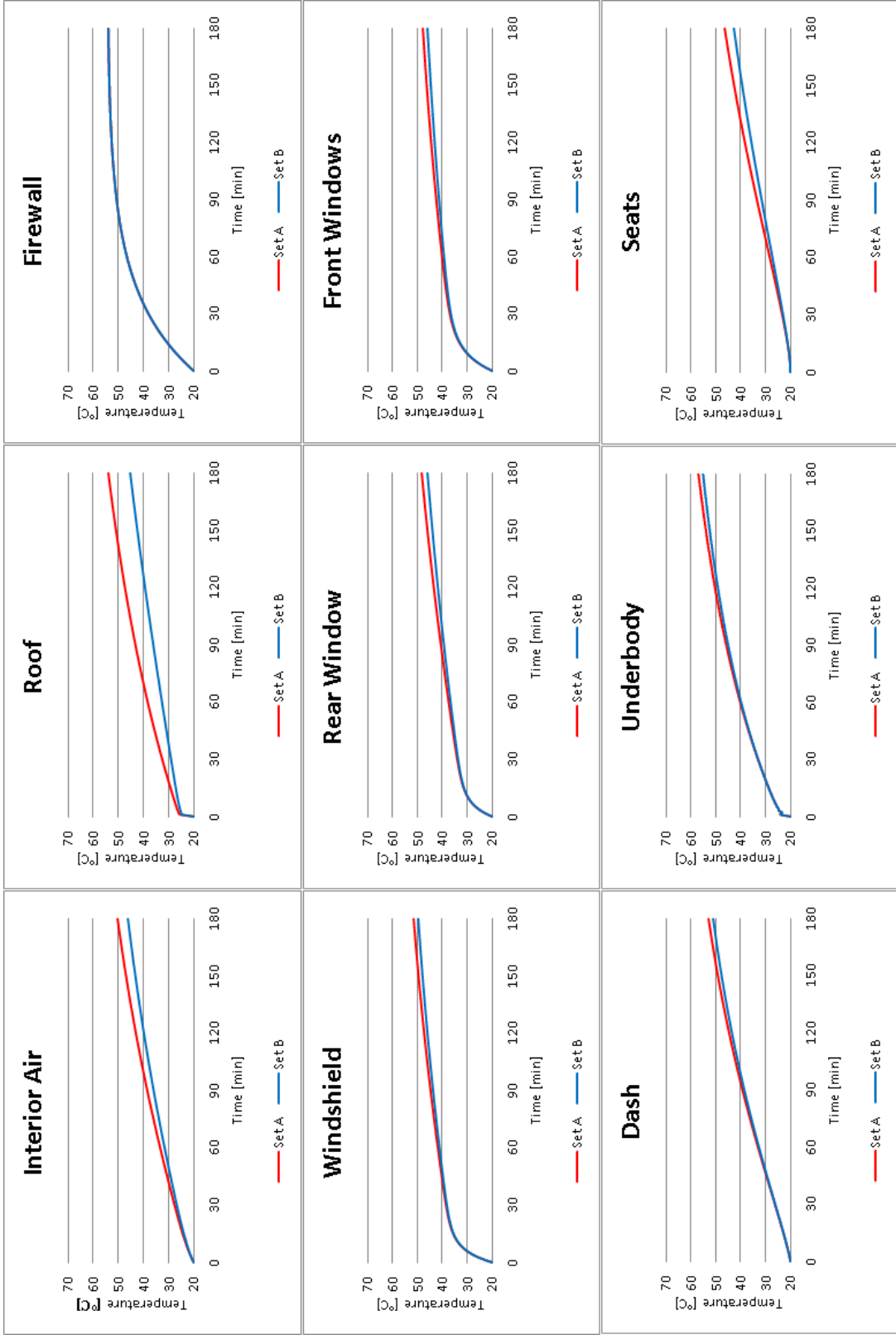


Figure A6: Roof-insulation at N2. Data set A = C2-default, Data set B=C1-doubled

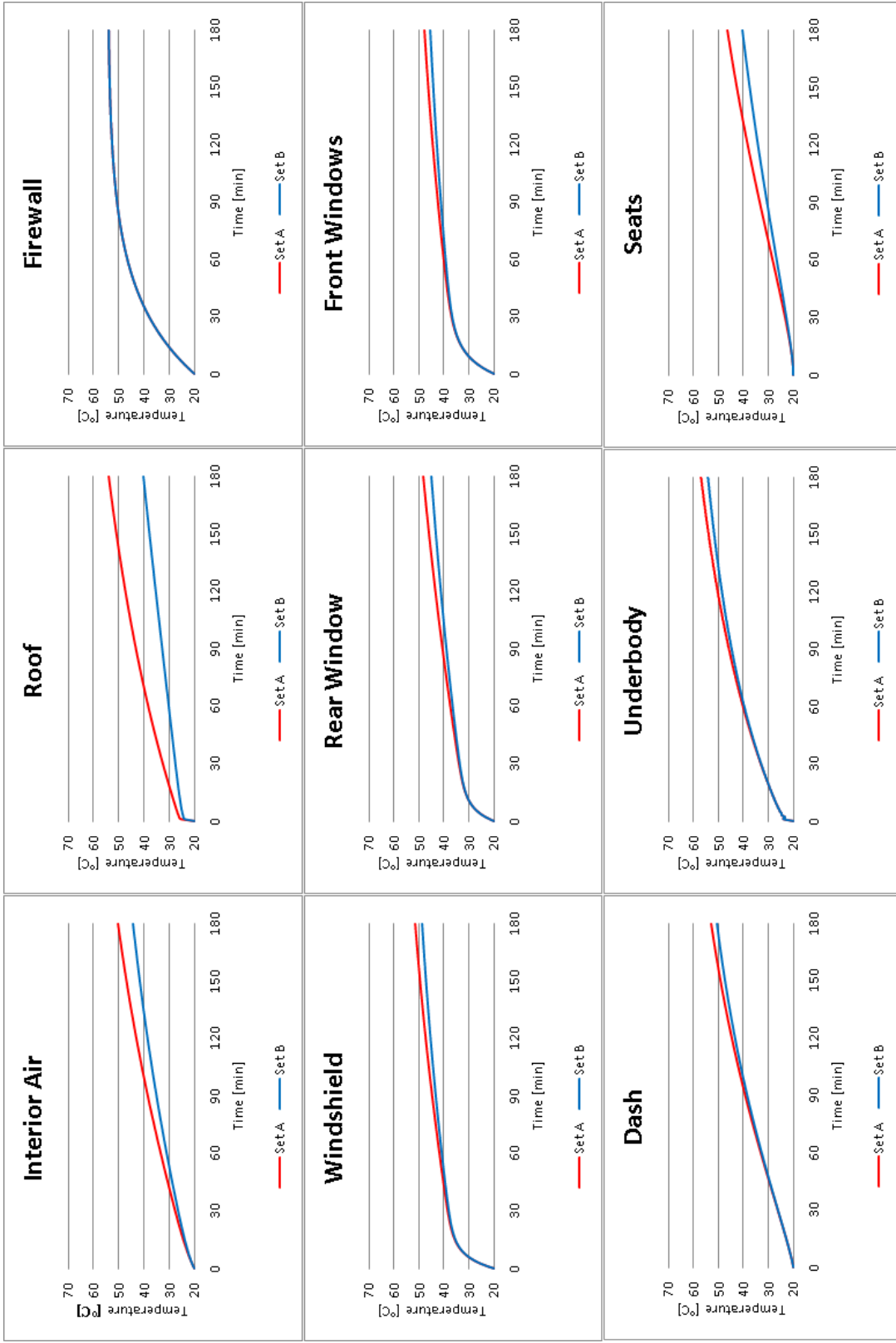


Figure A7: Roof-insulation at N2. Data set A = C2-default, Data set B = C3-trippled

Table A6: Final temperatures for thermal comfort

| Temperature at 3 hr [°C] | Interior Air | | Seat | | Dash | |
|---------------------------|--------------|-------|-------|-------|-------|-------|
| | N1 | N2 | N1 | N2 | N1 | N2 |
| F1: Black Colour Roof | 31.33 | 60.44 | 30.74 | 57.46 | 34.75 | 57.20 |
| F2: Green Colour Roof | 28.80 | 54.39 | 28.01 | 50.94 | 33.79 | 54.68 |
| F3: White Colour Roof | 27.03 | 50.16 | 26.13 | 46.49 | 33.13 | 52.97 |
| B1: Conventional Glass | 27.03 | 50.12 | 26.13 | 46.45 | 33.14 | 52.94 |
| B2: Reflective Glass | 24.61 | 46.36 | 24.25 | 42.78 | 27.27 | 44.51 |
| B3: Absorptive Glass | 25.80 | 47.77 | 25.16 | 43.87 | 30.62 | 47.90 |
| E1: Cut Pile 16oz Carpet | 27.03 | 50.16 | 26.13 | 46.49 | 33.13 | 52.97 |
| E2: Polyurethane Foam | 27.06 | 49.49 | 26.14 | 45.97 | 33.14 | 52.63 |
| E3: Nylon Carpet | 27.05 | 50.35 | 26.14 | 46.63 | 33.14 | 53.07 |
| C2: Default | 27.03 | 49.49 | 26.13 | 45.97 | 33.13 | 52.63 |
| C1: Last 3 layers doubled | 26.32 | 50.06 | 25.32 | 46.49 | 32.78 | 52.97 |
| C3: Last 3 layers tripled | 25.85 | 50.35 | 24.83 | 46.63 | 32.59 | 53.07 |

VITA AUCTORIS

NAME: Rehan Rashid
PLACE OF BIRTH: Lahore, Punjab, Pakistan

YEAR OF BIRTH: 1992

EDUCATION: Vincent Massey Secondary School, Windsor, ON,
2010

University of Windsor, B.ASc., Windsor, ON, 2015

University of Windsor, M.ASc., Windsor, ON, 2018